

University of New Orleans

ScholarWorks@UNO

University of New Orleans Theses and
Dissertations

Dissertations and Theses

5-20-2005

The Cloning and Characterization of Two ROP/RAC G-Proteins from *Gossypium Hirsutum*

Nicole Asprodites

University of New Orleans

Follow this and additional works at: <https://scholarworks.uno.edu/td>

Recommended Citation

Asprodites, Nicole, "The Cloning and Characterization of Two ROP/RAC G-Proteins from *Gossypium Hirsutum*" (2005). *University of New Orleans Theses and Dissertations*. 233.

<https://scholarworks.uno.edu/td/233>

This Thesis is protected by copyright and/or related rights. It has been brought to you by ScholarWorks@UNO with permission from the rights-holder(s). You are free to use this Thesis in any way that is permitted by the copyright and related rights legislation that applies to your use. For other uses you need to obtain permission from the rights-holder(s) directly, unless additional rights are indicated by a Creative Commons license in the record and/or on the work itself.

This Thesis has been accepted for inclusion in University of New Orleans Theses and Dissertations by an authorized administrator of ScholarWorks@UNO. For more information, please contact scholarworks@uno.edu.

THE CLONING AND CHARACTERIZATION OF TWO *ROP/RAC* G-PROTEINS FROM
GOSSYPIUM HIRSUTUM

A Thesis

Submitted to the Graduate Faculty of the
University of New Orleans
in partial fulfillment of the
requirements for the degree of

Master of Science
in
The Department of Biological Sciences

by

Nicole Marie Asprodites

B.S. Zoology Louisiana State University, 1996

May 2005

Dedication

I dedicate this thesis in loving memory to my father, Stephen Asprodites Jr., who offered unconditional love and support. He is no longer physically present to give me strength and support, but his spiritual presence continues to guide me, always.

Acknowledgement

Attending Graduate School at the University of New Orleans and performing my research work at the United States Department of Agriculture, Southern Regional Research Center has been a remarkable, challenging, and rewarding journey, and there are many people to thank at both facilities.

From the Southern Regional Research Center, I begin with my thesis supervisor, Dr. Barbara A. Triplett. It will be very difficult not to overstate my heartfelt gratitude. Thank you for welcoming me into the cotton fiber bioscience family with open arms and taking me under your wing. Words cannot describe my genuine gratitude for providing encouragement, sympathy, sound advice, and a passion for research. Besides being my mentor, she is my role model and a cherished friend.

I offer a most sincere thank you to Dr. Hee Jin Kim. He is a remarkable teacher and an excellent person. I appreciate his patience, understanding, experience, and advice.

To the rest of the Cotton Fiber Bioscience family, I am grateful for their friendship, emotional support, and words of encouragement. They were for always available when I needed to harvest field tissue or gin cotton fibers.

I thank the Southern Regional Research Center Journal Club for providing a forum to aid my development as a scientist.

From the University of New Orleans, I would like to thank my thesis advisors, Dr. Mary Clancy and Dr. Candace Timpte. They gave me the chance of a lifetime and found my home at the Southern Regional Research Center. Their doors were always open for academic advice, words of wisdom, and guidance. They are not only excellent teachers, but also, excellent people.

I also thank Dr. Kathleen Burt-Utley and Dr. Bernard Rees for their advice as Graduate Coordinators. I thank the faculty and staff in the Department of Biological Sciences for their academic and administrative help.

I thank the Louisiana Governor's Biotechnology Initiative for funding this project.

I cannot end without thanking my family, on whose constant encouragement and love I have relied throughout my life, especially my mother, Julie Asprodites and my sisters, Linzy Liuzza and Diane Sabatier. They encouraged me to go back to school and supported my decisions monetarily and emotionally. Without family, this journey would not have been possible. I hope now that my family understands what this voyage has been about.

Last but certainly never least; I thank my fiancé, Richard Miller. He entered my life unexpectedly. Now as the door to Graduate School closes, we open another door and prepare for our lifelong journey, together. The last few months have been especially difficult; thanks for all the love and emotional support.

TABLE OF CONTENTS

| | |
|---|------|
| List of Figures | vi |
| List of Tables | viii |
| List of Abbreviations | ix |
| Abstract | xii |
| Introduction | 1 |
| Materials and Methods | 26 |
| Results and Discussion | 40 |
| References | 74 |
| Appendix | |
| Buffers, Media, and Reagents | 83 |
| 3'-Rapid Amplification of cDNA Ends PCR Primers | 88 |
| Real-time Reverse Transcription PCR Primers | 89 |
| Vita | 91 |

List of Figures

| Figure Number | Figure Title | Page |
|----------------------|---|-------------|
| Figure 1-1 | Stages of cotton fiber development | 3 |
| Figure 1-2 | Mature <i>Gossypium hirsutum</i> bolls | 5 |
| Figure 1-3 | A general scheme for the regulation of monomeric G-proteins in plants and animals | 9 |
| Figure 1-4 | Animal monomeric G-protein superfamily | 11 |
| Figure 1-5 | Plant monomeric G-protein superfamily | 14 |
| Figure 1-6 | Phylogenetic analysis of the <i>Rho</i> family of monomeric G-proteins | 15 |
| Figure 1-7 | Phylogenetic analysis of the <i>Rop</i> G-protein subfamilies from <i>Arabidopsis thaliana</i> and <i>Gossypium hirsutum</i> | 20 |
| Figure 2-1 | Multiple sequence alignment of the <i>Gossypium arboreum</i> <i>Rop</i> EST sequences used to design PCR primers | 41 |
| Figure 2-2 | Multiple sequence alignment of the <i>Gossypium hirsutum</i> <i>Rop/Rac</i> GTPases used to determine amplicon length | 42 |
| Figure 2-3 | Agarose gel of PCR amplification products | 43 |
| Figure 2-4 | cDNA sequences of <i>GhRac2</i> and <i>GhRac3</i> | 45 |
| Figure 2-5 | Multiple sequence alignment of the <i>Gossypium hirsutum</i> <i>Rop/Rac</i> G-proteins at the amino acid level | 46 |
| Figure 2-6 | Phylogenetic analysis of the <i>Gossypium hirsutum</i> and <i>Arabidopsis thaliana</i> <i>Rop/Rac</i> G-proteins | 48 |
| Figure 2-7 | Phylogenetic analysis of the <i>Gossypium hirsutum</i> <i>Rop/Rac</i> G-proteins and the <i>Rop/Rac</i> G-protein TC sequences from the TIGR database | 49 |
| Figure 2-8 | Representative total RNA gel | 51 |
| Figure 2-9 | Developmental expression of <i>GhRac9</i> in TM1 fiber tissue | 54 |

List of Figures (continued)

| | | |
|-------------|---|----|
| Figure 2-10 | Developmental expression of <i>GhGLP1</i> in TM1 fiber tissue | 55 |
| Figure 2-11 | Developmental expression of <i>GhRac2</i> in TM1 fiber tissue | 56 |
| Figure 2-12 | Developmental expression of <i>GhRac3</i> in TM1 fiber tissue | 57 |
| Figure 2-13 | <i>GhRac1</i> transcript level comparison among <i>Gossypium hirsutum</i> TM1, N1, and Li1 ovules on the day of anthesis | 59 |
| Figure 2-14 | <i>GhRac2</i> transcript level comparison among <i>Gossypium hirsutum</i> TM1, N1, and Li1 ovules on the day of anthesis | 60 |
| Figure 2-15 | <i>GhRac3</i> transcript level comparison among <i>Gossypium hirsutum</i> TM1, N1, and Li1 ovules on the day of anthesis | 63 |
| Figure 2-16 | <i>GhRac9</i> transcript level comparison among <i>Gossypium hirsutum</i> TM1, N1, and Li1 ovules on the day of anthesis | 65 |
| Figure 2-17 | <i>GhRac13</i> transcript level comparison among <i>Gossypium hirsutum</i> TM1, N1, and Li1 ovules on the day of anthesis | 66 |
| Figure 2-18 | <i>GhRac2</i> transcript level comparison among <i>Gossypium hirsutum</i> TM1 and N1 ovules from 0 to 10 DPA | 68 |
| Figure 2-19 | <i>GhRac3</i> transcript level comparison among <i>Gossypium hirsutum</i> TM1 and N1 ovules from 0 to 10 DPA | 69 |
| Figure 2-20 | <i>GhRac9</i> transcript level comparison among <i>Gossypium hirsutum</i> TM1 and N1 ovules from 0 to 10 DPA | 70 |

List of Tables

| Table Number | Table Title | Page |
|---------------------|--|-------------|
| Table 2-1 | Single nucleotide polymorphisms in <i>GhRac2</i> and <i>GhRac3</i> | 50 |

List of Abbreviations

| | |
|---------------|--|
| * | Significant difference |
| A | <u>A</u> bsorbance |
| ABI | <u>A</u> pplyed <u>B</u> iosystems <u>I</u> ncorporated |
| ADP | <u>A</u> denosine <u>D</u> iphosphate |
| <i>AGB1</i> | <u>G</u> -protein <u>b</u> eta subunit gene 1 from <i>Arabidopsis thaliana</i> |
| <i>AGG1</i> | <u>G</u> -protein <u>g</u> amma subunit gene from <i>Arabidopsis thaliana</i> |
| <i>Arf</i> | <u>A</u> denosine diphosphate <u>r</u> ibosylation <u>f</u> actor |
| <i>AtRop</i> | <i>Arabidopsis thaliana</i> <u>R</u> ho-related GTPase from <u>p</u> lant gene |
| BLAST | <u>B</u> asic <u>L</u> ocal <u>A</u> lignment <u>S</u> earch <u>T</u> ool |
| C | <u>C</u> ytosine |
| CA | <u>C</u> onstitutively <u>A</u> ctive |
| <i>Cdc 42</i> | <u>C</u> ell <u>d</u> ivision <u>c</u> ycle |
| cDNA | <u>C</u> opied <u>D</u> eoxyribonucleic <u>A</u> cid |
| CLUSTAL W | Multiple sequence alignment program |
| dATP | <u>D</u> eoxyadenosine <u>T</u> riphosphate |
| dCTP | <u>D</u> eoxycytidine <u>T</u> riphosphate |
| DEPC | <u>D</u> iethylpyrocarbonate |
| dGTP | <u>D</u> eoxyguanosine <u>T</u> riphosphate |
| DN | <u>D</u> ominant <u>N</u> egative |
| DNA | <u>D</u> eoxyribonucleic <u>a</u> cid |
| DNase | <u>D</u> eoxyribonuclease |
| dNTP | <u>D</u> eoxynucleotide <u>T</u> riphosphate |
| DOA | <u>D</u> ay <u>O</u> f <u>A</u> nthesis |
| DPA | <u>D</u> ays <u>P</u> ost <u>A</u> nthesis |
| dTTP | <u>D</u> eoxythymidine <u>T</u> riphosphate |
| EDTA | <u>E</u> thylenediaminetetraacetic <u>A</u> cid |
| EGTA | <u>E</u> thylene <u>G</u> lycol Bis- <u>N,N,N',N'</u> - <u>T</u> etraacetic <u>A</u> cid |
| EST | <u>E</u> xpressed <u>S</u> equence <u>T</u> ag |
| ExpPASy | <u>E</u> xpert <u>P</u> rotein <u>A</u> nalysis <u>S</u> ystem |
| F | <u>F</u> orward |
| <i>g</i> | <u>G</u> ravity force |
| G | <u>G</u> uanosine |
| G α | <u>G</u> -protein <u>a</u> lpha subunit |
| G β | <u>G</u> -protein <u>b</u> eta subunit |
| G γ | <u>G</u> -protein <u>g</u> amma subunit |
| GAP | <u>G</u> TPase <u>A</u> ctivating <u>P</u> rotein |
| GB ID | <u>G</u> en <u>B</u> ank <u>I</u> dentification |
| <i>GCR1</i> | <u>G</u> -protein- <u>C</u> oupled <u>R</u> eceptor gene <u>1</u> from <i>Arabidopsis thaliana</i> |
| GEF | <u>G</u> uanine nucleotide <u>E</u> xchange <u>F</u> actor |
| GDI | <u>G</u> uanine nucleotide <u>D</u> issociation <u>I</u> nhibitor |
| GDP | <u>G</u> uanosine <u>D</u> iphosphate |
| <i>GhGLP1</i> | <i>Gossypium hirsutum</i> <u>G</u> ermin- <u>L</u> ike <u>P</u> rotein <u>1</u> |
| <i>GhRac</i> | <i>Gossypium hirsutum</i> <u>R</u> as-related <u>C</u> 3 botulinum toxin substrate gene |

List of Abbreviations (continued)

| | |
|-------------------|---|
| G-protein | <u>G</u> uanosine triphosphate-binding protein |
| <i>GPA1</i> | <u>G</u> -protein <u>α</u> subunit gene <u>1</u> from <i>Arabidopsis thaliana</i> |
| GPCR | <u>G</u> - <u>P</u> rotein- <u>C</u> oupled <u>R</u> eceptor |
| GTP | <u>G</u> uanosine <u>T</u> riphosphate |
| GTPase | <u>G</u> uanosine <u>T</u> riphosphatase |
| H ₂ O | chemical abbreviation for water |
| HCl | <u>H</u> ydro <u>cl</u> oric Acid |
| kb | <u>k</u> ilobase |
| kbp | <u>k</u> ilobase pair |
| kDa | <u>k</u> ilo <u>D</u> alton |
| <i>Lac</i> | <u>L</u> actose operon |
| LacZα | Lactose operon beta-galactosidase gene |
| LB | <u>L</u> uria- <u>B</u> ertani |
| Li1 | <u>L</u> igon lintless allele <u>1</u> |
| LiCl | <u>L</u> ithium <u>C</u> hloride |
| M | <u>M</u> olar |
| MgCl ₂ | <u>M</u> agnesium <u>C</u> hloride |
| n | sample size |
| N1 | <u>N</u> aked Seed allele <u>1</u> |
| NaCl | Sodium Chloride |
| NaOH | Sodium Hydroxide |
| NCBI | <u>N</u> ational <u>C</u> enter for <u>B</u> iotechnology <u>I</u> nformation |
| NS | <u>N</u> ot <u>S</u> ignificant |
| <i>ori</i> | <u>o</u> ri <u>g</u> in of replication |
| PCR | <u>P</u> olymerase <u>C</u> hain <u>R</u> eaction |
| PVPP | <u>P</u> olyvinylpolypyrrolidone |
| Q-RT-PCR | Real-time <u>R</u> everse <u>T</u> ranscription <u>P</u> olymerase <u>C</u> hain <u>R</u> eaction |
| R | <u>R</u> everse |
| <i>Rab</i> | <u>R</u> as gene from rat <u>b</u> rain |
| <i>Rac</i> | <u>R</u> as-related <u>C</u> 3 botulinum toxin substrate |
| RACE PCR | <u>R</u> apid <u>A</u> mplification <u>c</u> DNA <u>E</u> nds <u>P</u> olymerase <u>C</u> hain <u>R</u> eaction |
| <i>Ran</i> | <u>R</u> as-related <u>n</u> uclear |
| <i>Ras</i> | <u>R</u> at <u>s</u> arcoma |
| <i>Rho</i> | <u>R</u> as <u>h</u> omology |
| <i>Rho1P</i> | <u>R</u> as <u>h</u> omology-like protein <u>1</u> from the garden pea |
| RNA | <u>R</u> ibonucleic <u>A</u> cid |
| RNase | <u>R</u> ibonuclease |
| <i>Rop</i> | <u>R</u> ho-related GTPase from <u>P</u> lant |
| rRNA | <u>r</u> ibosomal <u>R</u> ibonucleic <u>A</u> cid |
| SDS | <u>S</u> odium <u>D</u> odecyl <u>S</u> ulfate |
| SNP | <u>S</u> ingle <u>N</u> ucleotide <u>P</u> olymorphism |
| T _m | <u>M</u> elting <u>T</u> emperature |

List of Abbreviations (continued)

| | |
|------------|---|
| TBE | <u>T</u> ris- <u>B</u> orate- <u>E</u> DTA |
| TC | <u>T</u> entative <u>C</u> onsensus |
| TIGR | <u>T</u> he <u>I</u> nstitute of <u>G</u> enomic <u>R</u> esearch |
| TM1 | <u>T</u> exas <u>M</u> arker <u>1</u> |
| tRNA | <u>t</u> ransfer <u>R</u> ibonucleic <u>A</u> cid |
| <i>UCP</i> | <u>U</u> biquitin- <u>C</u> onjugated <u>P</u> rotein |
| UTR | <u>U</u> ntranslated <u>R</u> egion |
| UV | <u>U</u> ltra <u>V</u> iolet |

Abstract

Rop/Rac proteins are plant-specific monomeric guanosine triphosphate-binding proteins (G-proteins) with important functions in plant development. Until recently, only three cotton (*Gossypium hirsutum*) *Rop/Rac* G-protein genes were sequenced, representing subfamilies III and IV of the plant monomeric G-protein family. In this project, members of subfamilies II and I were cloned, sequenced, and named *GhRac2* and *GhRac3*, respectively. Using real-time reverse transcription PCR, expression of *GhRac2* was highest during fiber elongation, decreasing significantly when cellulose biosynthesis began. Transcript abundance of *GhRac3* doubled between fiber elongation and secondary wall synthesis, remaining constant until 20 days post-anthesis. Expression of *GhRac2* and *GhRac3* was compared between the unfertilized ovules of *Gossypium hirsutum*, Texas Marker 1 and two near-isogenic fiber-impaired mutants. Expression of *GhRac2* and *GhRac3* was significantly higher in wild type ovules than in Ligon lintless, a mutant impaired in fiber elongation, but was not different in Naked Seed, a mutant impaired in fiber initiation.

Introduction

I. Cotton production, utilization, and taxonomy

Cotton is the most important textile crop, worldwide [Lee, 1984; Wendel and Cronn, 2003]. According to the latest estimates from the National Cotton Council, cotton is the number one value crop in the United States. Cotton generates approximately \$120 billion in annual revenue for the United States economy [<http://www.cotton.org>]. According to the latest estimates from the United States Department of Agriculture, Economic Research Service, Louisiana is the eighth highest cotton producing state. Generating over \$116 million of revenue, cotton is the second highest agricultural export for Louisiana [<http://www.ers.usda.gov>]. Fiber represents 90% of the value of the cotton crop with the remainder of the profit coming from cottonseed, a by-product of ginning. Fibers are used in making cotton cloth, plastics, explosives, and high quality paper products [Lee, 1984; <http://www.cotton.org>]. Fibers are also processed into batting for padding mattresses, furniture, automobile cushions, and other non-woven products [Lee, 1984; <http://www.cotton.org>]. Cottonseed oil is used primarily for culinary purposes: shortening, cooking oil, and salad dressing [Lee, 1984]. The meal and hulls that remain are used either separately or in combination as a protein rich fodder for livestock, poultry, and fish feed as well as fertilizer [Lee, 1984; <http://www.cotton.org>].

The word ‘cotton’, derived from the Arabic word ‘quoton’, refers to the genus *Gossypium*, a member of the *Malvaceae* (mallow) family [Lee, 1984]. The large and diverse *Gossypium* genus is divided into at least 45 diploid species ($2N=26$) and five tetraploid species ($2N=52$) distributed throughout arid and semi-arid tropic and sub-tropic regions [Brubaker et al., 1999; Wendel and Cronn, 2003]. The approximately 45 diploid *Gossypium* species are grouped into eight different genomes, designated A through G and K [Brubaker et al., 1999; Wendel and

Cronn, 2003]. The five tetraploid *Gossypium* species originated from a hybridization event that united an Old World AA genome with a New World DD genome [Brubaker et al., 1999; Wendel and Cronn, 2003]. How and when the original crosses occurred and the identity of the progenitor species are still a matter of speculation [Brubaker et al., 1999; Wendel and Cronn, 2003]. Comparative restriction fragment length polymorphism mapping of the tetraploid species, the AA genome diploid species, and the DD genome diploid species suggests that the closest living descendants of the progenitor species are *Gossypium raimondii* (DD genome) and *Gossypium herbaceum* (AA genome) [Brubaker et al., 1999]. Today, four independent species of *Gossypium* are cultivated [Lee, 1984; Brubaker et al., 1999; Wendel and Cronn, 2003]. Two species are New World (American) tetraploid species, *Gossypium hirsutum* L. (upland cotton) and *Gossypium barbadense* L. (Egyptian or pima cotton); two species are Old World (Africa-Asia) diploid species, *Gossypium arboreum* L. (tree cotton, AA genome) and *Gossypium herbaceum* L. (levant cotton, AA genome) [Lee, 1984; Brubaker et al., 1999; Wendel and Cronn, 2003]. *Gossypium hirsutum* is responsible for at least 90% of the commercially cultivated cotton, worldwide [Lee, 1984; Brubaker et al., 1999; Wendel and Cronn, 2003].

II. Cotton fiber development and fiber mutants

Cotton fibers are unicellular trichomes that differentiate from ovule epidermal cells [Basra and Malik, 1984; DeLanghe, 1986]. Cotton ovules bear two forms of trichomes: trichomes that differentiate into lint fibers and trichomes that differentiate into fuzz or linter fibers [Basra & Malik, 1984]. At present, the mechanisms for determining whether cotton ovule epidermal cells develop into lint, fuzz, or some other type of cell (i.e. stomatal cells) have not

been fully elucidated [Kim & Triplett, 2001]. There are four recognized stages of cotton fiber development that overlap each other in time: fiber initiation, cell elongation, cellulose biosynthesis, and maturation (Figure 1-1) [Basra and Malik, 1984; DeLanghe, 1986].

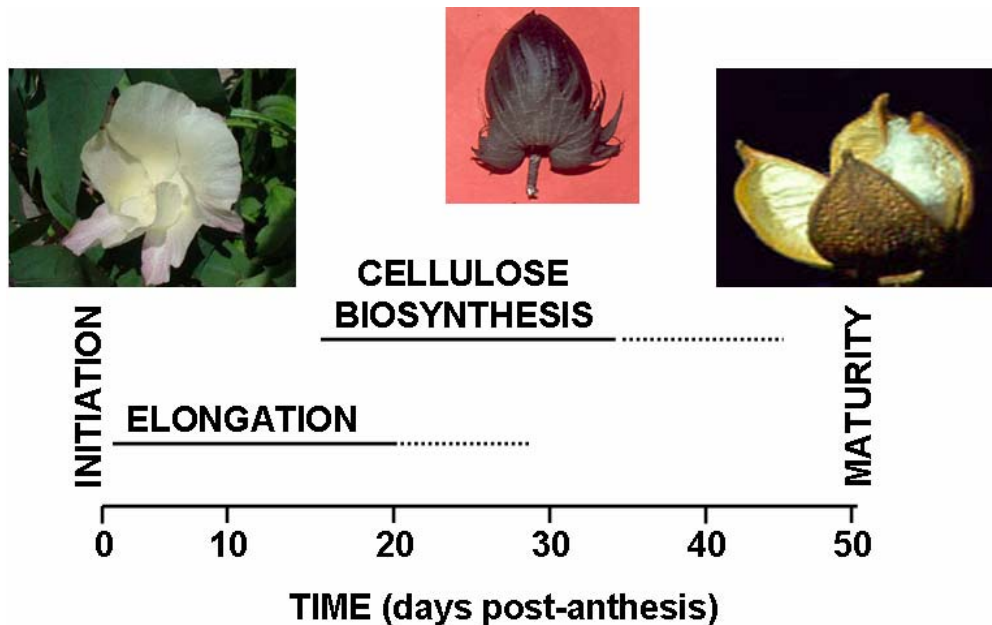


Figure 1-1. Stages of cotton fiber development. Cotton fibers pass through four stages of development: initiation, elongation, cellulose biosynthesis, and maturity. The area of overlap between elongation and cellulose biosynthesis is the transition period.

Initiation, the first stage of fiber development, involves the initial expansion of the epidermal cell above the surface of the ovule [Basra and Malik, 1984; DeLanghe, 1986]. The cotton flower blooms for only one day. Initiation is conveniently timed beginning on or near the day of anthesis (day of flowering) and lasts only a day or so for each fiber initial (Figure 1-1) [Basra and Malik, 1984]. Fiber initiation first appears at the chalazal part of the ovule and continues progressively toward the micropylar end [DeLanghe, 1986]. Initiated fibers immediately enter Stage 2 or fiber elongation (Figure 1-1) [Basra and Malik, 1984]. The elongation phase of cotton fiber development encompasses the major growth phase of the fiber [Basra and Malik, 1984]. Fibers initiating development on the day of anthesis (DOA) are destined to become lint fibers;

fibers that start to elongate beginning around the fourth to seventh day after anthesis are destined to become fuzz fibers [Basra and Saha, 1999]. Fiber growth occurs by a combination of tip growth and an intercalation of materials throughout the fiber length (diffuse growth) [Seagull, 1990]. In tip growth, post-Golgi vesicles are targeted and fused to the plasma membrane, resulting in unidirectional expansion of the cell membrane and cell wall. Diffuse growth is driven by turgor pressure with new cell wall materials deposited throughout the cell surface [Seagull, 1990]. The elongation stage of cotton fiber development continues from the day of anthesis to approximately 21 to 26 days post anthesis (DPA) (Figure 1-1) [Basra and Malik, 1984]. The third stage of cotton fiber development is the cellulose biosynthesis stage or the secondary cell wall deposition stage (Figure 1-1). Secondary cell wall synthesis begins slightly before the cessation of fiber elongation (16 to 18 DPA) [Basra and Malik, 1984; Delmer, 1999]. During the cellulose biosynthesis stage, the β -1,4-glucan chains that form the cellulose microfibrils of the secondary cell wall are synthesized [Basra and Malik, 1984; Delmer, 1999]. Successive layers of cellulose are deposited until the wall is 3 to 4 μm thick [Basra and Malik, 1984; Delmer, 1999]. At approximately 45 to 60 DPA, the fibers enter into the last stage of development, maturation (Figure 1-1) [Basra and Malik, 1984]. Maturation occurs concomitantly with boll opening and results from drying of the hydrated living fiber to a dried metabolically inactive fiber [Basra and Malik, 1984]. This is in contrast to the first three stages that occur while the fiber is alive and actively growing. During maturation, the seed capsule dehisces and the thin fiber cells quickly dehydrate [Basra and Malik, 1984]. As the cytoplasm dries, the cytoplasm adheres to the innermost layer of the fiber cell wall leaving a lumen where the central vacuole was once located [Basra and Malik, 1984].

Several near-isogenic mutants in cotton are impaired in fiber development. Each of these naturally occurring mutants has been repeatedly backcrossed into *Gossypium hirsutum*, Texas Marker 1 (TM1), a long-term inbred and the genetic standard line for cotton genetic studies (Figure 1-2) [Kohel et al., 1970].

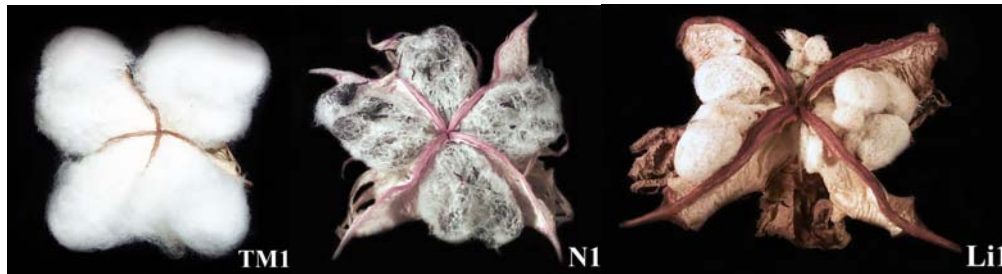


Figure 1-2. Mature *Gossypium hirsutum* bolls. TM1, wild type Texas Marker 1. N1, Naked Seed mutant. Li1, Ligon lintless mutant.

One mutant, known as Naked Seed (N1), is impaired in fiber initiation. N1 is a dominant mutation; N1 mutants are characterized by a small tuft of lint fiber at the chalazal end of the seed and fuzz fibers are completely absent (Figure 1-2) [Endrizzi et al., 1984]. A second mutant, Ligon lintless (Li1) is impaired in fiber elongation. Li1 is a dominant mutation; Li1 mutants are characterized by very short fiber (~6 mm long) and distorted (epinastic) plant growth in the leaves, stem and flower (Figure 1-2) [Kohel, 1974].

The desire to improve fiber productivity and quality is inherent to the culture of cotton; the challenge is to develop new varieties with both high quality and high productivity [Kohel, 1999]. New strategies are necessary to increase cotton fiber yield without sacrificing quality [Kim and Triplett, 2001] and must include biotechnological approaches. In order to achieve this long-term goal, the genes responsible for regulating the development of lint fiber must be identified and their roles characterized [Kim and Triplett, 2001]. Our research group has previously characterized cotton fiber guanosine triphosphate-binding proteins or G-proteins as

potentially important regulators of fiber development [Kim et al., 2000; Kim and Triplett, 2004a]. G-proteins are a subset of guanosine triphosphatases (GTPases) ubiquitously found in eukaryotes from yeast to humans. G-proteins act as pivotal molecular switches involved in eukaryotic signal transduction, though the entire signal transduction process has yet to be fully elucidated [for reviews see Bischoff et al., 1999; Takai et al., 2001; Yang, 2002; Vernoud et al., 2003; Gu et al., 2004]. G-proteins cycle between an active guanosine triphosphate (GTP) -bound or “on” state and an inactive guanosine diphosphate (GDP) -bound or “off” state, ensuring the flow of information at the expense of GTP [Bischoff et al., 1999; Takai et al., 2001; Yang, 2002; Gu et al., 2004]. Currently, two distinct classes of G-proteins are known: heterotrimeric G-proteins and monomeric G-proteins [Bischoff et al., 1999; Takai et al., 2001; Jones and Assmann, 2004].

III. Heterotrimeric G-proteins in animals and plants

Heterotrimeric G-proteins mediate a vast array of signaling processes in eukaryotes, including ion channel regulation, cell proliferation, hormone regulation, and light signaling [for reviews see Bischoff et al., 1999; Fujisawa et al., 2001; Jones and Assmann, 2004]. Heterotrimeric G-proteins are GTPase mediators that transmit external signals (i.e. light) via a plasma membrane G-protein-coupled receptor (GPCR) [Fujisawa et al., 2001; Jones and Assmann, 2004]. Heterotrimeric G-proteins consist of three different polypeptide subunits: alpha ($G\alpha$), beta ($G\beta$), and gamma ($G\gamma$) [Bischoff et al., 1999; Fujisawa et al., 2001; Jones and Assmann, 2004]. The $G\alpha$ domain is the regulatory domain for GDP-GTP exchange in heterotrimeric G-proteins; the $G\alpha$ subunit has a GDP/GTP-nucleotide-binding site and GTP-hydrolase activity [Bischoff et al., 1999; Fujisawa et al., 2001; Jones and Assmann, 2004]. In the inactive state, GDP is bound to an active site on the $G\alpha$ subunit [Bischoff et al., 1999; Fujisawa

et al., 2001; Jones and Assmann, 2004]. When an extracellular signal binds to the appropriate GPCR, GDP is released from the active site on the $G\alpha$ subunit [Fujisawa et al., 2001; Jones and Assmann, 2004]. Because the intrinsic cytoplasmic concentration of GTP is higher than GDP, GTP binding is favored [Bischoff et al., 1999; Fujisawa et al., 2001; Jones and Assmann, 2004]. Once GTP binds, the $G\alpha$ subunit resumes an activated conformation and dissociates from the $G\alpha\beta\gamma$ trimer complex [Bischoff et al., 1999; Fujisawa et al., 2001; Jones and Assmann, 2004]. The separated $G\alpha$ and/or $G\beta\gamma$ subunits transiently interact with the appropriate target proteins [Jones and Assmann, 2004]. The intrinsic hydrolase activity of the $G\alpha$ subunit eventually results in GTP hydrolysis, and the $G\alpha$ subunit re-associates with a $G\beta\gamma$ dimer [Bischoff et al., 1999; Fujisawa et al., 2001; Jones and Assmann, 2004].

In plants, heterotrimeric G-protein signaling has been implicated in an array of plant signal transduction pathways, including hormone signaling [Ullah et al., 2003; Pandey and Assmann, 2004], pathogen responses [Suharsono et al., 2002], ion channel regulation [Wang et al., 2001], seed germination [Ullah et al., 2002], and cell proliferation [Ullah et al., 2001]. To date, it appears that plants possess few heterotrimeric G-protein subunit genes, compared to animals. Only one heterotrimeric G-protein α subunit gene, *GPA1* (GenBank (GB) mRNA ID [M32887](#)) [Ma et al., 1990] and one heterotrimeric G-protein β subunit gene, *AGB1* (GB mRNA ID [U12232](#)) [Weiss et al., 1994] have been identified in *Arabidopsis thaliana*. Two putative heterotrimeric G-protein γ subunit genes, *AGG1* (GB mRNA ID [AF283673](#)) [Mason and Botella, 2000] and *AGG2* (GB mRNA ID [AF347077](#)) [Mason and Botella, 2001] have been identified in *Arabidopsis thaliana*. Finally, only one G-protein-coupled receptor gene similar to an animal G-protein-coupled receptor, *GCRI* (GB mRNA ID [U95143](#)) has been identified in *Arabidopsis* [Josefsson and Rask, 1997; Plakidou-Dymock et al., 1998]. In addition, sequences released very

recently by the TIGR database [http://www.tigr.org/tigr-scripts/tgi/T_index.cgi?species=cotton] revealed one tentative consensus (TC) sequence for a putative heterotrimeric G-protein α -like subunit ([TC28475](#)) derived from various expressed sequence tags (EST) clones from *Gossypium arboreum* [Wing et al., unpublished] and *Gossypium raimondii* [Kim et al., unpublished]. At present, no heterotrimeric G-protein α -subunit ESTs have been identified from *Gossypium hirsutum*. Four TC sequences for a putative heterotrimeric G-protein β -like subunit ([TC27639](#), [TC32268](#), [TC32269](#), [TC32270](#)) have been assembled from various EST clones from *Gossypium arboreum* [Wing et al., unpublished], *Gossypium hirsutum* [Blewitt et al., unpublished], and *Gossypium raimondii* [Kim et al., unpublished]. One TC sequence for a putative GPCR ([TC36932](#)) has been assembled from two *Gossypium raimondii* EST clones [Kim et al., unpublished]. In addition, one EST clone similar to a GPCR (GB mRNA ID [AI728327](#)) has been identified in *Gossypium hirsutum* [Blewitt et al., unpublished]. At present, heterotrimeric G-protein γ subunit ESTs have not been identified in *Gossypium arboreum*, *Gossypium hirsutum*, or *Gossypium raimondii*.

IV. Monomeric G-proteins in animals

The second class of signaling G-proteins are monomeric G-proteins [for reviews see Mackay and Hall, 1998; Bischoff et al., 1999; Takai et al., 2001]. In contrast to heterotrimeric G-proteins, monomeric G-proteins are small, single subunit proteins with molecular masses of 20-40 kDa [Bischoff et al., 1999; Takai et al., 2001]. Like heterotrimeric G-proteins, the activity of monomeric G-proteins depends on their association with GTP or GDP [Bischoff et al., 1999]. The active GTP-bound form activates downstream target molecules and signaling pathways, but an intrinsic GTPase activity hydrolyses GTP to GDP, inactivating the G-protein [Bischoff et al., 1999; Takai et al., 2001]. In contrast to heterotrimeric G-proteins, monomeric G-proteins are

controlled by three classes of regulatory proteins in animal cells: guanine nucleotide exchange factor (GEF), GTPase activating protein (GAP), and guanine nucleotide dissociating inhibitor (GDI) [Boguski and McCormick, 1993; Takai et al., 2001]. In response to different cellular conditions, GEF, GAP, and GDI proteins maintain the equilibrium between the active GTP-bound form and inactive GDP-bound form of monomeric G-proteins [Boguski and McCormick, 1993].

A series of reactions, constituting the GTPase switch, appears to be conserved in eukaryotes (Figure 1-3) [for review see Boguski and McCormick, 1993; Bischoff et al., 1999; Takai et al., 2001].

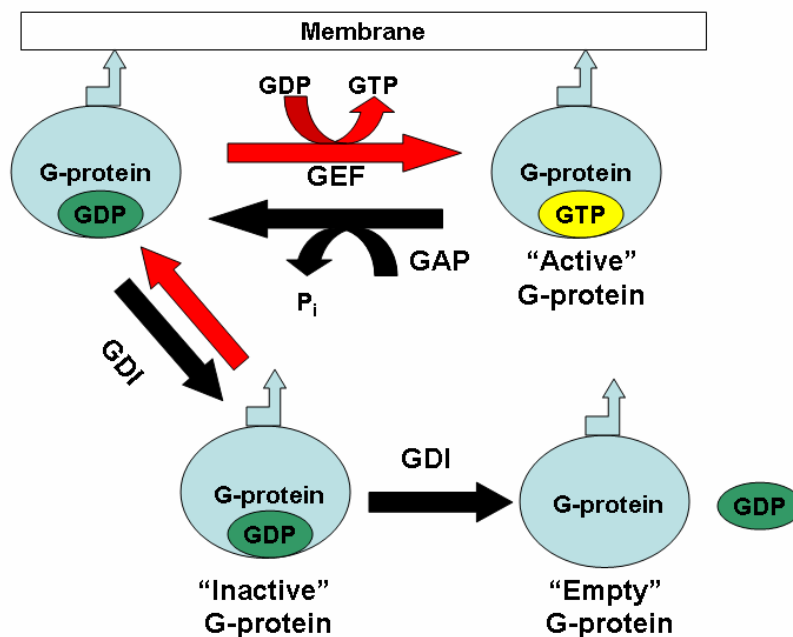


Figure 1-3. A general scheme for the regulation of monomeric G-proteins in plants and animals. Figure adapted from Yang (2002). GAP (GTPase-activating protein), GDI (guanine nucleotide dissociating inhibitor), GEF (guanine nucleotide exchange factor). Bent arrowhead indicates a lipid moiety that becomes attached to membranes. The red arrow indicates activation of the monomeric G-protein. The black arrow indicates inactivation of the monomeric G-protein.

GDI, an inhibitor of GAP, is postulated to shuttle GDP-bound inactive cytosolic monomeric G-proteins, except *Ras* and *Ran* G-proteins to the plasma membrane (Figure 1-3) [Boguski and

McCormick, 1993; Bischoff et al., 1999; Takai et al., 2001]. Membrane localization is achieved through a post-translational lipid modification of the G-protein at the C-terminus [Boguski and McCormick, 1993; Takai et al., 2001]. Upon stimulation by an upstream signal, GEF converts the GDP-bound inactive G-protein into the GTP-bound active form through GDP/GTP replacement (Figure 1-3) [Boguski and McCormick, 1993; Takai et al., 2001]. In order to be activated by GEF, the GDP-bound G-protein must be membrane-bound [Boguski and McCormick, 1993; Takai et al., 2001]. Through the effector domain, the GTP-bound active G-protein can interact with other proteins to perform a myriad of functions [Bischoff et al., 1999; Takai et al., 2001]. The GTP-bound form of the enzyme exhibits a weak intrinsic activity for GTP hydrolysis [Boguski and McCormick, 1993; Takai et al., 2001]. GAPs promote the intrinsic GTP hydrolyzing activity, leading to the rapid conversion of the active monomeric G-protein to the inactive GDP-bound form (Figure 1-3) [Boguski and McCormick, 1993; Takai et al., 2001]. Then, GDI binds to the inactive GDP-bound G-protein and releases the G-protein from the membrane (Figure 1-3) [Boguski and McCormick, 1993; Takai et al., 2001]. GDI subsequently dissociates GDP from the guanine nucleotide-binding site leaving the G-protein “empty” (Figure 1-3) [Boguski and McCormick, 1993]. This complex series of reactions ensures the flow of information at the expense of guanosine triphosphate. The irreversibility of GTP hydrolysis makes the cycle unidirectional [Boguski and McCormick, 1993].

Animal monomeric G-proteins belong a gene superfamily and are structurally divided into at least five distinct families: *Arf*, *Rab*, *Ran*, *Ras*, and *Rho* (Figure 1-4) [for reviews see Bischoff et al., 1999; Takai et al., 2001].

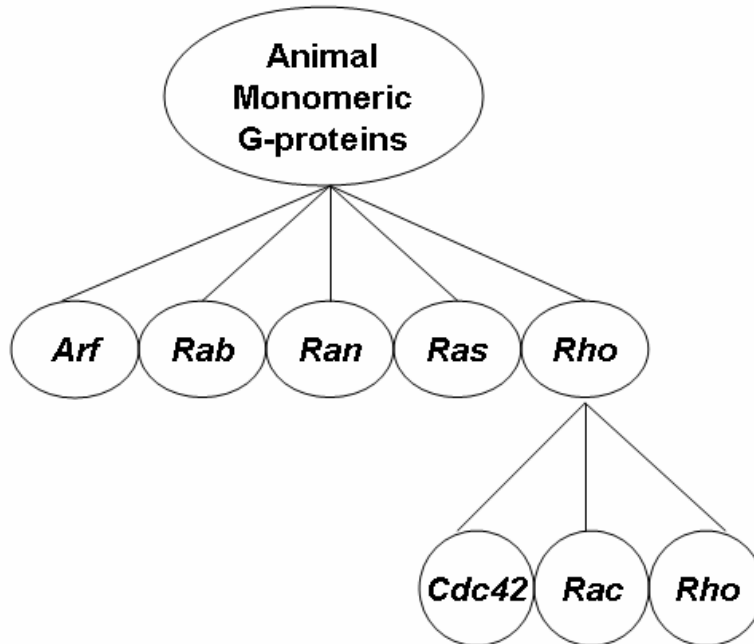


Figure 1-4. Animal monomeric G-protein superfamily. Animal monomeric G-proteins are structurally divided into 5 distinct families: *Arf* (adenosine diphosphate-ribosylation factor), *Rab* (*ras* gene from rat brain), *Ran* (*ras*-related nuclear), *Ras* (rat sarcoma), and *Rho* (*ras* homology). The *Rho* family of monomeric G-proteins is divided into 3 distinct subfamilies: *Cdc42* (cell division cycle), *Rac* (*ras*-related C3 botulinum toxin substrate), and *Rho* (*ras* homology).

Monomeric G-proteins have two domains responsible for GTPase activity and two domains for guanine nucleotide binding [Takai et al., 2001]. Moreover, monomeric G-proteins have an effector domain for interacting and binding with downstream proteins [Bischoff et al., 1999; Takai et al., 2001]. In addition, the *Ras*, *Rab*, and *Rho* families have a membrane localization domain at their C-termini. *Ras*, *Rab*, and *Rho* G-proteins are post-translationally modified with lipid for plasma membrane binding [Bischoff et al., 1999; Takai et al., 2001]. The *Arf* G-proteins are post-translationally modified at the N-terminus with a myristate fatty acid for plasma membrane binding [Bischoff et al., 1999; Takai et al., 2001]. The *Rho* family of monomeric G-proteins contains a variable domain or an insert region that is responsible for interacting with effector molecules [Mackay and Hall, 1998; Bischoff et al., 1999; Takai et al., 2001].

Adenosine diphosphate (ADP) -ribosylation factors (*Arfs*) were initially identified due to their ability to stimulate the ADP-ribosyltransferase activity of cholera toxin A [Kahn and Gilman, 1986]. *Arf* G-proteins function in vesicular trafficking pathways as regulators of vesicle transport between the endoplasmic reticulum and the Golgi network [for reviews see Bischoff et al., 1999; Takai et al., 2001; Vernoud et al., 2003; Memon, 2004; Molendijk et al., 2004].

Rab (*ras* gene from rat brain) G-proteins organize intracellular membrane trafficking during three consecutive stages of transport: vesicle formation, vesicle motility, and the tethering of vesicles to target compartments preceding membrane-fusion events [for reviews see Bischoff et al., 1999; Takai et al., 2001; Vernoud et al., 2003; Molendijk et al., 2004].

Ran (*ras*-related nuclear) G-proteins cycle between GDP- and GTP-bound states, like other monomeric G-proteins, but GTP binding and hydrolysis is linked to transport into or out of the nucleus. *Ran* G-proteins function in nucleocytoplasmic transport and microtubule organization [for reviews see Bischoff et al., 1999; Takai et al., 2001; Vernoud et al., 2003]. Unlike other small monomeric G-proteins, *Ran* G-proteins are not post-translationally modified with lipid and do not associate with cellular plasma membranes.

Ras (rat sarcoma) G-proteins regulate cell proliferation in yeast and mammalian systems. *Ras* G-proteins are essential for cell viability, cell differentiation, cell morphology, and apoptosis [for reviews see Bischoff et al., 1999; Takai et al., 2001; Vernoud et al., 2003]. An interesting characteristic of *Ras* G-proteins is that *Ras* genes and/or mutations in *Ras* regulator genes have been implicated in over 30% of human carcinomas [for reviews see Drivas et al., 1990; Campbell and Der, 2004]. *Rho* (*ras* homology) G-proteins control key cellular processes such as cell proliferation, apoptosis, lipid metabolism, adhesion, migration, cell polarity, and

transcriptional regulation [for reviews see Mackay and Hall, 1998; Bischoff et al., 1999; Takai et al., 2001; Vernoud et al., 2003; BurrIDGE and Wennerberg, 2004].

The *Rho* family of monomeric G-proteins is structurally divided into at least three subfamilies in animals: *Rho*, *Rac*, and *Cdc42* (Figure 1-4) [for reviews see Bischoff et al., 1999; Takai et al., 2001; Vernoud et al., 2003]. In mammalian fibroblasts, the *Rac* (*ras*-related C3 botulinum toxin substrate) subfamily of *Rho* G-proteins regulates growth factor-induced membrane ruffling [Ridley et al., 1992; BurrIDGE and Wennerberg, 2004]. *Rac* G-proteins are also involved in signal transduction pathways involving stress fiber formation [Ridley et al., 1992; BurrIDGE and Wennerberg, 2004]. In addition, *Rac* G-proteins control the production of reactive oxygen species by directly associating with and regulating the activity of plasma membrane-associated nicotinamide adenine dinucleotide phosphate oxidase complexes resulting in oxidative bursts [Heyworth et al., 1993; Hassanain et al., 2000]. In yeast and mammals, the *Rho* G-proteins play a key role in the control of microfilament organization; *Rho* G-proteins are crucial components of signal transduction pathways mediated by the actin cytoskeleton such as establishing cell polarity and influencing cell morphogenesis [Ridley and Hall, 1992; BurrIDGE and Wennerberg, 2004]. In yeast and mammals, *Cdc42* (cell division cycle) G-proteins are involved in regulating cell polarity and cell morphogenesis [for a review see Etienne-Manneville, 2004].

V. Monomeric G-proteins in plants

Numerous *Rab*, *Arf*, *Ran*, and *Rho*-related G-protein orthologs have been identified in many plants species, including *Gossypium hirsutum*, but to date, no *Ras* orthologs have been identified in plants (Figure 1-5).

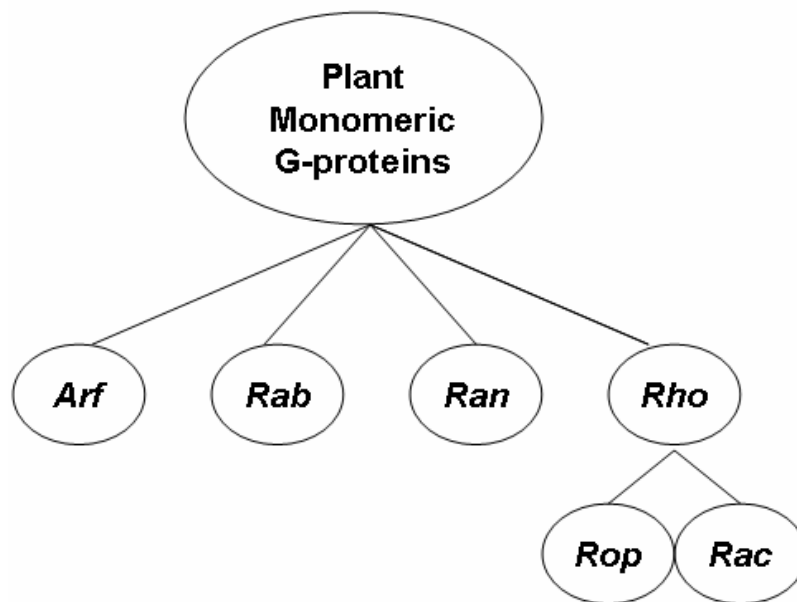


Figure 1-5. Plant monomeric G-protein superfamily. Plant monomeric G-proteins are divided into four structurally distinct families: *Arf* (adenosine diphosphate-ribosylation factor), *Rab* (*ras* gene from rat brain), *Ran* (*ras*-related nuclear), and *Rho* (*ras* homology). At present, *Ras* (rat sarcoma) G-proteins have not been identified *in planta*. The *Rho* family is comprised of a monomeric G-protein subfamily exclusive to plants, *Rop* (*rho*-related GTPase from plant). Even though *Rac* G-protein orthologs have not been identified in plants, both terms *Rop* and *Rac* are used in literature to identify the same type of plant G-protein.

The monomeric G-protein orthologs identified in plants, so far, are assumed to regulate the same biological processes: membrane trafficking, cytoskeletal assembly, vesicle fusion, vesicle budding, nuclear transport, and gene expression [for reviews see Bischoff et al., 1999; Vernoud et al., 2003]. To date, no *Rho*, *Rac*, or *Cdc42* orthologs have been identified in plants. Instead, plants seem to possess a novel and unique group of G-proteins, termed *Rop* (*rho*-related GTPase from plants, Figure 1-5) [Bischoff et al., 1999; Yang, 2002; Vernoud et al., 2003; Gu et al., 2004]. *Rho1P* (GB mRNA ID [L19093](#)) from the garden pea was the first plant monomeric G-protein to be cloned and characterized [Yang and Watson, 1993]. Yang and Watson (1993) demonstrated that *Rho1P* encoded an active GTP-binding-protein and that the *Rho1P* transcript was expressed in all organs of pea seedlings and was quite abundantly expressed in root tips. Since 1993, numerous G-proteins unique to plants have been cloned and characterized [Yang and

Watson, 1993; Delmer et al., 1995; Winge et al., 1997; Kawasaki et al., 1999; *Arabidopsis* Genome Initiative, 2000; Kim et al., 2000; Morel et al., 2004]. Phylogenetic analyses of human *Rho*, *Rac*, and *Cdc42* G-proteins, yeast *Rho* and *Cdc42* G-proteins, and *Arabidopsis thaliana* *Rho*-related G-proteins suggest that the plant *Rho*-related G-proteins belong to a distinct subfamily (Figure 1-6) [Zheng and Yang, 2000b].

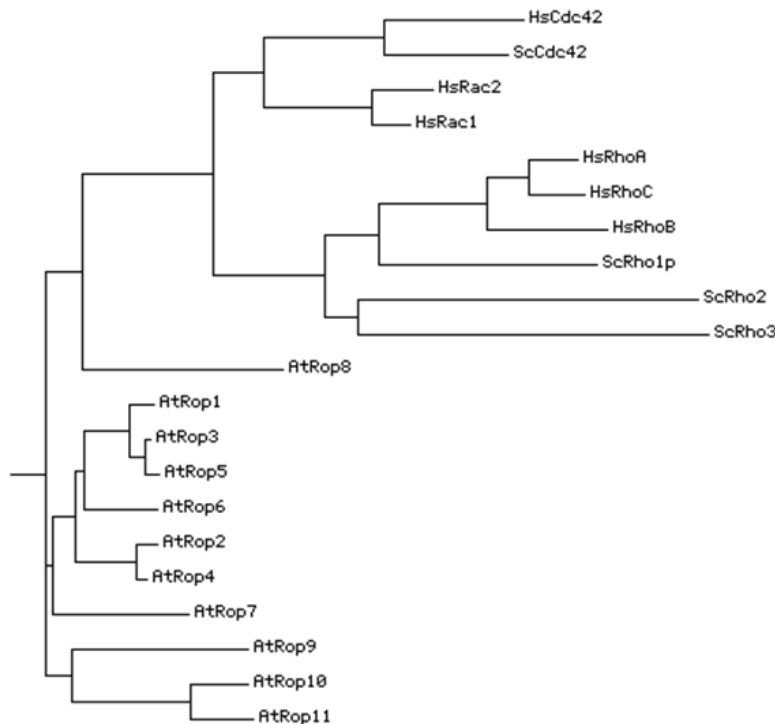


Figure 1-6. Phylogenetic analysis of the *Rho* family of monomeric G-proteins. Figure adapted from Zheng and Yang (2000b). The phylogenetic tree file was obtained from amino acids aligned with CLUSTAL W [Thompson et al., 1994]. A web-based program, Phylo dendron Phylogenetic tree printer, created the phenogram [Gilbert, 1997]. HsRhoA (*Homo sapiens*, GB protein ID [NP001655](#)); HsRhoB (GB protein ID [AAH66954](#)); HsRhoC (GB protein ID [AAH52808](#)); HsCdc42 (GB protein ID [P60953](#)); HsRac1 (GB protein ID [P15154](#)); HsRac2 (GB protein ID [P15153](#)); ScRho1p (*Saccharomyces cerevisiae*, GB protein ID [NP015491](#)); ScRho2 (GB protein ID [P06781](#)); ScRho3 (GB protein ID [Q00245](#)); ScCdc42 (GB protein ID [NP013330](#)); AtRop1 (*Arabidopsis thaliana*, GB protein ID [NP190698](#)); AtRop2 (GB protein ID [NP173437](#)); AtRop3 (GB protein ID [AAF40237](#)); AtRop4 (GB protein ID [NP177712](#)); AtRop5 (GB protein ID [NP195320](#)); AtRop6 (GB protein ID [NP195228](#)); AtRop7 (GB protein ID [NP199409](#)); AtRop8 (GB protein ID [NP566024](#)); AtRop9 (GB protein ID [NP194624](#)); AtRop10 (GB protein ID [NP566897](#)); AtRop11 (GB protein ID [NP201093](#)).

Based on amino acid sequence similarities with human *Rac* G-proteins, plant *Rho*-related G-proteins are termed *Rac* G-proteins in some literature [Yang and Watson, 1993; Delmer et al., 1995; Tranin et al., 1996; Winge et al., 1997; Kawasaki et al., 1999; Kost et al., 1999; Potikha et al., 1999; Hassanain et al., 2000; Kim et al., 2000; Winge et al., 2000; Lemichez et al., 2001; Lavy et al., 2002; Tao et al., 2002; Kim and Triplett, 2004a; Morel et al., 2004]. Due to amino acid differences between plant *Rho*-related G-proteins, fungal *Rho* and *Cdc42* G-proteins, and animal *Rho*, *Rac*, and *Cdc42* G-proteins, it has been suggested to rename the plant *Rho*-related G-proteins *Rop* (*rho*-related GTPase from plant) G-proteins [Zheng and Yang, 2000b; Yang, 2002; Vernoud et al., 2003]. Both terms *Rac* and *Rop* are currently used in the literature to identify the same type of plant monomeric G-protein. For clarity and consistency in this thesis, plant monomeric G-proteins will be called *Rop/Rac* G-proteins. Since the *Rop/Rac* G-protein genes identified from *Arabidopsis thaliana* have been renamed *Rop*, *Arabidopsis thaliana* *Rop/Rac* G-protein genes will be called *AtRop* throughout this thesis. *Rac* is still used in literature to identify *Gossypium hirsutum* G-protein genes; cotton *Rop/Rac* G-protein genes will be referred to as *GhRac* throughout this thesis.

Full-length *Rop/Rac* G-proteins contain four conserved domains, two for guanine nucleotide binding and two for GTPase activity, that have been found in all the monomeric G-proteins identified, so far [Winge et al., 2000; Zheng and Yang, 2000b; Yang, 2002]. A fifth conserved domain is an effector domain, the domain for binding target proteins [Winge et al., 2000; Zheng and Yang, 2000b; Yang, 2002]. In addition, full-length *Rop/Rac* G-proteins possess a variable domain termed the *Rho* insert region that functions in target protein recognition and binding. The insert region is unique to the *Rho* family of monomeric G-proteins

[Mackay and Hall, 1998; Winge et al., 2000; Zheng and Yang, 2000b; Yang 2002]. *Rop/Rac* G-proteins also have a post-translational lipid modified C-terminal motif for plasma membrane binding [Zheng and Yang, 2000b; Yang, 2002].

Rop/Rac G-proteins undergo one of two types of post-translational lipid modification that may be necessary for interaction with effector proteins or for relocation from the cytoplasm to cellular membranes [Takai et al., 2001; Yang 2002]. One form of lipid modification of *Rop/Rac* G-proteins is prenylation. Prenylation is the addition of a 15 carbon (farnesyl) or a 20 carbon (geranylgeranyl) group to a CAAX or CAAL motif (C= cysteine, A= an aliphatic amino acid, X= any amino acid except leucine, L= leucine) at the C-terminus of *Rop/Rac* G-proteins [Yalvosky et al., 1999; Zheng and Yang 2000b; Yang 2002]. Prenylated *Rop/Rac* G-proteins can localize to nuclei, the cytoplasm, or plasma membrane [Molendijk et al., 2001; Lavy et al., 2002]. Eight of the *Arabidopsis thaliana* *Rop/Rac* G-proteins (*AtRop1-AtRop8*) and the three *Gossypium hirsutum* *Rop/Rac* G-proteins (*GhRac1*, *GhRac9*, and *GhRac13*) terminate with a CAAL motif specifying prenylation [Delmer et al., 1995; Tranin et al., 1996; Winge et al., 2000; Kim and Triplett, 2004a]. Prenylated *Rop/Rac* G-proteins have been implicated in regulating polar cell division and elongation [Li et al., 1999; Fu et al., 2001; Fu et al., 2002, Molendijk et al., 2001; Jones et al., 2002]. The second form of post-translational lipid modification of *Rop/Rac* G-proteins is prenylation independent, requiring palmitoylation. Palmitoylation is the reversible attachment of 16-carbon palmitate molecule to one or multiple cysteine residues by a reversible thioester bond [Lavy et al., 2002]. Three of the *Arabidopsis* *Rop/Rac* G-proteins, *AtRop9-AtRop11*, are palmitoylated [Lavy et al., 2002]. *AtRop9* and *AtRop11* are palmitoylated multiple times. *AtRop10* is palmitoylated once [Lavy et al., 2002]. The palmitoylated *Rop/Rac* G-proteins are targeted to the plasma membrane [Lavy et al., 2002] and have been implicated in

regulating plant hormone responses and stress responses [Kawasaki et al., 1999; Zheng et al., 2002]. In addition, unlike the prenylated *Rop/Rac* G-proteins, *in vitro* assays suggest that palmitoylated *Rop/Rac* G-proteins do not interact with the regulator protein GDI [Lavy et al., 2002].

At present, the *Rop/Rac* signal transduction pathway is poorly characterized in plants. Presumably, the complex series of reactions constituting the GTPase switch as described for animal cells also regulates *Rop/Rac* G-protein activity (Figure 1-3) [Yang, 2002; Gu et al., 2004]. *Rop/Rac* GTPase activating-proteins [Wu et al., 2000] and *Rop/Rac* guanine nucleotide disassociation inhibitor proteins [Bischoff et al., 2000] have been identified in *Arabidopsis thaliana* and many other plant species. Recently, a gene orthologous to a human guanine nucleotide exchange factor has been identified in *Arabidopsis thaliana* and is postulated to be a putative *Rop/Rac* guanine nucleotide exchange factor [Qiu et al., 2002]. A recent survey of the TIGR database [http://www.tigr.org/tigr-scripts/tgi/T_index.cgi?species=cotton] has revealed five cotton *Rop/Rac* GAP putative TC sequences. The TCs were derived from *Gossypium arboreum* ESTs ([TC35528](#)) [Wing et al., unpublished] and *Gossypium raimondii* ESTs ([TC28980](#), [TC28981](#), [TC30195](#), [TC31609](#)) [Kim et al., unpublished]. At present, putative *Rop/Rac* GAP ESTs have not been identified in *Gossypium hirsutum*. Three TC sequences weakly similar to a guanine nucleotide exchange-like protein have been assembled from *Gossypium raimondii* ESTs ([TC31563](#), [TC39393](#), [TC40595](#)) [Kim et al., unpublished]. In addition, two ESTs weakly similar to a guanine nucleotide exchange protein have been identified in *Gossypium hirsutum* (GB mRNA ID [A1731844](#), [AW187291](#)) [Blewitt et al., unpublished] and *Gossypium arboreum* (GB mRNA ID [BE053450](#)) [Wing et al., unpublished]. At present,

Rop/Rac GDI ESTs have not been identified in *Gossypium arboreum*, *Gossypium raimondii*, or *Gossypium hirsutum*.

In addition, sequences released very recently by the TIGR database revealed six tentative consensus sequences for putative *Rop/Rac* G-proteins assembled from various expressed sequence tag clones from *Gossypium arboreum* [Wing et al., unpublished], *Gossypium raimondii* [Kim et al., unpublished], and *Gossypium hirsutum* [Blewitt et al., unpublished]. [TC28011](#) is similar to *Lotus japonicus* mRNA sequence *Rac1* (GB mRNA ID [Z73961](#)). [TC29458](#) is similar to *Arabidopsis thaliana* mRNA *AtRop9* (GB mRNA ID [NM_119039](#)). [TC30900](#) is similar to *Nicotiana tabacum* mRNA *Rac4* (GB mRNA ID [AJ496228](#)). [TC32824](#) and [TC32825](#) are similar to *Gossypium hirsutum* mRNA sequence *GhRac1* (GB mRNA ID [AF165925](#)). [TC38099](#) is similar to *Oryza sativa* (rice) mRNA sequence *OsRac3* (GB mRNA ID [XM467730](#)) [Blewitt et al., unpublished; Wing et al., unpublished; Kim et al., unpublished].

Gain-of-function studies, involving constitutively active (CA - GTP permanently bound) and dominant negative (DN - GDP permanently bound) *Rop/Rac* mutants, loss-of-function studies involving knockouts, and overexpression studies have been used to investigate the physiological roles of *Rop/Rac* G-proteins in many plant species [Yang, 2002]. Collectively, these experiments suggest a pivotal role for *Rop/Rac* signaling in many plant processes, including stress responses [Baxter-Burrell et al., 2002; Suharsono et al., 2002; Park et al., 2004], defense responses [Kawasaki et al., 1999; Hassanain et al., 2000; Agrawal et al., 2003; Morel et al., 2004], hormone responses [Lemichez et al., 2001; Li et al., 2001; Tao et al., 2002; Zheng et al., 2002], secondary cell wall differentiation [Potikha et al., 1999], pollen tube growth [Lin and Yang, 1997; Li et al., 1998; Kost et al., 1999; Li et al., 1999], root hair initiation [Molendijk et

al., 2001; Jones et al., 2002], and actin cytoskeleton organization [Fu et al., 2001; Fu et al., 2002; Jones et al., 2002; Chen et al., 2003; Gu et al., 2003; Kim and Triplett, 2004a].

Phylogenetic analyses suggest that *Rop/Rac* G-proteins are divided into at least four subfamilies based on their amino acid sequence (Figure 1-7) [Winge et al., 1997; Zheng and Yang, 2000b; Yang, 2002; Vernoud et al, 2003].

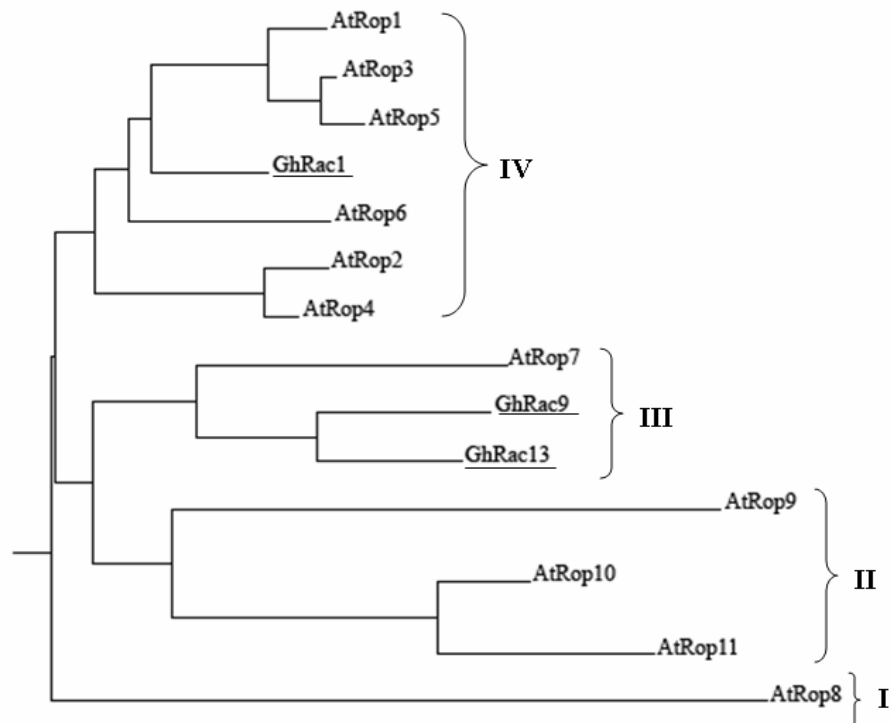


Figure 1-7. Phylogenetic analysis of the *Rop/Rac* G-protein subfamilies from *Arabidopsis thaliana* and *Gossypium hirsutum*. The phylogenetic tree file was obtained from amino acids aligned with CLUSTAL W [Thompson et al., 1994]. A web-based program, Phylodendron Phylogenetic tree printer, created the phenogram [Gilbert, 1997]. The *Rop/Rac* G-proteins are divided into at least four distinct subfamilies and designated with the Roman numerals I through IV. The *Gossypium hirsutum* *Rop/Rac* G-proteins are underlined. AtRop1 (*Arabidopsis thaliana*, GB protein ID [NP190698](#)); AtRop2 (GB protein ID [NP173437](#)); AtRop3 (GB protein ID [AAF40237](#)); AtRop4 (GB protein ID [NP177712](#)); AtRop5 (GB protein ID [NP195320](#)); AtRop6 (GB protein ID [NP195228](#)); AtRop7 (GB protein ID [NP199409](#)); AtRop8 (GB protein ID [NP566024](#)); AtRop9 (GB protein ID [NP194624](#)); AtRop10 (GB protein ID [NP566897](#)); AtRop11 (GB protein ID [NP201093](#)); GhRac1 (*Gossypium hirsutum*, GB protein ID [AAD47828](#)), GhRac9 (GB protein ID [Q41254](#)), GhRac13 (GB protein ID [Q41253](#)).

The function of the subfamily I *Rop/Rac* G-proteins is unknown, at present. *AtRop8* (GB mRNA ID [NM130033](#)) from *Arabidopsis* is a subfamily I *Rop/Rac* G-protein. Although Li and colleagues (1998) demonstrated that *AtRop8* is expressed in pollen tubes, the function of *AtRop8* is still undetermined [Gu et al., 2004]. Prior to beginning this research project, no members of the subfamily I class of *Rop/Rac* genes in *Gossypium hirsutum* had been cloned or characterized (Figure 1-7).

Subfamily II contains three *Rop/Rac* G-proteins from *Arabidopsis*, *AtRop9* (GB mRNA ID [NM119039](#)), *AtRop10* (GB mRNA ID [NM114673](#)), and *AtRop11* (GB mRNA ID [NM125682](#)) (Figure 1-7). Subfamily II *Arabidopsis* *Rop/Rac* G-proteins are hypothesized to be involved in stress responses and hormone responses [for reviews see Yang, 2002; Vernoud et al., 2003; Gu et al., 2004]. The CA form of *OsRac1* (GB mRNA ID [AB029508](#)), a subfamily II *Rop/Rac* G-protein from *Oryza sativa* (rice), induces H₂O₂ production and cell death in transgenic rice and the DN form of *OsRac1* inhibits H₂O₂ production and cell death in transgenic rice [Kawasaki et al., 1999]. Two other subfamily II *Rop/Rac* G-proteins (*AtRop9* and *AtRop10*) act as general negative regulators of the hormone abscisic acid in higher plants [Zheng et al., 2002]. In loss-of-function experiments, double null mutants of *AtRop9/AtRop10* specifically enhanced various abscisic acid responses, including increased seed dormancy, inhibition of seed germination and root elongation, and stimulation of stomatal closure [Zheng et al., 2002]. Although *AtRop11* is expressed in pollen tubes [Li et al., 1998], the function of this gene has yet to be determined [Gu et al., 2004]. At the time this research project was initiated, no members of the subfamily II *Rop/Rac* G-protein class from *Gossypium hirsutum* had been cloned or characterized (Figure 1-7).

Subfamily III includes one *Rop/Rac* G-protein from *Arabidopsis*, *AtRop7* (GB mRNA ID [NM123965](#)), and two *Rop/Rac* G-proteins from *Gossypium hirsutum*, *GhRac9* (GB mRNA ID [S79309](#)) and *GhRac13* (GB mRNA ID [S79308](#)) (Figure 1-7). Overexpression of *AtRop7* inhibited root hair tip growth in *Arabidopsis thaliana* [Jones et al., 2002]; however, the function of this gene is currently unknown [Gu et al., 2004]. Similarly, the functions of the cotton subfamily III *Rop/Rac* genes are not well established. Delmer and colleagues (1995) reported that *GhRac9* is expressed at low levels in root tissue and in cotton fiber during the cellulose biosynthesis stage. This group also demonstrated that *GhRac13* was preferentially expressed in cotton fiber at the time of transition between primary and secondary cell wall synthesis (14 to 18 DPA) [Delmer et al., 1995]. Constitutive expression of *GhRac13* induced the production of reactive oxygen species in cultured soybean and *Arabidopsis* cells. The DN form of *GhRac13* had the opposite effect suggesting that *GhRac13* may be involved in the H₂O₂ signaling pathway [Potikha et al., 1999]. More recently, Kim and Triplett (2004a) demonstrated that *GhRac13* was also expressed in young cotton leaves, 1- and 6-week old cotton roots, and fully expanded cotton leaves, in addition to its transient expression in fiber during the transition phase.

Subfamily IV is the largest group of plant monomeric G-proteins, including at least six members from *Arabidopsis*, *AtRop1* (GB mRNA ID [NM114989](#)), *AtRop2* (GB mRNA ID [NM101863](#)), *AtRop3* (GB mRNA ID [AF115466](#)), *AtRop4* (GB mRNA ID [NM106234](#)), *AtRop5* (GB mRNA ID [NM119762](#)), and *AtRop6* (GB mRNA ID [NM119668](#)) (Figure 1-7). Only one subfamily IV *Rop/Rac* G-protein has been characterized from *Gossypium hirsutum*, *GhRac1* (GB mRNA ID [AF165925](#)). Subfamily IV *Arabidopsis Rop/Rac* G-proteins are hypothesized to control cell growth by regulating the dynamic assembly of cortical F-actin [Li et al., 1999; Li et al., 2001; Fu et al., 2001; Fu et al., 2002] or by controlling actin binding and activity of actin-

depolymerizing factors [Chen et al., 2003]. At present, mechanisms for regulating the actin cytoskeleton in plants are not well understood [Gu et al., 2004]. *AtRop1*, *AtRop3*, and *AtRop5* are preferentially expressed in pollen and may be functionally redundant during pollen tube growth [Li et al., 1998; Kost et al., 1999; Gu et al., 2003]. Pollen tubes overexpressing *AtRop1* assume a spoon- or balloon-shaped morphology at the tip suggesting that this gene is involved in the conversion from polar tube growth to isotropic growth [Li et al., 1999; Fu and Yang, 2001; Fu et al., 2002]. Pollen tube elongation was inhibited by microinjecting anti-Rop1Ps antibodies or by overexpressing of DN forms of *AtRop1* [Lin and Yang, 1997]. Expression of the DN form of *AtRop5* inhibited pollen tube elongation; expression of the CA form of *AtRop5* induced depolarized growth. The other three *Arabidopsis* Rop/Rac G-proteins belonging to this group: *AtRop2*, *AtRop4*, and *AtRop6* may also be functionally redundant and involved in multiple signal transduction pathways. Li and colleagues (2001) reported that the CA form of *AtRop2* is involved in multiple developmental processes in *Arabidopsis*: embryo development, seed dormancy, seedling development, shoot apical dominance, lateral root initiation, morphogenesis, and orientation of shoot lateral organs. Overexpression of *AtRop2* induced multiple root hair swellings but often inhibited root hair formation [Jones et al., 2002]. Expression of CA and DN forms of *AtRop2* controlled root hair initiation and modulated polar expansion of various cells within differentiating tissues during *Arabidopsis* organogenesis by spatially regulating a diffuse form of cortical fine F-actin throughout the cell cortex [Fu et al., 2002]. In addition, a CA form of *AtRop2* and phosphotidic acid, through a reactive oxygen species-generated pathway, induced leaf cell death [Park et al., 2004]. *AtRop4* and the CA form of *AtRop6* may regulate cell polarity in *Arabidopsis* roots [Molendijk et al., 2001]. *AtRop2* and *AtRop4* localize to the tips of elongating root hairs [Molendijk et al., 2001; Jones et al., 2002]. CA forms of *AtRop2*, *AtRop4*,

and *AtRop6* either cause isotropic growth or increased root hair length in *Arabidopsis*, whereas the DN form of *AtRop2* inhibited root hair elongation. These observations indicate that *AtRop2*, *AtRop4*, and *AtRop6* also control tip growth during root hair development [Molendijk et al., 2001; Jones et al., 2002]. In both root hairs and pollen tubes, *Rop/Rac* G-proteins control growth by modulating the formation of both the dynamic fine tip F-actin and a cytosolic calcium gradient [Li et al., 1999; Fu and Yang, 2001; Li et al., 2001; Molendijk et al., 2001; Fu et al., 2001; Fu et al., 2002; Jones et al., 2002].

GhRac1, a subfamily IV *Rop/Rac* G-protein from cotton (Figure 1-7), is highly expressed during the elongation stage of cotton fiber development and is minimally expressed when secondary cell wall synthesis begins [Kim and Triplett, 2004a]. *GhRac1* is also expressed at high levels in elongating cotton tissues such as 1-week old hypocotyls and 1-week old roots [Kim and Triplett, 2004a]. The association of highest *GhRac1* expression during maximal cotton elongation, expression in other elongating tissues, and the sequence similarities between *GhRac1* and subfamily IV *Rop/Rac* genes from *Arabidopsis* suggested that *GhRac1* might regulate cotton fiber elongation by controlling cytoskeletal assembly [Kim and Triplett, 2004a].

When this research project was initiated, only three *Rop/Rac* G-proteins had been cloned from *Gossypium hirsutum*: *GhRac1* (subfamily IV *Rop/Rac* G-protein) [Kim et al., 2000], *GhRac9* (subfamily III *Rop/Rac* G-protein), and *GhRac13* (subfamily III *Rop/Rac* G-protein) [Delmer et al., 1995]. In an ongoing effort to characterize genes involved in cotton fiber development, a project to clone and characterize subfamily II and subfamily I *Rop/Rac* G-proteins from *Gossypium hirsutum* was initiated. Monitoring changes in the expression of *Gossypium hirsutum* *Rop/Rac* G-proteins in a wild type and mutants during fiber development

and in young ovules may provide clues about how fiber development is regulated and offers the opportunity to gain additional insights about the potential functions of these genes during fiber development.

Materials and Methods

I. Enzymes, chemicals, reagents, and kits

Primers for 3' rapid amplification of cDNA ends polymerase chain reaction (3'-RACE PCR) and real-time reverse transcription PCR (Q-RT-PCR) were purchased from Sigma-Genosys (The Woodlands, TX). TaqMan® reverse transcriptase enzyme and reagents, SYBR® Green PCR master mix, 96-well optical reaction plates, and adhesive covers were purchased from Applied Biosystems (Foster City, CA). Accuprime™ *Taq* DNA polymerase, molecular mass markers for RNA, and restriction enzymes were purchased from Invitrogen (Carlsbad, CA). Molecular mass markers for DNA were purchased from Sigma-Aldrich Co. (St. Louis, MO). Unless otherwise noted, all chemical reagents were purchased from Sigma-Aldrich Co. Water used in the preparation of all buffers, media, and other reagents was purified using a Milli-Q water purification system (Millipore, Bedford, MA).

II. Plant materials and growth conditions

Three near-isogenic lines of upland cotton (*Gossypium hirsutum* L.), Texas Marker 1 (TM1), Naked Seed (N1), and Ligon lintless (Li1) were grown under standard field conditions at the Southern Regional Research Center in New Orleans, LA during the summer of 2004. Developing TM1 ovules with attached fiber were collected at 2-day intervals from DOA to 20 DPA. Developing N1 ovules with attached fiber were collected at 2-day intervals from DOA to 10 DPA. Li1 ovules were collected at DOA, only. For stages younger than 10 DPA, when it is difficult to strip fiber from the seeds, immature seeds with attached fiber were used. For some experiments, elongating TM1 fibers (10-20 DPA) were manually removed from freshly harvested ovules using a pair of straight micro-dissecting forceps. All bolls of the appropriate age and cell line were harvested from individual *Gossypium hirsutum* plants by 9:00 a.m. and

stored, briefly at 4°C until the ovule and/or fiber tissues were harvested. All plant tissue harvested from individual bolls was rapidly frozen in liquid nitrogen and stored at -80°C until use.

III. Cloning of the *Rop/Rac* G-Proteins from *Gossypium hirsutum*

Primer design. Three forward primers were designed from the 5' ends of 10 *Gossypium arboreum* *Rop/Rac* G-protein ESTs that were deposited in GenBank at the time this research project was initiated. The *Gossypium arboreum* nucleotide sequences were aligned with the web-based program CLUSTAL W [Thompson et al., 1994] version 1.82 from the European Bioinformatics Institute. Reverse primers were not designed from G-protein sequences because cDNAs were prepared with an adapter sequence that could be used as a primer. One primer (G1) was degenerate and designed to amplify a *Gossypium hirsutum* *Rop/Rac* G-protein from any subfamily (5'-ATGAGYRCYKCVARRTTYATMAARTGY-3'; translation codes: Y= C+T, R= A+G, K= G+T, V= A+C+G, M= A+C). The second primer (G2) was designed to amplify a subfamily II *Rop/Rac* G-protein from *Gossypium hirsutum* (5'-ATGGCTTCAAGCGCTTCAAGATTTATC-3'). The third primer (Nic1) was designed to amplify a subfamily I *Rop/Rac* G-protein from *Gossypium hirsutum* (5'-ATGAGCGCCTCGAGATTCATAAAGTGC-3'). All three primers were designed to amplify the protein-coding region and the 3' untranslated region (UTR). Based on CLUSTAL W sequence analyses of the protein-coding regions and 3' UTRs from *Gossypium hirsutum* *Rop/Rac* G-proteins available in GenBank, an amplicon length of 800-900 base pairs was expected.

3' Rapid amplification of cDNA ends polymerase chain reaction. The full-length protein-coding region and 3' UTR for new *Gossypium hirsutum* *Rop/Rac* G-proteins were obtained by 3'-RACE PCR following a protocol outlined by Clontech (Palo Alto, CA) [Clontech,

Marathon™ cDNA Amplification Kit User Manual PT1115-1] and using the AccuPrime™ *Taq* DNA Polymerase System from Invitrogen. The AccuPrime™ *Taq* DNA polymerase was used because this enzyme preparation contained anti-*Taq* polymerase antibodies that inhibited polymerase activity prior to reaching 60-80°C. This feature, called a “hot start”, permitted ambient temperature set-up of the reactions [Chou et al., 1992; Sharkey et al., 1994] and an improved recovery of amplification products, specific to the primer pairs, by not catalyzing the reactions until the primer pairs were annealed [Chou et al., 1992]. The following components were added to a sterile PCR tube at ambient temperature: 10% (v/v) 10X Accuprime™ PCR Buffer II (Invitrogen) to amplify products in the 200 base pair to 4 kb range, 0.2 μM primer, 100 ng template cDNA (4 DPA TM1 ovule or 20 DPA TM1 fiber, kindly provided by Dr. Hee Jin Kim), 2 units Accuprime™ *Taq* DNA Polymerase (2 U/μL, Invitrogen), 5 μM Adaptor I primer (Clontech) to reduce nonspecific amplification, 5 mM dNTP mix (1.25 mM each: dATP, dGTP, dCTP, and dTTP, Clontech), and autoclaved H₂O to adjust the final reaction volume to 50 μL. The contents were vortexed (1 minute) and were briefly centrifuged (at 20,196 x g for 30 seconds at room temperature) in an Eppendorf 5417C microcentrifuge with a standard 45° fixed angle rotor (Brinkmann Instruments, Westbury, NY) to collect the reaction mixture at the bottom of each tube. Reactions were incubated in a GeneAmp 9700 Thermal Cycler (Applied Biosystems, Foster City, CA) at 94°C for 2 minutes to denature the template and to activate the polymerase. Thirty-five cycles of PCR were performed as follows: 94°C (30 seconds) to denature the double-stranded cDNA template, 52°C (30 seconds) to allow stringent annealing of primers to the template, 68°C (60 seconds) for amplification of template cDNA, and 68°C (10 minutes) for a final extension. All reactions were maintained at 4°C after cycling and stored at

-20°C until use. Six different PCR reactions were performed using the three primers, G1, G2, and Nic1, with either 4 DPA TM1 ovule cDNA or 20 DPA TM1 fiber cDNA.

Gel electrophoresis of PCR amplification products. After each round of 3'-RACE PCR, the PCR products were separated on a 10 cm by 8.5 cm 0.8% agarose gel (5 mm thick, Appendix 1) in 1X TBE buffer (Appendix 1) and electrophoresed at 100 V for 90 minutes at room temperature [Sambrook et al., 1989]. The total volume in each electrophoresis lane was 24 μ L, 20 μ L from each PCR reaction and 4 μ L of 6X DNA gel-loading buffer (Appendix 1). A DNA ladder (1 kb, Invitrogen) was used as the molecular mass marker. The gel was stained with ethidium bromide solution (Appendix 1) diluted to a final concentration of 0.5 μ g/mL [Sambrook et al., 1989]. The gel was rocked gently (30 minutes) on Hoefer Red Rocker (Hoefer Scientific Instruments, San Francisco, CA). After staining, the gel was washed in H₂O to remove unbound ethidium bromide. The DNA bands were visualized with a Gel Doc 1000 Imager (Bio-Rad, Hercules, CA) and analyzed with the Bio-Rad Molecular Analyst software (version 1.5).

Recovery of PCR amplification products. The gel was placed on a Fotodyne Transilluminator (Fotodyne Incorporated, Hartland, WI) and transmitted UV light (312 nm) was utilized to visualize the ethidium bromide-stained DNA bands. All DNA bands of the appropriate size (800-900 base pairs) were excised from the gel and were extracted using the Bio-Rad Quantum Prep™ Freeze 'N Squeeze DNA Gel Extraction Kit. The manufacturer's directions were followed [Thuring et al., 1975; Bio-Rad, Quantum Prep™ Freeze 'N Squeeze DNA Gel Extraction Spin Columns].

Ligation and cloning reactions. Extracted DNA was cloned into the pCR[®]-XL TOPO[®] cloning vector from Invitrogen, following the manufacturer's instructions [Invitrogen TOPO[®] XL PCR Cloning Kit Manual, Version M]. The pCR[®]-XL-TOPO[®] cloning vector is a

3.5 kb vector designed for direct selection of recombinants in *Escherichia coli*, because the vector contains the lethal *Escherichia coli ccdB* gene [Bernard et al., 1994] fused to the C-terminus of the *LacZ α* fragment. Ligation of a PCR product disrupts the expression of the *lacZ α -ccdB* fusion gene that permits growth of only positive recombinants upon transformation [Bernard et al., 1994]. In addition, the vector contains the *Lac* promoter region for gene expression, a multiple cloning site with 16 unique restriction sites to facilitate in-frame cloning, a TOPO[®] cloning site (single 3' thymidine overhangs) for efficient insertion of the PCR amplification product, kanamycin and zeocin antibiotic resistance genes for selection of transformants, and a *pUC ori* for replication in *Escherichia coli* [Invitrogen TOPO[®] XL PCR Cloning Kit Manual, Version M]. Furthermore, the vector is supplied with Topoisomerase I from the *Vaccinia* virus covalently bound to each 3' phosphate for efficient ligation of the PCR amplification product within the multiple cloning site of the vector [Shuman, 1994]. The total volume for each ligation/cloning reaction was 2.5 μ L, 2 μ L from the recovered PCR product and 0.5 μ L of the pCR[®]-XL-TOPO[®] vector (10 ng/ μ L plasmid DNA). After a 5-minute incubation period at room temperature, 6X TOPO[®] cloning stop solution (0.3 M NaCl and 0.06 M MgCl₂) diluted to a 1X final concentration was added to each reaction to prevent the topoisomerase enzyme from re-binding the plasmid and nicking the DNA [Invitrogen TOPO[®] XL PCR Cloning Kit Manual, Version M].

Transformation. The pCR[®]-XL-TOPO[®] constructs from above were transformed into chemically competent One Shot[®] TOP10 *Escherichia coli* cells (provided in Invitrogen's TOPO[®] XL PCR Cloning Kit). The manufacturer's directions for transforming chemically competent cells were followed [Invitrogen, TOPO[®] XL PCR Cloning Kit Manual, Version M]. The total volume for each transformation event was 278 μ L: 3 μ L from the pCR[®]-XL-TOPO[®]

cloning reaction, 25 μL of chemically competent One Shot[®] TOP10 *Escherichia coli* cells, and 250 μL SOC medium (Appendix 1). From each transformation event, 150 μL of cells were spread onto a pre-warmed Luria-Bertani (LB) agar plate (Appendix 1) and incubated overnight in a 37°C incubator.

IV. Recombinant DNA procedures

Bacterial cell culture. Individual *Escherichia coli* colonies were isolated with a disposable sterile inoculating loop and transferred to 5 mL liquid LB media (Appendix 1) containing 3 μL of 50 $\mu\text{g}/\text{mL}$ kanamycin (Appendix 1). Bacterial cell cultures were incubated at 37°C, overnight with shaking (500 rpm).

Plasmid DNA isolation. Plasmid DNA was isolated and purified with the Wizard[®] Plus Miniprep DNA Purification System Kit from Promega (Madison, WI). Promega's Miniprep Kit was selected because only a small amount of highly purified plasmid DNA was required for DNA sequencing. The manufacturer's protocol for 3-5 mL of bacterial cell culture and plasmid purification using a vacuum manifold was followed [Promega, Technical Bulletin Number 117]. Multiple minipreps were processed simultaneously.

DNA quality and yield. Plasmid DNA samples were diluted 1: 200 with autoclaved H₂O and the absorbance (A) at 260, 280, and 320 nm was measured with a Pharmacia Biotech Ultrospec 3000 UV/Visible Spectrophotometer (Amersham Biosciences, Piscataway, NJ). A solution of DNA whose $A_{260} = 1$ contains approximately 50 μg DNA/mL [Sambrook et al., 1989]. The A_{260}/A_{280} absorbance ratio was calculated to assess the purity of the sample. Pure DNA preparations have an A_{260}/A_{280} value of 1.8 [Sambrook et al., 1989].

Restriction enzyme digestion. Restriction enzyme digestion was performed on the plasmid DNA samples to liberate the PCR amplification product (~ 800-900 base pairs) from the plasmid vector. The multiple cloning site of the pCR[®]-XL-TOPO[®] plasmid vector contains 16 unique restriction enzyme sites including flanking *EcoRI* sites [Invitrogen, TOPO[®] XL PCR Cloning Kit Manual, Version M]. The following components were added to a sterile tube: 5 units *EcoRI* (Invitrogen), up to 5 µg of purified plasmid DNA, 0.1 volumes 10X REact3 buffer (Appendix 1) from Invitrogen, and autoclaved H₂O to adjust the final reaction volume to 20 µL. Each reaction was placed into a 37°C bath for 1 hour to digest the plasmid DNA [Sambrook et al., 1989]. The restriction enzyme digests were electrophoresed on a 0.8% agarose gel (Appendix 1) in 1X TBE buffer (Appendix 1) at 100 V for 90 minutes at room temperature. The gel was visualized with the Bio-Rad Gel Doc 1000 imager and analyzed with the Bio-Rad Molecular Analyst software (version 1.5).

V. Sequencing and bioinformatics

Sequencing. The multiple cloning site of the pCR[®]-XL-TOPO[®] vector contains the T7 promoter/priming site and the M13-forward and –reverse priming sites. The M13-reverse priming site and T7 promoter/primer site were the closest priming sites to the ligated PCR product. All samples were sequenced with both the T7 primer and the M13 reverse primers by the Auburn University Genomics Center (Auburn, AL). Raw sequence data files were received in the Applied Biosystems (ABI) file format and were converted with the web-based program Chromas version 1.45 (Technelysium Pty Ltd, Tewantin, Australia). The sense and anti-sense nucleotide sequences for each sample were aligned with CLUSTAL W [Thompson et al., 1994]

to resolve ambiguous nucleotides. Plasmid vector sequences were identified and removed by the web-based Vecscreen software at the National Center for Biotechnology Information (NCBI) [Altschul et al., 1997].

Bioinformatics. A web-based basic local alignment search tool (BLAST) from NCBI was used to perform a rapid sequence comparison, using the *blastn* algorithm, for each sequenced DNA sample [Altschul et al., 1990]. Samples identified as putative *Rop/Rac* G-proteins were translated with a web-based program from the ExPASy (Expert Protein Analysis System) proteomics server of the Swiss Institute of Bioinformatics [Gasteiger et al., 2003]. After translation, amino acid sequences were aligned with known *Gossypium hirsutum* *Rop/Rac* G-protein amino acid sequences with CLUSTAL W [Thompson et al., 1994].

Cryogenic preservation of bacterial cultures growing in liquid media. Glycerol stocks were prepared for bacterial cultures containing PCR amplification products putatively identified as *Rop/Rac* G-proteins. Five hundred microliters of each bacterial cell culture was transferred to a sterile 2.0 mL Corning cryogenic vial. An equal volume of sterile 80% (v/v) glycerol solution (Appendix 1) was added. The glycerol stocks were vortexed and stored at -80°C [Sambrook et al., 1989].

VI. Gene expression of the cloned *Rop/Rac* G-Proteins

Total RNA isolation. Total RNA from cotton tissues of different developmental stages was isolated using a phenol-based extraction and LiCl-precipitation procedure [Schultz et al., 1994]. Tissue samples were ground in liquid nitrogen-filled mortars before maceration in 30 mL Total RNA Extraction Buffer (Appendix 1) with a Tekmar Tissumizer and 10N Homogenizer (Tekmar, Cincinnati, OH). The cellular debris was pelleted by centrifugation (23, 708 x g for 15 minutes at 4°C) in a Sorvall RC5C centrifuge with a HB-4 swinging bucket

rotor (Kendro Laboratory Products, Newton, CT). The aqueous phase was extracted sequentially with an equal volume chloroform, an equal volume phenol/chloroform/isoamyl alcohol (25:24:1), and again with an equal volume chloroform. Between each extraction, the samples were vortexed (2 minutes) and centrifuged (23,708 x g for 15 minutes at 4°C). After the final extraction, the aqueous phase (approximately 10 mL) was transferred to a fresh tube. Nucleic acids were precipitated with 0.1 volume 3 M sodium acetate, pH 5.2 (Appendix 1), and 2.5 volumes cold 100% ethanol. The samples were stored at -20°C overnight. The following day, the samples were centrifuged (23,708 x g for 45 minutes at 4°C) in a Sorvall RC5C centrifuge with a HB-4 swinging bucket rotor. After the supernatant liquid was discarded, the remaining pellet was rinsed with a small amount of 70% ethanol (Appendix 1), air-dried (5 minutes), and was dissolved in 10 mL Total RNA Re-suspension Buffer (Appendix 1). To selectively precipitate polysaccharides contaminating the sample, an equal volume of 2-butoxyethanol was added¹. The samples were vortexed (2 minutes) and incubated on ice (1 hour) before centrifugation (23,708 x g for 15 minutes at 4°C) in a Sorvall RC5C centrifuge with a HB-4 swinging bucket rotor. The supernatant liquid was transferred to fresh tubes. An additional 50% (v/v) 2-butoxyethanol was added to the RNA preparation to precipitate the nucleic acids. Samples were vortexed (2 minutes) and incubated on ice (1 hour) before centrifugation (23,708 x g 15 minutes at 4°C). The nucleic acid pellets were washed with a small volume of 70% ethanol (Appendix 1), air-dried (5 minutes), and were dissolved in 1 mL diethylpyrocarbonate (DEPC)-treated water (Appendix 1). To precipitate RNA, 8 M LiCl (Appendix 1) was added to a final concentration of 2 M before incubation on ice at 4°C overnight. The following day, all samples were centrifuged (20,196 x g for 30 minutes at room

¹ The selective precipitation of polysaccharides with 2-butoxyethanol was omitted in all samples extracted from cotton fiber to avoid precipitating nucleic acids with the polysaccharides, thereby reducing total RNA yields.

temperature) in an Eppendorf 5417C microcentrifuge with a standard fixed 45° angle rotor. The supernatant liquid was discarded; the nucleic acid pellets were rinsed in a small volume of 70% ethanol (Appendix 1), air-dried (5 minutes), and dissolved in 300 µL DEPC-treated water (Appendix 1). To each RNA sample, 0.1 volume 3M sodium acetate, pH 5.2, (Appendix 1) and 2.5 volume 100% ethanol was added. The samples were stored at -80°C for 2.5 hours. Total RNA was recovered by microcentrifugation (20,196 x g for 30 minutes at room temperature), the pellet was rinsed with a small volume of 70% ethanol (Appendix 1), air-dried (5 minutes), dissolved in 300 µL of DEPC-treated water (Appendix 1), and stored at -80°C.

Quality and yield of total RNA. The concentration of total RNA was determined by measuring the A_{260} of a 1:50 dilution of each total RNA sample. A solution of RNA whose $A_{260}= 1$ contains approximately 40 µg RNA/mL [Sambrook et al., 1989]. The absorbance was monitored at 230, 260, 270, 280, and 320 nm with a Pharmacia Biotech Ultraspec 3000 UV/Visible spectrophotometer to determine the quality, concentration, and yield of each total RNA sample. The A_{260}/A_{280} absorbance ratio was calculated to assess sample purity. Pure RNA preparations have an A_{260}/A_{280} value of 2.0 [Sambrook et al., 1989].

Gel electrophoresis of total RNA. Total RNA (5 µg) was separated on a 10 cm by 8.5 cm 0.8% agarose gel (5 mm thick, Appendix 1) in 1X TBE buffer (Appendix 1) and electrophoresed at 100 V for 60 minutes at room temperature. An equal volume of 2X RNA dye (Appendix 1) was added to each sample to visualize the RNA bands [Sambrook et al., 1989]. A RNA ladder (0.24-9.5 kb, Invitrogen) was used as the molecular mass marker. The bands were visualized with the Bio-Rad Gel Doc 1000 imager and analyzed with the Bio-Rad Molecular Analyst software (version 1.5).

DNase digestion of genomic DNA contaminating total RNA samples. DNase digestion was performed using the Turbo DNA-free™ Kit (Ambion, Austin, TX) following the manufacturer's instructions. The Turbo DNase is designed to remove up to 50 µg contaminating DNA/mL RNA [Ambion, TURBO DNase Treatment and Removal Protocol, Version 0405]. For each DNase digestion reaction: 100 ng of total RNA, 2 units Turbo DNase (2 U/µL), 0.1 volume 10X Buffer, and DEPC-treated water to adjust the total volume to 100 µL. Samples were incubated in a 37°C water bath (30 minutes), and 0.1 volume Turbo DNase Inactivation reagent was added to inactivate the DNase. The samples were centrifuged (20,196 x g at room temperature for 90 seconds) in an Eppendorf 5417C microcentrifuge with a standard 45° fixed angle rotor from Brinkmann Instruments to pellet the DNase Inactivation reagent. The DNA-free total RNA was recovered and transferred to sterile microcentrifuge tubes.

Purification of DNA-free total RNA. The DNA-free total RNA samples were purified with the RNeasy® Plant Mini Kit from Qiagen (Valencia, CA), following the protocol for RNA cleanup [Qiagen, RNeasy® Mini Handbook, Third Edition]. Absorbance readings at 260, 280, and 320 nm were measured for all purified RNA samples with a Pharmacia Biotech Ultraspec 3000 UV/Visible spectrophotometer.

Reverse transcription of total RNA to cDNA. Purified DNA-free total RNA was reverse transcribed using the TaqMan® Reverse Transcriptase Reagent Kit from Applied Biosystems. All reagents, except the total RNA sample and DEPC-treated water (Appendix 1), were supplied in the kit. The final reaction in a sterile PCR tube contained the following components: 500 ng DNA-free purified total RNA, 10% (v/v) 10X Buffer, 5.5 mM MgCl₂, 2 mM dNTP mix (0.5 mM each: dATP, dTTP, dCTP, and dGTP), 2 µM random hexamer primers, 25 units MultiScribe™ reverse transcriptase (50 U/µL), 8 units RNase inhibitor

(20 U/μL), and DEPC-treated water (Appendix 1) to adjust the final volume to 20 μL. Random hexamer primers were used instead of an oligo (dT) primer because 18S rRNA, which does not have a polyA tail, needed to be reverse-transcribed for use in real-time reverse transcription PCR experiments. All reverse transcription reactions were incubated in a GeneAmp 9700 Thermal Cycler from Applied Biosystems at 25°C (10 minutes) for primer binding, 48°C (30 minutes) to reverse transcribe the total RNA template, and 95°C (5 minutes) to stop the reverse transcription reaction. Each reverse transcription reaction produced 500 ng of double-stranded cDNA. Autoclaved water was added to each reaction to dilute the cDNA to a 2.5 ng/μL final concentration. The cDNA samples were stored at -80°C until used.

VII. Characterization of the cloned *Rop/Rac* G-proteins

Real-time reverse transcription PCR primer design. Real-time reverse transcription PCR gene specific primers for cotton *Rop/Rac* G-proteins were designed with Primer Express, version 2.0 from Applied Biosystems. Forward (F) and reverse (R) primer pairs were designed for three *Gossypium hirsutum* *Rop/Rac* G-proteins: *GhRac2*, *GhRac3*, and *GhRac9*. Primers pairs designed were as follows: *GhRac2-F* (5'-GAGGAACTTCGTGCCTGCTAA-3'), *GhRac2-R* (5'-GCAAGAGGAACACAAGCATTTG-3'), *GhRac3-F* (5'-AGATTGCGGCTCCTGCATAC-3'), *GhRac3-R* (5'-TGCATCAAACACTGCCTTCAC-3'), *GhRac9-F* (5'-ACGTCGAGGTTTATCAAGTGTGTC-3'), and *GhRac9-R* (5'-TTGCTAGTATACGAAATAAGCATGCA-3'). The primer pairs for *GhRac1-F* (5'-GAAATGGATTCCAGAAT TGAGACA-3'), *GhRac1-R* (5'-TGTTGGGACTAAGCTTGATCTT-3'), *GhRac13-F* (5'-GTGAAGGCTGTTTTTCGATGCT-3'), *GhRac13-R* (5'-CCAAAGAGAAAGCCTTGCAAAA-3'), *18S rRNA-F* (5'-CGTCCCTGCCCTTTGTACA-3'), *18S rRNA-R* (5'-AACACTTCACCGGACCATTCA-3'), cotton *α-tubulin4-F* (5'-GATCTCGCTGCCCTGGAA-3'), cotton *α-*

tubulin4-R (5'-ACCAGACTCAGCGCCAACCTT-3'), *Gossypium hirsutum Germin-like protein (GhGLP1-F)* (5'-CCGTACCGCAGGCAACAC-3'), *GhGLP1-R* (5'-CGGGAATTGAGTCGA AAAGG-3'), *ubiquitin-conjugating protein (UCP-F)* (5'-CGGAAAGAGGTGAAGATGTC AAC-3'), and *UCP-R* (5'-GGATCTTGCTGCAACCTCTTAAA-3') were previously designed and purchased by Dr. Hee Jin Kim. The specificity of the gene specific primers was carefully monitored by examining the dissociation curves at the completion of each Q-RT-PCR reaction.

Real-time reverse transcription polymerase chain reaction. All Q-RT-PCR experiments utilized SYBR® Green as the fluorescent reporter. SYBR® green is a fluorogenic minor groove binding dye that exhibits little fluorescence when in solution but emits a strong fluorescent signal upon binding to double-stranded DNA [Morrison, 1998]. Reaction components were assembled in a 96-well optical reaction plates from Applied Biosystems that were sealed with optical adhesion covers. The following components were added to each reaction well: 0.25 µM forward primer, 0.25 µM reverse primer, 7.5 ng cDNA template, 50% (v/v) of 2X SYBR® Green PCR master mix, and autoclaved water to adjust the final volume to 18 µL. Q-RT-PCR experiments were performed using an ABI 7900HT Sequence Detection System from Applied Biosystems. The samples were incubated at 50°C (2 minutes) followed by 95°C (10 minutes). Fifty cycles of amplification were performed at 95°C (15 seconds) to denature double-stranded cDNA template and 60°C (1 minute) for primer annealing and extension. A dissociation stage at 95°C (15 seconds), 60°C (15 seconds), and 95°C (15 seconds) followed amplification. The amplicon sizes of *GhRac2* (71 base pairs), *GhRac3* (71 base pairs), *GhRac9* (73 base pairs), *GhRac1* (73 base pairs), *GhRac13* (73 base pairs), *α-tubulin4* (51 base pairs), *18S rRNA* (61 base pairs), *GLP1* (70 base pairs), and *UCP* (74 base pairs) were designed to be less than 150 base pairs to make amplification efficiencies

equivalent. For samples using cDNA prepared from TM1 fiber (10-20 DPA), the reported values are the average of 2-4 independent PCR reactions. For all other real-time PCR experiments, reported values are the average of 3-6 independent PCR reactions. The experiments were repeated 2 to 4 times independently beginning with RNA isolation. *Rop/Rac* G-protein relative transcript levels were determined by a comparative C_T method ($2^{-\Delta\Delta C_T}$) [Livak and Schmittgen, 2001]. Statistical analyses and construction of graphs were performed using Graph Pad Prism, version 4.00.

Results and Discussion

I. Cloning of the *Rop/Rac* G-proteins from *Gossypium hirsutum*

Rop/Rac G-proteins are involved in numerous plant signal transduction pathways, including those for stress responses [Baxter-Burrell et al., 2002; Suharsono et al., 2002; Park et al., 2004], hormone responses [Lemichez et al., 2001; Li et al., 2001; Tao et al., 2002; Zheng et al., 2002], defense responses [Kawasaki et al., 1999; Hassanain et al., 2000; Agrawal et al., 2003; Morel et al., 2004], secondary cell wall differentiation [Potikha et al., 1999], and actin cytoskeleton organization [Fu et al., 2001; Fu et al., 2002; Jones et al., 2002; Chen et al., 2003; Gu et al., 2003; Kim and Triplett, 2004a]. At the time this research project was initiated, only three *Gossypium hirsutum* *Rop/Rac* G-protein sequences were available in GenBank, *GhRac1* (subfamily IV *Rop/Rac* G-protein, GB mRNA ID [AF165925](#)) [Kim et al., 2000], *GhRac9* (subfamily III *Rop/Rac* G-protein, GB mRNA ID [S79309](#)), and *GhRac13* (subfamily III *Rop/Rac* G-protein, GB mRNA ID [S79308](#)) [Delmer et al., 1995]. All three cotton *Rop/Rac* G-proteins were characterized as potentially important regulators of fiber development [Delmer et al., 1995; Delmer, 1999; Kim et al., 2000; Kim and Triplett, 2004a]. No subfamily I or II *Rop/Rac* genes had been cloned from *Gossypium hirsutum*. The central role of *Rop/Rac* genes in *Arabidopsis thaliana* pollen tube [Lin and Yang, 1997; Li et al., 1998; Zheng and Yang, 2000a; Fu and Yang, 2001; Fu et al., 2001; Fu et al., 2002; Chen et al., 2003] and root hair development [Fu and Yang, 2001; Molendijk et al., 2001; Jones et al., 2002], two cells with exaggerated polar growth, suggested that elucidating the function of cotton *Rop/Rac* G-proteins might provide important clues about the regulation of cotton fiber development.

PCR primer design. PCR primers were designed from the 5' ends of 10 known *Gossypium arboreum* *Rop/Rac* EST sequences in GenBank at the time this research project was initiated (Figure 2-1).

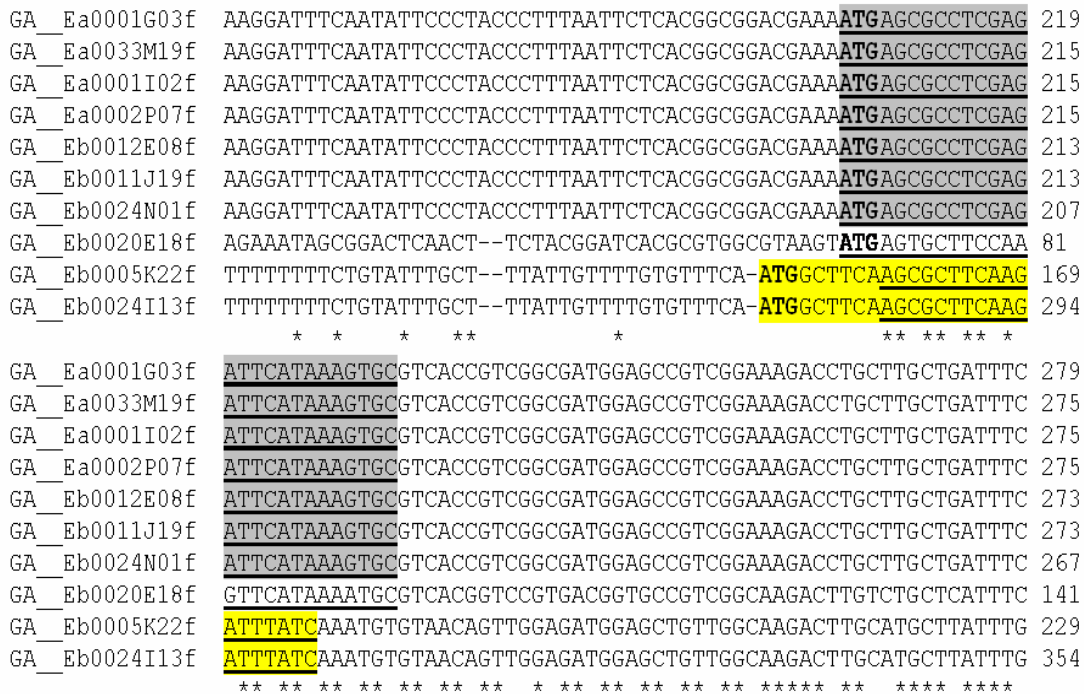


Figure 2-1. Multiple sequence alignment of the *Gossypium arboreum* *Rop* EST sequences used to design PCR primers. *Gossypium arboreum* *Rop/Rac* EST sequences aligned with CLUSTAL W [Thompson et al., 1994]. Primer G1 is indicated by the black underline. Primer G2 is indicated by the yellow highlight. Primer Nic1 is indicated by the grey highlight. The translation start codon is indicated by the boldface font.

We designed forward primers at the 5' end of the genes because we could choose a defined internal site, such as the translation start site, for alignment (Figure 2-1). Three forward primers were designed to amplify the entire protein-coding region and 3' UTR. Primer G1 was degenerate and designed to amplify a *Rop/Rac* G-protein from any subfamily (Figure 2-1). Primer G2 was designed to amplify a *Rop/Rac* G-protein from subfamily II (Figure 2-1). Primer Nic1 was designed to amplify a *Rop/Rac* G-protein from subfamily I (Figure 2-1). Reverse primers were not designed from G-protein sequences because cDNAs were prepared with an adapter sequence that was used as a primer.

3'-RACE PCR. Since the 5' end of the *Gossypium arboreum Rop/Rac* ESTs were more defined than the 3' end, we chose 3'-RACE PCR to amplify the newly cloned *Rop/Rac* G-proteins from *Gossypium hirsutum*. We chose 4 DPA TM1 ovule cDNA as one template to amplify *Rop/Rac* G-proteins from the elongation stage of fiber development. We chose 20 DPA TM1 fiber cDNA as a second template to amplify *Rop/Rac* G-proteins from the cellulose biosynthesis stage. Six different PCR reactions were performed using the three primers, G1, G2, and Nic1 with either 4 DPA TM1 ovule cDNA or 20 DPA TM1 fiber cDNA. Based on a multiple sequence alignment of the protein-coding region and the 3' UTR from known *Gossypium hirsutum Rop/Rac* G-proteins, an amplicon length of 800-900 base pairs was expected (Figure 2-2).

```

GhRac1      ATGAGTGCCTCCAGGTTTCATAAAATGCGTCCACGGTCGGTGACGGTGCCGTCCGGCAAGACT 60
GhRac13    ATGAGCACTGCAAGATTTATCAAGTGTGTCACGGTCGGTGATGGAGCTGTGGGGAAAAC 60
GhRac9     ATGAAATACGTCGAGGTTTATCAAGTGTGTCACAGTAGGTGATGGAGCAGTGGGGAAGACT 60
          *****
GhRac1      TGTCTGCTCATTTCCTACACTAGCAATACTTTCCCTACCGATTATGTGCCAACTGTCTTT 120
GhRac13    TGTATGCTCATTTCATATACCAAGCAATACTTTCCCAACCGATTATGTGCCAACTGTCTTT 120
GhRac9     TGCATGCTTATTTTCGTATAC TAGCAATACGTTCCCAACCGACTATGTGCCCACTGTCTTT 120
          **  ***  *****  **  **  *****  *****  **  **  *****  **  **  ***

GhRac1      541 CCAAAGAAGAAGAAGAAA-----AAGAAGAGAA-AGGCACA-----AAAAGCTTGCT 586
GhRac13    541 CCAAACCCAAAGAGAAAACCTTTCAAAAGGAGAACATGTGCTTTCCTTTGAAATATTGGAT 600
GhRac9     541 CCAAACCCAAAGAGAAAACCTATAAAAAGAAGATCATGTGCTTTCCTTTGAAACCTCAATT 600
          *****  *****  **  *  *  *  *  *  *  *  *  *  *  *  *  *
GhRac1      CAATATTGTAATCATGCAAG--AAGTGATATTGGTGCAG----- 624
GhRac13    CATTTTACAGTCAAAAACAGTTAAACAAAAGCTGTTGCAGATAAACACTGAATCTGCTAT 660
GhRac9     CTACATTACAATCAAATTTATTTTGTATATAC TTTTGT TTTT TATTTT TATTTT TTT 660
          *  ***  ***  *  *  *

GhRac1      -----
GhRac13    AGTTTGT TTTTGGTTTACATATGTTCCACGTGAAACTATGAAGCA TCTCTAAGAAAACCC 720
GhRac9     CACATAAAATTT-CATATGTAACCATGAAGGATCTCTAAAAGGGGATTGATTTGAAATTG 719

GhRac1      -----
GhRac13    AAACATCATATCAACCCATCGATCAATGAATCGATTTCAATTTTCGAGTATAAGTTCC 780
GhRac9     CAATGGTATTTGTAA TGTATAAAAAGAAAAAAAATATATA TTTT-----GTAATAGTTTA 775

GhRac1      -----
GhRac13    TTTTAATCCTTCTTTTACTTCA TTTTAACGAATTC TATGGATAATGTTCCCTACAA 840
GhRac9     AACTCATTCATTTGTTATTACCTTATTTCTTTCCA TTTTAAAAAAAAAAAAAAAAAAAA--- 832

GhRac1      -----
GhRac13    ACATGTCATTACAATGTTTAAATTAATAAATCCATTCCTTC TATTTTACTAAAAAAAAAAAA 900
GhRac9     -----

GhRac1      --
GhRac13    AA 902
GhRac9     --

```

Figure 2-2. Multiple sequence alignment of the *Gossypium hirsutum Rop/Rac* GTPases used to determine amplicon length. The nucleotide sequences of *GhRac1* (*Gossypium hirsutum*, GB mRNA ID [AF165925](#)), *GhRac9* (GB mRNA ID [S79309](#)), and *GhRac13* (GB mRNA ID [S79308](#)) were aligned with CLUSTAL W [Thompson et al., 1994]. The first 120 nucleotides are shown to represent the beginning of the protein-coding region. Sequences between 120 and 541 are omitted for brevity. Starting at nucleotide 541, the last 50 nucleotides of the protein-coding region are shown. The translation start codon is indicated by the yellow highlight. The translation stop codon is indicated by the grey highlight. The polyA tail is underlined.

Gel electrophoresis and recovery of amplification products. PCR products were separated on an agarose gel (Figure 2-3).

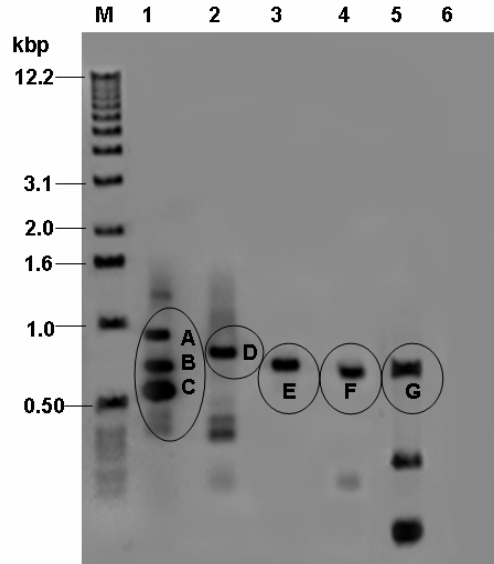


Figure 2-3. Agarose gel of PCR amplification products. 3'-Race PCR products were separated on a 0.8% (w/v) agarose gel. The gel was stained with ethidium bromide, visualized with the Bio-Rad Gel Doc 1000 imager, and analyzed with the Bio-Rad Molecular Analyst Software. The DNA molecular mass marker (Invitrogen) is shown in the lane labeled M. Lane 1 is 4 DPA TM1 ovule cDNA amplified with primer G1. Lane 2 is 4 DPA TM1 ovule cDNA amplified with primer G2. Lane 3 is 20 DPA TM1 fiber cDNA amplified with primer G1. Lane 4 is 20 DPA TM1 fiber cDNA amplified with primer G2. Lane 5 is 4 DPA TM1 ovule cDNA amplified with primer Nic1. Lane 6 is 20 DPA TM1 fiber cDNA amplified with primer Nic1. The bands circled and labeled (A-G) are the bands that were excised, cloned, and sequenced.

Seven PCR amplification products ranging in size between 0.50 and 1.0 kb were excised from the gel and labeled A through G (Figure 2-3). Bands A (~ 1.0 kb), B (~ 0.75 kb), and C (~ 0.6 kb) were extracted from lane 1. Bands D (~ 0.9 kb), E (~ 0.8 kb), F (~ 0.8 kb), and G (~ 0.8 kb) were extracted from lanes 2, 3, 4, and 5, respectively (Figure 2-3). No PCR amplification products were evident in lane 6 (Figure 2-3).

Recombinant DNA procedures. A small volume of DNA extracted from each PCR product was ligated into the multiple cloning site of the pCR[®]-XL-TOPO vector (Invitrogen). The key to using this cloning vector was the enzyme DNA topoisomerase I that functions as both a restriction enzyme and a ligase to enable fast ligation of DNA sequences with compatible ends

[Shuman, 1994]. After only 5 minutes at room temperature, ligation was complete and ready for transformation into *Escherichia coli*. We also chose this vector because we could directly select recombinants via disruption of a lethal *Escherichia coli* gene, *ccdB* [Bernard et al., 1994]. Each PCR product was ligated in frame between flanking *EcoRI* restriction sites, and kanamycin was used for chosen the antibiotic selection. Chemically competent *Escherichia coli* was transformed with plasmid DNA corresponding to one of the seven PCR amplification products. For each transformation event, at least six individual *Escherichia coli* colonies were isolated. Plasmid DNA was isolated, purified, quantified, and digested with *EcoRI* to liberate the PCR amplification product.

Sequencing and bioinformatics. One representative DNA sample (concentration \geq 150 ng/ μ L) from each PCR amplification product was sequenced at the Auburn University Genomics Facility. The nucleotide-nucleotide or *blastn* algorithm of BLAST at NCBI [Altschul et al., 1990; 1997] was used to determine sequence relatedness with previously characterized genes. Two DNA sequences amplified from 4 DPA TM1 ovule cDNA (A and B from Figure 2-3) and two DNA sequences amplified from 20 DPA TM1 fiber cDNA (E and F from Figure 2-3) were similar to an *Arabidopsis thaliana* mRNA sequence for importin alpha protein, *IMPA4* (GB mRNA ID [NM179292](#)). A third DNA sequence amplified from 4 DPA TM1 ovule cDNA (C from figure 2-3) was similar to an *Arabidopsis thaliana* mRNA for a mitochondrial ATP binding cassette transporter gene, *STAI* (GB mRNA ID [AJ272202](#)). Two DNA sequences amplified from 4 DPA TM1 ovule cDNA (D and G from Figure 2-3) were similar to putative GTP-binding proteins. Fragment D was similar to a *Nicotiana tabacum* mRNA sequence for GTP-binding protein, *NtRac4* (GB mRNA ID [AJ496228](#)) and was named *GhRac2* (GB mRNA ID [AY965615](#)). Fragment G was similar to a *Lotus japonicus* mRNA sequence for GTP-binding

protein, *Rac1* (GB mRNA ID [Z73961](#)) and was named *GhRac3* (GB mRNA ID [AY965614](#)).

The only amplification products determined to be *Rop/Rac* G-proteins were amplified from TM1 4 DPA ovule cDNA. These *Rop/Rac* G-proteins were transcribed during the fiber elongation stage.

***GhRac2* encodes a full-length *Rop/Rac* G-protein.** The cDNA sequence of *GhRac2* is shown in Figure 2-4A.

A *GhRac2* cDNA

```

1 ATGGCTTCAAGCGCTTCAAGATTTATCAAATGTGTAACAGTTGGAGATGGAGCTGTTGGCAAGACTTGCA 70
  TGCTTATTTGCTATACAAGTAACAAGTTCCCGACCGATTACATACCAACAGTTTTTGGATAACTTCAGTGC 140
  CAACGTTGTAGTTGAAGGCACAACCTGTGAACCTAGGTCCTTGGGGACACGGCTGGACAAGAGGATTACAAC 210
  AGACTAAGGCCATTGAGCTACAGAGGTGCAGATGCTTTGTCCTTAGCTTTCTCATTAGTTAGTCGAGCAA 280
  GCCATGAGAACGTAATAAAAAAGTGGATTCCCTGAACCTCAGCATTATGCCCCAGGCGTCCCTGTGGTTCT 350
  GGTGGCACC AATTTGGATCTTCGTGAGGATAAACATTATCTGGCTGATCCTCGGCTTGCTGCCGGTT 420
  AGCACCGCACAGGGCGAGGAGCTCCGCAAACAGATAGGTGCTGCTTATTACATTGAGTGCAGCTCAAAAA 490
  CTCAGCAGAACGTGAAAGCAGTTTTTGTATGATGCAATCAAAGTTGTAATCAAGCCACCCAGAAACAGAA 560
  GGAGAAGAAGAAAAAGCC AAGTTCGAGGATGTCTAATAAATGCTTCTGCGGGAGGAACTTCGTGCCTGCT 630
  AAATGAGACGGATTGGCTTCAGTCAAAAATCAAATGCTTGTGTTCTCTTGTACCTAGAGATTCTTTTT 700
  AGACAAACAGGATCAAGTCGGCTTGTATTATCATGCAACGCTTTTAGCATACAGATTTATTTCTAATCTTA 770
  CGCTTTAATTCGGATGCTAATTTACCATAGTGATTTCTTGTATAGAGTTAAAGCTTAATGGACTTGTGGT 840
  TTTATGCATGAAAAAAAAAAAAAAAAAAAAAAAAAAAAAAAAAAAAA 877
  
```

B *GhRac3* cDNA

```

1 ATGAGCGCCTCGAGATTCATAAAGTGCCTCACCGTCGCGATGGAGCCGTCGGAAGACCTGCTGCTGA 70
  TTTCTACACCAGCAACACTTTCCCTACGGACTATGTCCCAGCTGTTTTTCGACAATTCAGTGC AATGT 140
  CGTCGTGATGGCAGCACTGTCAACTTAGGTTTATGGGACACTGTGTCAGGAGGATTACAATAGACTA 210
  CGACCACTGAGCTATCGTGGGGCTGATGTGTTTATTCTTGCATTTCTCTCATCAGCAAGGCCAGTTATG 280
  AAAACGTTGCCAAGAAGTGGATTCCCTGAAC TAAAGCATTATGCCCTGGTGTCCGATAGTTCTTGTGG 350
  AACTAAGCTTGATCTCCGAGATGATCAACAATTCTTAACAGACCATCCTAACGCAGTGCCCAATTTCTACA 420
  GCTCAGGGAGAGGAATTAAGAAACAGATTGCGGCTCCTGCATACATTGAGTGTAGCTCAAAAACACAGC 490
  AGAATGTGAAGGCAGTGTTTGATGCAGCCATTAAGGTAGTGTGCTGCAGCCTCCGAATAAAAAAAGAA 560
  AAAGTCAGGTGGTTGCTCAATATTATGATCAGATGAAGATTCTTCAAGTCTGAAAAAGATGGAAACCACT 630
  GCCAGCTTCTCGCTGCTGCTATCTATATCAATTTTACTCTTATTTTTTTTCTAGTTC AAGGAAAACAG 700
  CAAGCCATCATGTTTAGCATCAAGTCTTAACCTGACTTCTATGGACTTTCTGTGAAAGCATCAGGTGAT 770
  TTTGTTTCGTGTTTTTTACTTAGATGACAAGTATTCCTTGTAAAAA AAAAAAAAAAAAAAAAAAAAAA 839
  
```

Figure 2-4. cDNA sequences of *GhRac2* and *GhRac3*. A) The full-length cDNA sequence of *GhRac2* (GB mRNA ID [AY965615](#)) is 877 nucleotides. The protein-coding region (nucleotides 1-636) is underlined in red. The 3' UTR (nucleotides 637-877) is underlined in black. The translation start codon (nucleotides 1-3) is highlighted in yellow. The translation stop codon (nucleotides 633-636) is highlighted in green. The polyA tail (nucleotides 850-877) is highlighted in grey. B) The full-length cDNA sequence of *GhRac3* (GB mRNA ID [AY965614](#)) is 839 nucleotides. The protein-coding region (nucleotides 1-588) is underlined in red. The 3' UTR (nucleotides 589-839) is underlined in black. The translation start codon (nucleotides 1-3) is highlighted in yellow. The translation stop codon (nucleotides 585-588) is highlighted in green. The polyA tail (nucleotides 812-839) is highlighted in grey.

Translated with a web-based program from the ExPASy proteomics server [Gasteiger et al., 2003], the deduced GhRac2 (GB protein ID [AAX77218](#)) is a 211 amino acid polypeptide with a

predicted molecular weight of 23.3 kDa. Conserved domains found in all *Rop/Rac* G-proteins identified thus far are shown in Figure 2-5.

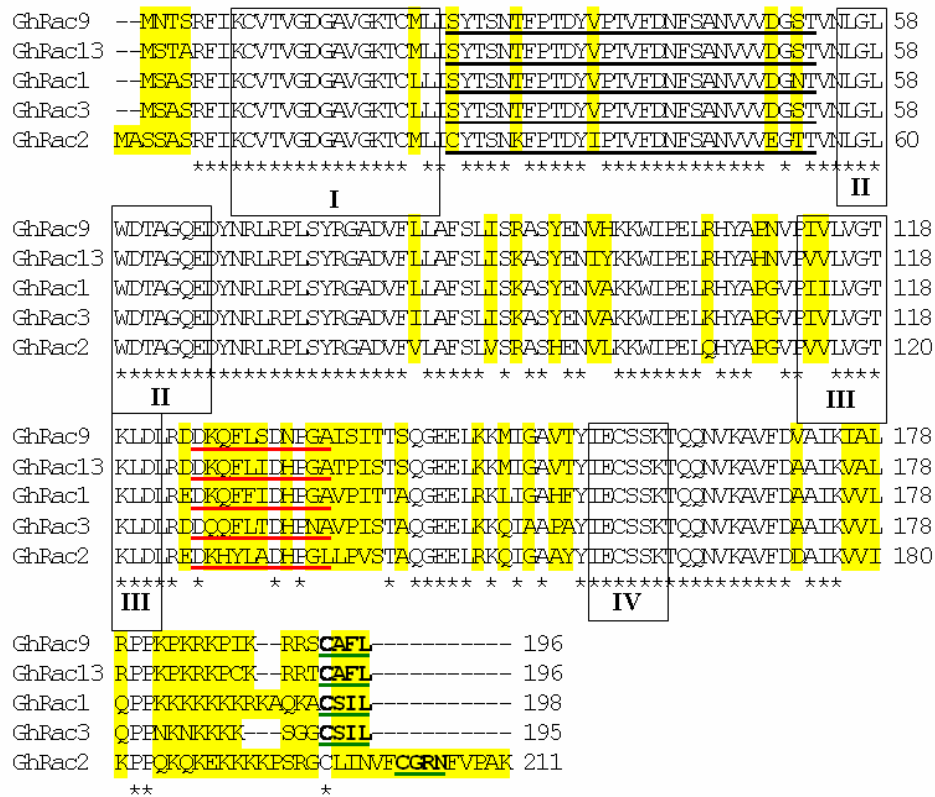


Figure 2-5. Multiple sequence alignment of the *Gossypium hirsutum* *Rop/Rac* G-proteins at the amino acid level. Amino acid sequences were aligned with CLUSTAL W [Thompson et al., 1994]. Amino acid differences are highlighted in yellow. The predicted *Rop/Rac* GTPase domains are boxed and labeled I and II. The predicted *Rop/Rac* guanine nucleotide binding domains are boxed and labeled II and IV. The predicted *Rop/Rac* effector domain is underlined in black. The predicted *Rho* insert region is underlined in red. The predicted *Rop/Rac* membrane localization domain is indicated by the boldface font and underlined in green.

The predicted *Rop/Rac* GTPase domains (amino acids 10-25, 58-67), predicted *Rop/Rac* effector domain (amino acids 27-55), predicted *Rop/Rac* guanine nucleotide binding domains (amino acids 115-123, 157-163), and predicted *Rho* insert region (amino acids 127-137), and the predicted *Rop/Rac* membrane localization domain (amino acids 203-206) were found in the open reading frame (Figure 2-5). We predict that this protein is post-translationally modified by the addition of palmitoyl residues, because GhRac2 does not terminate with the consensus carboxyl

motif CAAL (C = cysteine, A = an aliphatic amino acid, L = leucine) or CAAX (X = any amino acid, except leucine, Figure 2-5). Palmitoylated *Rop/Rac* G-proteins have been implicated in regulating plant defense responses [Kawasaki et al., 1999; Hassanain et al., 2000; Agrawal et al., 2003; Morel et al., 2004] and hormone responses [Lemichez et al., 2001; Li et al., 2001; Tao et al., 2002; Zheng et al., 2002].

***GhRac3* encodes a full-length *Rop/Rac* G-protein.** The cDNA sequence of *GhRac3* is illustrated in Figure 2-4B. Translated with a web-based program from the ExPASy proteomics server [Gasteiger et al., 2003], GhRac3 (GB protein ID [AAX77217](#)) is a 195 amino acid polypeptide with a predicted molecular weight of 21.2 kDa. The predicted *Rop/Rac* GTPase domains (amino acids 8-23, 56-65), the predicted *Rop/Rac* effector domain (amino acids 25-53), the predicted *Rop/Rac* guanine nucleotide binding domain (amino acids 113-121, 155-161), the predicted *Rho* insert region (amino acids 125-135), and the predicted *Rop/Rac* membrane localization domain (amino acids 192-195) were found in the open reading frame of GhRac3 (Figure 2-5). We postulate that GhRac3 undergoes prenylation post-translationally, because GhRac3 terminates with the consensus carboxyl motif CAAL (C = cysteine, A = any aliphatic amino acid, L = leucine, Figure 2-5). Other prenylated *Rop/Rac* G-proteins have been implicated in regulating polar cell division and elongation [Li et al., 1999; Fu et al., 2001; Fu et al., 2002, Molendijk et al., 2001; Jones et al., 2002; Chen et al., 2003].

Phylogenetic analysis of *GhRac2* and *GhRac3*. *GhRac2* showed the greatest sequence similarity to subfamily II *Rop/Rac* G-proteins from *Arabidopsis thaliana*; *GhRac3* showed the greatest sequence similarity to subfamily I *Rop/Rac* G-proteins from *Arabidopsis thaliana* (Figure 2-6).

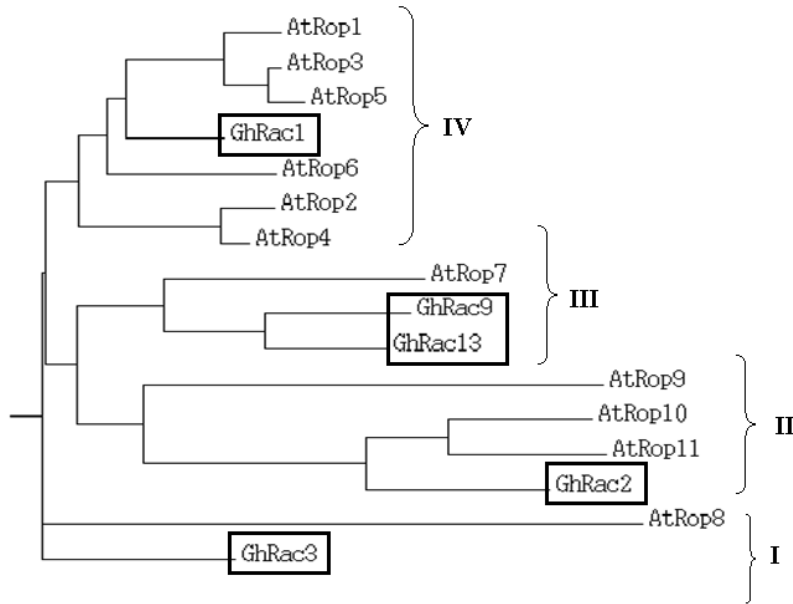


Figure 2-6. Phylogenetic analysis of the *Gossypium hirsutum* and *Arabidopsis thaliana* Rop/Rac G-proteins. The phylogenetic tree file was obtained from amino acids aligned with CLUSTAL W [Thompson et al., 1994]. A web-based program, Phylodendron Phylogenetic tree printer, created the phenogram [Gilbert 1997]. AtRop1 (*Arabidopsis thaliana*, GB protein ID [NP190698](#)); AtRop2 (GB protein ID [NP173437](#)); AtRop3 (GB protein ID [AAF40237](#)); AtRop4 (GB protein ID [NP177712](#)); AtRop5 (GB protein ID [NP195320](#)); AtRop6 (GB protein ID [NP195228](#)); AtRop7 (GB protein ID [NP199409](#)); AtRop8 (GB protein ID [NP566024](#)); AtRop9 (GB protein ID [NP194624](#)); AtRop10 (GB protein ID [NP566897](#)); AtRop11 (GB protein ID [NP201093](#)); GhRac1 (*Gossypium hirsutum*, GB protein ID [AAD47828](#)); GhRac2 (GB protein ID [AAX77218](#)), GhRac3 (GB protein ID [AAX77217](#)), GhRac9 (GB protein ID [Q41254](#)); and GhRac13 (GB protein ID [Q41253](#)). The *Gossypium hirsutum* Rop/Rac G-proteins are boxed. The Rop/Rac subfamilies are indicated by the Roman numerals (I-IV).

At the amino acid level, GhRac2 shared an 87% similarity with two *Arabidopsis* subfamily II Rop/Rac members AtRop10 and AtRop11, and a 73% similarity with the third *Arabidopsis* subfamily II Rop/Rac member, AtRop9. In addition, GhRac2 shared a 76%-80% deduced amino acid similarity with the cotton Rop/Rac G-proteins, GhRac1, GhRac9, and GhRac13. GhRac3 shared a 75% amino acid similarity with the only *Arabidopsis thaliana* subfamily I Rop/Rac member, AtRop8. GhRac3 also shared an 81%-87% deduced amino acid similarity with GhRac1, GhRac9, and GhRac13 and a 79% similarity with GhRac2.

Sequences released very recently by the TIGR database [http://www.tigr.org/tigr-scripts/tgi/T_index.cgi?species=cotton] revealed six tentative consensus sequences ([TC28011](#), [TC29458](#), [TC30900](#), [TC32824](#), [TC32825](#), and [TC38099](#)) for putative Rop/Rac G-proteins

assembled from expressed sequence tag clones from *Gossypium arboreum* [Wing et al., unpublished], *Gossypium raimondii* [Kim et al., unpublished], and *Gossypium hirsutum* [Blewitt et al., unpublished]. At the nucleotide level, *GhRac2* most closely identifies with TC38099 (Figure 2-7).

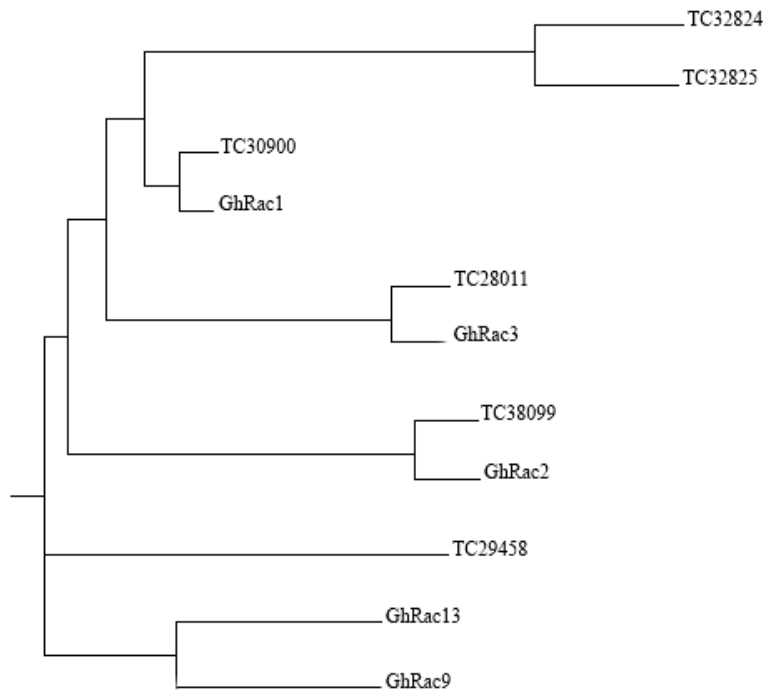


Figure 2-7. Phylogenetic analysis of the *Gossypium hirsutum* Rop/Rac G-proteins and the Rop/Rac G-protein TC sequences from the TIGR database. The phylogenetic tree file was obtained from the protein coding region and 3' UTR nucleotide sequences that were aligned with CLUSTAL W [Thompson et al., 1994]. The web-based program, Phylodendron Phylogenetic tree printer, created the phenogram [Gilbert, 1997].

The protein coding region and 3' UTR of *GhRac2* and TC38099 shared a 97% sequence similarity at the nucleotide sequence level. *GhRac3* is most closely related to TC28011 (Figure 2-7) with a 96% nucleotide sequence similarity.

***GhRac2* and *GhRac3* single nucleotide polymorphism analysis.** Single-nucleotide polymorphisms (SNPs) are the most frequent type of variation found in DNA [Brookes, 1999]. SNPs are a rich source of variability because of their high frequency of occurrence in genomes

[Brookes, 1999]. *Gossypium hirsutum* is a tetraploid species (AADD genome) that arose from a hybridization event that united an Old World diploid species (AA genome) and a New World diploid species (DD genome) [Brubaker et al., 1999; Wendel and Cronn, 2003]. Identifying single nucleotide polymorphisms in *GhRac2* and *GhRac3* could provide genetic markers useful to breeders for improving *Gossypium hirsutum* fiber length, strength, and quality. The SNP analysis of *GhRac2* and *GhRac3* compared to their closest TC sequences from *Gossypium raimondii* and *Gossypium arboreum* is listed in Table 2-1.

| Species | EST Clone Name | Full Length Sequence | # of Bases | Similarity with <i>GhRac2</i> | <i>GhRac2</i> SNP Location |
|----------------------------|----------------|----------------------|------------|-------------------------------|--|
| <i>Gossypium raimondii</i> | GR_Eb0038J16.f | No | 471 | 97% | 282, 448, 683, 720, 796, 851, 856, 862, 864 |
| | GR_Eb0038J14.r | No | 802 | 99% | |
| <i>Gossypium arboreum</i> | GA_Eb0024I13.f | No | 719 | 97% | 105, 253, 284, 292, 426, 435, 445, 521, 537, 552, 621, 640, 641, 651, 654, 659, 660, 661, 664, 707 |
| | GA_Eb0005K22.f | No | 567 | 97% | |

| Species | EST Clone Name | Full Length Sequence | # of Bases | Similarity with <i>GhRac3</i> | <i>GhRac3</i> SNP Location |
|----------------------------|----------------|----------------------|------------|-------------------------------|--|
| <i>Gossypium raimondii</i> | GR_Eb10C10.f | No | 684 | 99% | 387, 416, 668, 673, 674, 676, 683, 815, 839 |
| | GR_Eb10C10.r | No | 650 | 93% | |
| <i>Gossypium arboreum</i> | GA_Eb0011J19.f | No | 613 | 98% | 563, 565, 574, 629, 630, 640, 641, 644, 658, 659, 686, 689, 692, 694, 697, 699, 708, 710 |
| | GA_Eb0012E08.f | No | 690 | 91% | |

Table 2-1. Single nucleotide polymorphisms in *GhRac2* and *GhRac3*. A) *GhRac2*, the *Gossypium raimondii* EST clones GR_Eb0038J16.f and GR_Eb0038J14.r, and the *Gossypium arboreum* EST clones GA_Eb0024I13.f and GA_Eb0005K22.f. B) *GhRac3*, the *Gossypium raimondii* EST clones GR_Eb10C10.f and GR_Eb10C10.r, and the *Gossypium arboreum* EST clones GA_Eb0011J19.f and GA_Eb0012E08.f. The protein coding regions and 3' UTRs were aligned with CLUSTAL W [Thompson et al., 1994]. SNP locations are relative to the ATG start codon in *GhRac2* and *GhRac3*.

The results indicate that informative SNPs exist in *GhRac2* and *GhRac3* that could form the basis for distinguishing between the three species.

II. Gene expression of *GhRac2* and *GhRac3*

Total RNA was extracted from *Gossypium hirsutum* TM1, N1, and Li1 ovule tissue and TM1 fiber tissue at different developmental stages, using a phenol-based extraction protocol and precipitation with LiCl [Schultz et al., 1994]. A representative gel of purified total RNAs is illustrated in Figure 2-8.

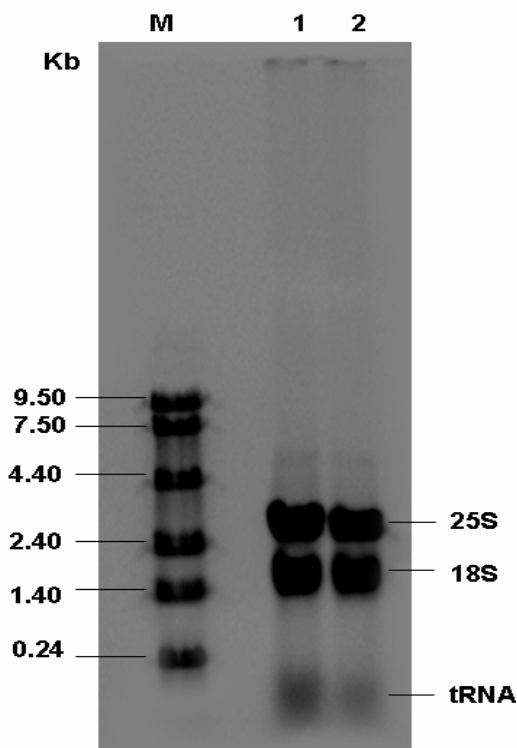


Figure 2-8. Representative total RNA gel. Five micrograms of total RNA was separated on a 0.8% (w/v) agarose gel. The gel was stained with ethidium bromide, visualized with the Bio-Rad Gel Doc 1000 imager, and analyzed with the Bio-Rad Molecular Analyst software. Lane M is the RNA molecular mass marker (Invitrogen). Lane 1 is 4 DPA TM1 ovule total RNA [4.7 mg/mL]. Lane 2 is 6 DPA TM1 ovule total RNA [2.1 mg/mL]. The 25S and 18S ribosomal RNA and tRNA bands are labeled.

The 25S ribosomal RNA band was ~ 3.0 kb, the 18S ribosomal RNA band was ~ 2.0 kb, and the tRNA band was less than 0.24 kb (Figure 2-8). Genomic DNA was often detected near the loading well when RNA gels were visualized (Figure 2-8). Even though each total RNA sample was precipitated in LiCl overnight, residual genomic DNA still co-purified. This problem was

mainly encountered when total RNA was extracted from ovule tissue. Therefore, in order to prevent problems with downstream applications, all total RNA samples were digested with DNaseI to eliminate contaminating genomic DNA.

III. Characterization of the *Gossypium hirsutum* Rop/Rac G-proteins

Cellular decisions concerning growth and development are reflected in altered patterns of gene expression. The ability to quantify transcript levels of specific genes has always been central to any research into gene function [Bustin, 2000]. Delmer et al. (1995) showed that *GhRac9* and *GhRac13* were developmentally regulated genes during cotton fiber development. Kim and Triplett (2004a) demonstrated that *GhRac1* was also developmentally regulated during cotton fiber development. Elucidation of the temporal and tissue-specific expression patterns of the newly cloned *GhRac2* and *GhRac3* genes will be important for defining their role in fiber development. Our lab previously characterized the temporal expression pattern of *GhRac1* and *GhRac13* using real-time reverse transcription PCR (Q-RT-PCR) and northern blot analysis [Kim and Triplett, 2004a]. Northern analysis provided information about mRNA size and integrity of the RNA sample. The main limitations of northern analysis are low sensitivity, large amounts of starting material are required, and the semi-quantitative nature of the analysis [Bustin 2000]. On the other hand, Q-RT-PCR measures the amplified PCR product at each cycle throughout the PCR reaction allowing the amplification to be followed in real-time during the exponential phase [Gachon et al., 2004]. Q-RT-PCR is a more advantageous technique since it was a quantitative method that provides reliable data rapidly, requires less starting material, can more specifically determine a target sequence than northern analysis, and is more sensitive than

northern analysis in detecting low abundance mRNAs [Gachon et al., 2004]. Since the temporal expression patterns of *GhRac1* and *GhRac13* as determined by real-time PCR were consistent with the results obtained by northern blot analysis, we chose Q-RT-PCR to test how *GhRac2* and *GhRac3* were regulated during fiber development.

Primer design. To verify the relative transcript levels of *GhRac2* and *GhRac3*, gene specific primers were designed using Primer Express software 2.0 from Applied Biosystems. The following important parameters were considered in the design of real-time PCR primers: (1) the G/C content of the primer pair was kept in the 20-80% range, (2) the T_m was kept between 58-60°C, and (3) the last five nucleotides at the 3' end did not contain more than two G and/or C base pairs [ABI User Bulletin No. 2]. Primer specificity was confirmed by analyzing the dissociation curves when the PCR reaction was complete.

Optimization of Q-RT-PCR conditions. The expression of two genes, *GhRac9* and *GhGLP1* was monitored as a test to show that all reaction conditions were optimal. Previously, the developmental regulation of *GhRac9* in cotton fiber was determined by Delmer et al. (1995) using northern blot analysis. Since Q-RT-PCR technology was unavailable at the time Delmer and colleagues published their results, we determined the expression pattern of *GhRac9* using Q-RT-PCR and compared our results with Delmer et al. (1995) results to verify that conditions for conducting Q-RT-PCR were optimized. Delmer and colleagues (1995) reported that the level *GhRac9* mRNA was lowest during fiber elongation and highest during secondary wall synthesis. The expression pattern of *GhRac9* transcript levels in TM1 10-20 DPA fiber using real-time PCR is illustrated in Figure 2-9.

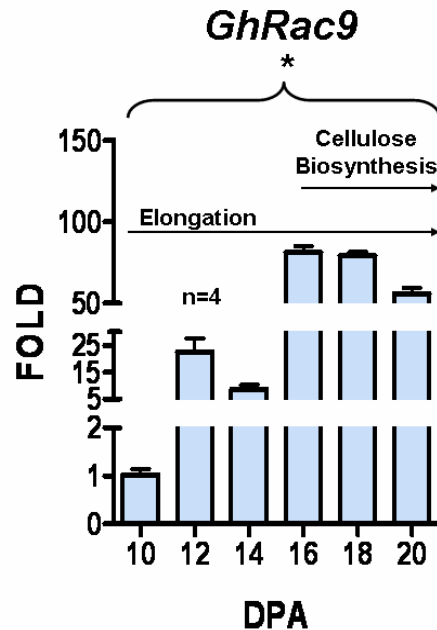


Figure 2-9. Developmental expression of *GhRac9* in TM1 fiber tissue. cDNA was synthesized from DNA-free total RNA by priming with random hexamer primers. Quantitative RT-PCR was performed using the SYBR® Green PCR master mix in the ABI Prism 7900HT Sequence Detection System (Applied Biosystems) with gene specific primers for *GhRac9*. The transcript levels of *GhRac9* are normalized with respect to the transcript level of cotton *α -tubulin4*. The asterisk (*) indicates significant difference and n indicates the sample size.

Transcript levels of *GhRac9* peaked at 16 and 18 DPA and were lowest at 10 DPA. Transcript abundance of *GhRac9* in 16 and 18 DPA fibers was 79 times higher than 10 DPA fibers (Figure 2-9). A one-way analysis of variance (ANOVA) with the Tukey-Kramer multiple comparison post-test was performed to compare the mean *GhRac9* transcript accumulation from 10 to 20 DPA in TM1 fiber. The ANOVA determined that the mean *GhRac9* transcription levels from 10 to 20 DPA in fiber was significantly different ($p < 0.0001$, $n = 6$). The Tukey-Kramer multiple comparison post-test confirmed the ANOVA result. *GhRac9* transcript levels were significantly different in 10 versus 12 DPA ($p < 0.01$), 14 versus 16 DPA ($p < 0.001$), and 18 versus 20 DPA ($p < 0.01$), but there was no significant difference in transcript accumulation between 12 versus 14 DPA ($p > 0.05$) and 16 versus 18 DPA ($p > 0.05$). Collectively, these results suggested that *GhRac9* transcripts levels were highest during the cellulose biosynthesis stage of fiber

development and lowest during the elongation stage, a result consistent with the results obtained by Delmer et al. (1995).

Kim and Triplett (2004b) reported that a germin-like protein (*GhGLP1*) showed tissue-specific accumulation in *Gossypium hirsutum* fiber. Expression of *GhGLP1* was regulated developmentally as shown by northern blot analysis. The abundance of *GhGLP1* transcripts was high during fiber elongation (10–14 DPA) and dropped dramatically when secondary cell wall synthesis began at ~ 16 DPA. The function of this protein in fiber growth and development remains unknown [Kim and Triplett, 2004b; Kim et al., 2004]. The temporal expression pattern of *GhGLP1* using real-time PCR is summarized in Figure 2-10.

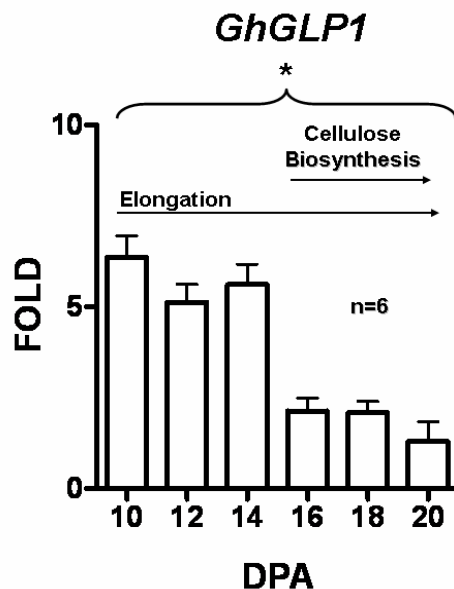


Figure 2-10. Developmental expression of *GhGLP1* in TM1 fiber tissue. The relative transcript abundance of *GhGLP1* measured by Q-RT-PCR with gene specific primers for *GhGLP1*. Conditions for Q-RT-PCR are identical to those shown in Figure 2-9. The transcript levels of *GhGLP1* are normalized with respect to the transcript level of cotton *α -tubulin4*. The asterisk (*) indicates a significant difference and n indicates the sample size.

The abundance of *GhGLP1* transcripts was three times higher during fiber elongation (10-14 DPA) and declined coincidentally with the transition to cellulose biosynthesis at 16 DPA. A one-way ANOVA analysis was performed and showed that the mean *GhGLP1* transcript levels were

significantly different ($p < 0.0001$, $n = 6$) in TM1 10-20 DPA fiber. The Tukey-Kramer multiple comparison post-test confirmed that the mean *GhGLP1* transcript accumulation in 10, 12, and 14 DPA TM1 fiber tissue (elongation stage) was significantly different from the mean *GhGLP1* transcript accumulation in 16, 18, and 20 DPA fiber tissue or the cellulose biosynthesis stage ($p < 0.001$). However, there was no significant difference among *GhGLP1* transcripts levels at 10, 12, or 14 DPA ($p > 0.05$) and at 16, 18, or 20 DPA ($p > 0.05$). The results were consistent with the results obtained by Kim and Triplett (2004b).

Developmental regulation of *GhRac2* and *GhRac3* in TM1 fiber. The temporal expression pattern of the *GhRac2* in TM1 10-20 DPA fibers is illustrated in Figure 2-11.

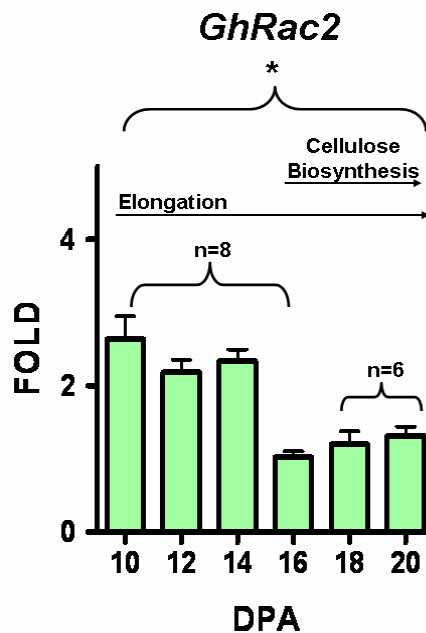


Figure 2-11. Developmental expression of *GhRac2* and in TM1 fiber tissue. The relative transcript abundance of *GhRac2* measured by Q-RT-PCR with gene specific primers for *GhRac2*. Conditions for Q-RT-PCR are identical to those shown in Figure 2-9. The transcript levels of *GhRac2* are normalized with respect to the transcript level of cotton *α -tubulin4*. The asterisk (*) indicates a significant difference and n indicates the sample size.

The transcript levels of *GhRac2* were highest during the period of fiber elongation (10-14 DPA) and decreased by half when cellulose biosynthesis begins (16-18 DPA). A one-way ANOVA analysis comparing *GhRac2* transcript levels in 10 to 20 DPA fiber suggested that the mean

transcript levels differ significantly ($p < 0.0001$, $n = 6$). The Tukey-Kramer post-test determined that *GhRac2* transcript level accumulation during the elongation stage (10-14 DPA) was significantly different from transcript accumulation during the cellulose biosynthesis stage (16-20 DPA, $p < 0.01$). However, there was no significant difference among *GhRac2* transcription levels between 10, 12, and 14 DPA or between 16, 18, and 20 DPA ($p > 0.05$). The significance of the real-time PCR results was that *GhRac2* was expressed at maximal stages of cotton fiber elongation (10-14 DPA) with transcripts levels significantly decreasing as fibers enter into the cellulose biosynthesis stage of development.

The temporal expression pattern of *GhRac3* in TM1 10-20 DPA fibers is illustrated in Figure 2-12.

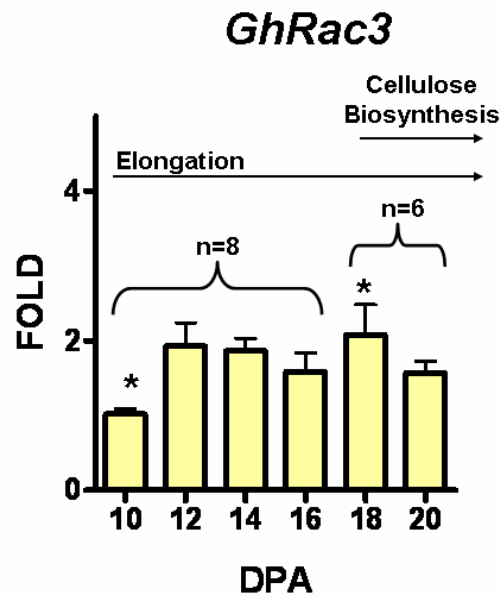


Figure 2-12. Developmental expression of *GhRac3* and in TM1 fiber tissue. The relative transcript abundance of *GhRac3* measured by Q-RT-PCR with gene specific primers for *GhRac3*. Conditions for Q-RT-PCR are identical to those shown in Figure 2-9. The transcript levels of *GhRac3* are normalized with respect to the transcript level of cotton *α -tubulin4*. The asterisk (*) indicates a significant difference and n indicates the sample size.

GhRac3 transcript levels doubled between 10 and 12 DPA and plateau from 14 to 20 DPA. A one-way ANOVA analysis comparing *GhRac3* transcript levels from 10 and 20 DPA suggested that the mean *GhRac3* transcript level was significantly different ($p=0.0453$, $n=6$). The Tukey-Kramer post-test determined that the only mean difference in *GhRac3* transcript levels that was significantly different was the *GhRac3* transcript level at 10 DPA compared to 18 DPA ($p<0.05$). The significance of the real-time PCR analysis of the temporal transcript expression pattern of *GhRac3* was that in TM1 fiber *GhRac3* transcripts increased during the elongation stage between 10 and 12 DPA and remained at a constant level throughout fiber development.

Comparison of the temporal expression pattern of cotton *Rop/Rac* GTPases in TM1, N1, and Li1 ovules on the day of anthesis. Several near-isogenic mutants in cotton are impaired in fiber development. One of these mutants, Naked Seed (N1) is impaired in fiber initiation. N1 mutants are completely devoid of fuzz fibers and have a substantial reduction in the number of lint fibers [Endrizzi et al., 1984]. A second mutant is Ligon lintless (Li1); Li1 mutants are impaired in fiber elongation. Li1 mutants are characterized by very short fiber [Kohel, 1974]. We compared the relative transcript abundance of *GhRac1*, *GhRac2*, *GhRac3*, *GhRac9*, and *GhRac13* between a genetic standard (TM1) and the two mutants (N1 and Li1) using Q-RT-PCR. Since lint fibers initiate elongation on the day of anthesis [Basra and Malik, 1984], we chose to measure transcript abundance for ovules.

Cotton *α -tubulin4* is preferentially expressed in cotton fiber and expressed at very low levels in other tissues such as ovules [Whittaker and Triplett, 1999]. We compared *Rop/Rac* G-protein transcript levels normalized with respect to the transcript level of *18S rRNA* and *Rop/Rac* G-protein transcript levels normalized with ubiquitin-conjugated protein (UCP), an enzyme that catalyzes the covalent attachment of ubiquitin to proteins targeted for degradation. We chose

18S rRNA and *UCP* as normalizers because they represent housekeeping genes that have been used as normalizers in other plant Q-RT-PCR experiments [Bustin, 2000; Kim et al., 2003; Burton et al., 2004; Iskandar et al., 2004].

The transcript levels of *GhRac1* in TM1, N1, and Li1 ovules normalized with respect to the transcript level of *18S rRNA* are shown in Figure 2-13A.

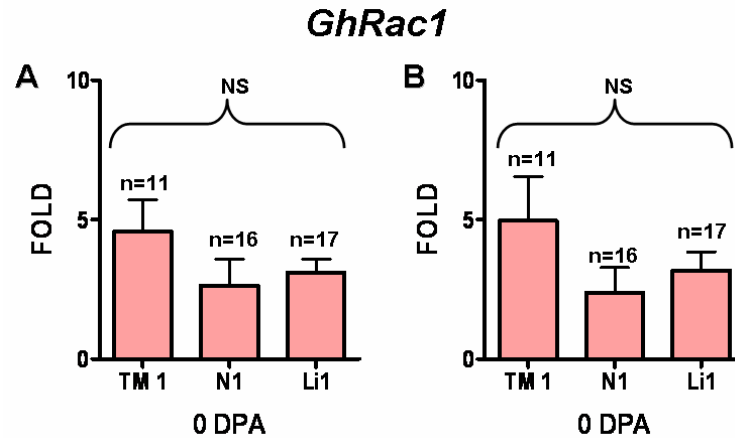


Figure 2-13. *GhRac1* transcript level comparison among *Gossypium hirsutum* TM1, N1, and Li1 ovules on the day of anthesis. The relative transcript abundance of *GhRac1* measured by Q-RT-PCR with gene specific primers for *GhRac1*. Conditions for Q-RT-PCR are identical to those shown in Figure 2-9. A) *GhRac1* transcript levels normalized with respect to the transcript level of *18S rRNA*. B) *GhRac1* transcript levels normalized with respect to the transcript level of *UCP*. NS indicates no significant difference and n equals the sample size.

There appeared to be slight differences among the genotypes in transcript accumulation; however, the one-way ANOVA analysis determined that the mean *GhRac1* transcript level was not significantly different in a wild type line (TM1) versus the two fiber mutants (N1 and Li1, $p=0.3010$, $n=3$). The Tukey-Kramer multiple comparison post-test confirmed the results obtained in the ANOVA analysis ($p>0.05$). Figure 2-13B illustrates the transcript levels of *GhRac1* in TM1, N1, and Li1 ovules normalized with respect to the transcript level of *UCP*.

Although it appeared that *GhRac1* transcripts accumulated more in TM1 than N1 and Li1, the ANOVA analysis determined that the mean *GhRac1* transcript level was not significantly

different in TM1, N1, or Li1 ovules ($p=0.2337$, $n=3$). The results obtained from the Tukey-Kramer post-test confirmed the ANOVA results ($p>0.05$).

The transcript levels of *GhRac2* in TM1, N1, and Li1 ovules normalized with respect to the transcript level of *18S rRNA* are shown in Figure 2-14A.

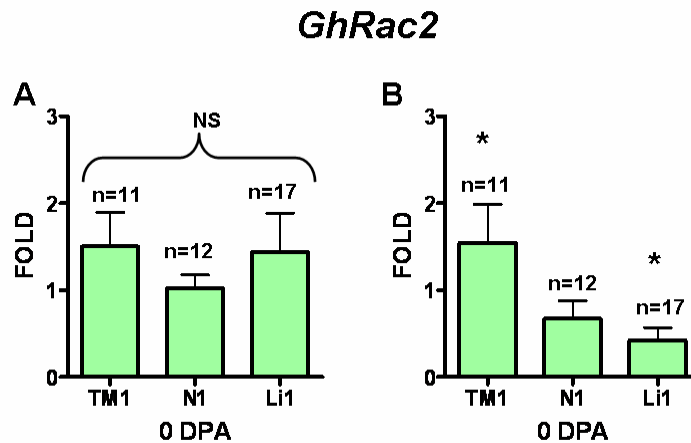


Figure 2-14. *GhRac2* transcript level comparison among *Gossypium hirsutum* TM1, N1, and Li1 ovules on the day of anthesis. The relative transcript abundance of *GhRac2* measured by Q-RT-PCR with gene specific primers for *GhRac2*. Conditions for Q-RT-PCR are identical to those shown in Figure 2-9. A) *GhRac2* transcript levels normalized with respect to the transcript level of *18S rRNA*. B) *GhRac2* transcript levels normalized with respect to the transcript level of *UCP*. The asterisks (*) indicate significant differences, NS indicates no significant difference, and n indicates the sample size.

GhRac2 transcripts accumulated at similar levels in TM1, N1, and Li1 ovules on the day of anthesis. A one-way ANOVA analysis determined that the mean *GhRac2* transcript level was not significantly different in TM1, N1, and Li1 ovules ($p=0.6592$, $n=3$). The Tukey-Kramer multiple comparison post-test confirmed the ANOVA analysis ($p>0.05$). When the transcript levels of *GhRac2* were normalized with respect to the transcript levels of *UCP*, a different profile resulted (Figure 2-14B). *GhRac2* transcripts accumulated the most in TM1 ovules and the least in Li1 ovules. The ANOVA analysis determined that the mean *GhRac2* transcript accumulation was significantly different in a wild type line versus two fiber-impaired mutants ($p=0.0189$, $n=3$). The results obtained from the Tukey-Kramer post-test determined that the *GhRac2*

transcript expression level was significantly different in TM1 ovules versus Li1 ovules ($p < 0.05$), but *GhRac2* transcript expression levels in TM1 versus N1 ovules and N1 ovules versus Li1 ovules was not significantly different ($p > 0.05$).

GhRac2 transcript levels in TM1, N1, and Li1 day of anthesis ovules were different depending on which normalizer gene was used. Relative gene expression comparisons work best when gene expression of the endogenous control, in this case *18S rRNA* or *UCP*, is more abundant than expression of the gene of interest (the cotton *Rop/Rac* G-proteins) and expression of the normalizer remains constant among the samples [Bustin, 2000]. We performed a cursory investigation of the cycle threshold (C_T) values for *18S rRNA* and *UCP*. The cycle threshold value is the cycle number at which the fluorescence generated within a reaction crosses a user-defined threshold [Bustin, 2000]. *UCP* and *18S rRNA* are more abundant in the transcriptome than the cotton *Rop/Rac* G-proteins, but the C_T values quantified for *UCP* were more constant among the TM1, N1, and Li1 ovule samples than the C_T values for *18S*, suggesting that *UCP* may be a more dependable normalizer than *18S rRNA*. In addition, the *UCP* C_T values were more similar to *GhRac2* C_T values than the *18S rRNA* C_T values. Bustin (2000) and Iskandar et al. (2004) report that the high abundance of *18S rRNA* may require template dilutions to bring *18S rRNA* measurement in the cDNA samples within the dynamic range of Q-RT-PCR. Template dilutions require more work and impose a level of potential error, adding to inaccuracy in the PCR analysis [Bustin, 2000]. The conclusion that *18S rRNA* transcripts may not be suitable normalizers for Q-RT-PCR of plant transcripts is consistent with the report of Burton et al. (2004), but varies from the findings of Kim et al. (2003) and Iskandar et al. (2004).

Collectively, these Q-RT-PCR results provide clues about the potential function of *GhRac2*. *GhRac2* is a subfamily II *Rop/Rac* G-protein (Figure 2-6). The GTP permanently

bound form of *OsRac1*, a subfamily II *Rop/Rac* G-protein from *Oryza sativa* (rice), induces H₂O₂ production and cell death in transgenic rice, and the DN form of *OsRac1* inhibits H₂O₂ production and cell death in transgenic rice [Kawasaki et al., 1999]. *AtRop9* and *AtRop10*, subfamily II *Rop/Rac* G-proteins from *Arabidopsis thaliana*, act as general negative regulators of the hormone abscisic acid in higher plants [Zheng et al., 2002]. In loss-of-function experiments, double null mutants of *AtRop9/AtRop10* specifically enhanced various abscisic acid responses, including increased seed dormancy, inhibition of seed germination and root elongation, and stimulation of stomatal closure [Zheng et al., 2002]. The Q-RT-PCR analysis of *GhRac2* in TM1, N1, and Li1 day of anthesis ovules does not suggest *GhRac2* involvement in hormone responses or stress responses, but Li et al. (1998) reported that *Arabidopsis* subfamily II *Rop/Rac* G-proteins were expressed in pollen tubes. The function of *AtRop9*, *AtRop10*, and *AtRop11* in pollen tubes is still undetermined. Several other *Arabidopsis* *Rop/Rac* G-protein members control the exaggerated growth in root hair development and pollen tubes; their common mechanism of regulating growth is actin cytoskeleton organization [Kost et al., 1999; Li et al., 1999; Molendijk et al., 2001; Fu et al., 2001; Fu et al., 2002; Jones et al., 20002]. The actin cytoskeleton plays an important role in cell morphogenesis in plants. The actin cytoskeleton is involved in the transportation of organelles and vesicles carrying membranes and cell wall components to sites of cell growth in root hairs, pollen tubes, and cotton fibers [Li et al., 2005]. Cotton fibers elongate by a combination of tip growth and diffuse growth [Seagull, 1990], and actin filaments may control the orientation of cortical microtubules during diffuse growth [Li et al., 2005]. In cotton and other higher plants, the regulation of actin cytoskeleton assembly remains unclear. Li et al. (2005) reported that actin is preferentially expressed in cotton fiber, developmentally regulated, and critical for fiber cell elongation. Our Q-RT-PCR results showing

maximum expression during fiber elongation suggest that *GhRac2* is involved in fiber expansion, a process that is regulated by actin cytoskeletal assembly. This hypothesis is further substantiated by the observation that accumulation of *GhRac2* transcripts in TM1 was significantly higher than *GhRac2* expression in a mutant impaired in fiber elongation (Li1).

The transcript levels of *GhRac3* in TM1, N1, and Li1 ovules normalized with *18S rRNA* are shown in Figure 2-15A.

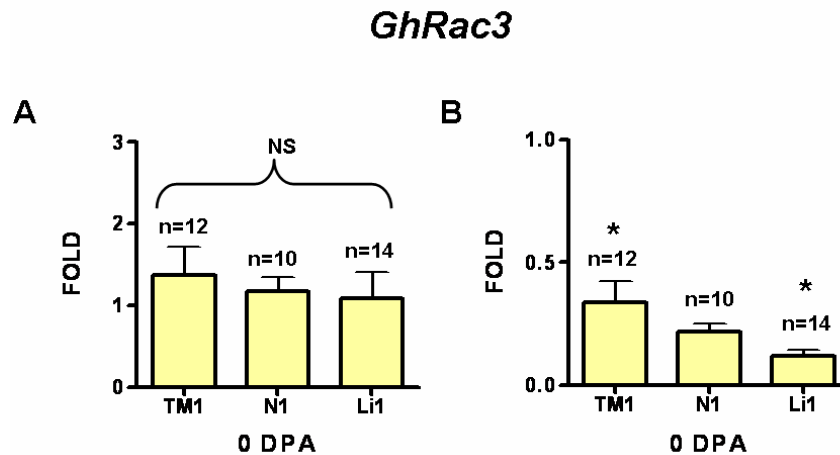


Figure 2-15. *GhRac3* transcript level comparison among *Gossypium hirsutum* TM1, N1, and Li1 ovules on the day of anthesis. The relative transcript abundance of *GhRac3* was measured by Q-RT-PCR with gene specific primers for *GhRac3*. Conditions for Q-RT-PCR were identical to those shown in Figure 2-9. A) *GhRac3* transcript levels normalized with respect to the transcript level of *18S rRNA*. B) *GhRac3* transcript levels normalized with respect to the transcript level of *UCP*. The asterisks (*) indicate significant differences, NS indicates no significant difference, and n indicates the sample size.

GhRac3 transcript levels were nearly identical in all three lines. The one-way ANOVA analysis results determined that the mean *GhRac3* transcript level in TM1, N1, and Li1 ovules on the day of anthesis was not significantly different ($p=0.7909$, $n=3$). The Tukey-Kramer multiple comparison post-test confirmed the ANOVA analysis results ($p>0.05$). Figure 2-15B illustrates the *GhRac3* transcripts levels in TM1, N1, and Li1 ovules normalized with respect to the transcript levels of *UCP*. *GhRac3* transcripts accumulated the most in TM1 ovules and the least in Li1 ovules. In addition, transcript levels accumulated more in N1 ovules than Li1 ovules. The

ANOVA analysis results determined that the mean *GhRac3* transcript accumulation in TM1, N1, and Li1 ovules on the day of anthesis was significantly different ($p=0.0382$, $n=3$). The results obtained from the Tukey-Kramer post-test determined that *GhRac3* transcript levels were significantly different in TM1 and Li1 ovules ($p<0.05$), but there was no significant difference in *GhRac3* transcript levels in N1 and Li1 ovules or in TM1 and N1 ovules on the day of anthesis ($p>0.05$).

Comparing the level of *GhRac3* transcript accumulation in TM1, N1, and Li1 ovules on the day of anthesis provided clues about the potential function of *GhRac3*. *GhRac3* is similar to the *Arabidopsis* subfamily I *Rop/Rac* G-protein, *AtRop8* (Figure 2-6). Although Li and colleagues (1998) demonstrated that *AtRop8* was preferentially expressed in pollen tubes, the function of *AtRop8* is still undetermined. The Q-RT-PCR results showing elevated expression of *GhRac3* immediately prior to the transition to secondary wall synthesis is intriguing. Higher levels of *GhRac3* expression in day of anthesis wild type ovules compared to a mutant impaired in fiber elongation (Li1) suggests that *GhRac3* may also be important for early stages of fiber elongation. Little is known about the regulation of this stage in fiber development.

Transcript levels of *GhRac9* in TM1, N1, and Li1 normalized with respect to *18S rRNA* transcripts are shown in Figure 2-16A.

GhRac9

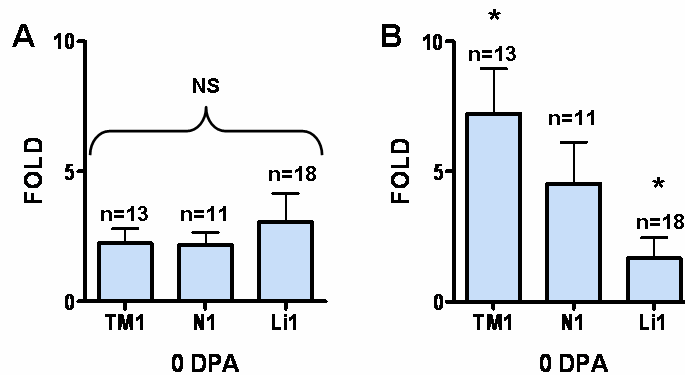


Figure 2-16. *GhRac9* transcript level comparison among *Gossypium hirsutum* TM1, N1, and Li1 ovules on the day of anthesis. The relative transcript abundance of *GhRac9* measured by Q-RT-PCR with gene specific primers for *GhRac9*. Conditions for Q-RT-PCR are identical to those shown in Figure 2-9. A) *GhRac9* transcript levels normalized with respect to the transcript level of *18S rRNA*. B) *GhRac9* transcript levels normalized with respect to the transcript level of *UCP*. The asterisks (*) indicate significant differences, NS indicates no significant difference, and n indicates the sample size.

GhRac9 transcripts accumulated more in Li1 ovules than either TM1 or N1 ovules, and *GhRac9* transcript levels were similar in TM1 and N1 ovules. The one-way ANOVA analysis determined that the mean *GhRac9* transcript level in TM1, N1, and Li1 day of anthesis ovules was not significantly different ($p=0.7236$, $n=3$). The results of the Tukey-Kramer multiple comparison post-test confirmed the ANOVA analysis ($p>0.05$). *GhRac9* transcript levels in TM1, N1, and Li1 ovules were also normalized with respect to the transcript level of *UCP* (Figure 2-16B). *GhRac9* transcripts accumulated 4.5 times more in TM1 ovules than in Li1 ovules and 1.6 times more in TM1 ovules than N1 ovules. The one-way ANOVA analysis results determined that the mean *GhRac9* transcript accumulation in TM1, N1, and Li1 ovules on the day of anthesis was significantly different ($p=0.0183$, $n=3$). The Tukey-Kramer post-test results reported that *GhRac9* transcript levels were significantly different in TM1 ovules versus Li1 ovules ($p<0.05$), but transcription expression was not significantly different between TM1 and N1 ovules or between N1 and Li1 ovules ($p>0.05$).

Similar to *GhRac2* and *GhRac3*, *GhRac9* transcripts were not significantly different in TM1, N1, and Li1 ovules when the *Rop/Rac* genes were normalized with *18S rRNA* transcripts. When the transcript levels of *GhRac2*, *GhRac3*, and *GhRac9* were standardized with respect to *UCP*, expression was significantly different in a wild type (TM1) compared to mutant impaired in fiber elongation (Li1). Expression of *GhRac2*, *GhRac3*, and *GhRac9* in the two fiber-impaired mutants was not significantly different. *GhRac2*, *GhRac3*, and *GhRac9* transcript levels expressed in a wild type versus a mutant impaired in fiber initiation (N1) was also not significantly different.

GhRac13 transcript levels in TM1, N1, and Li1 ovules normalized with respect to *18S rRNA* transcripts are shown in Figure 2-17A.

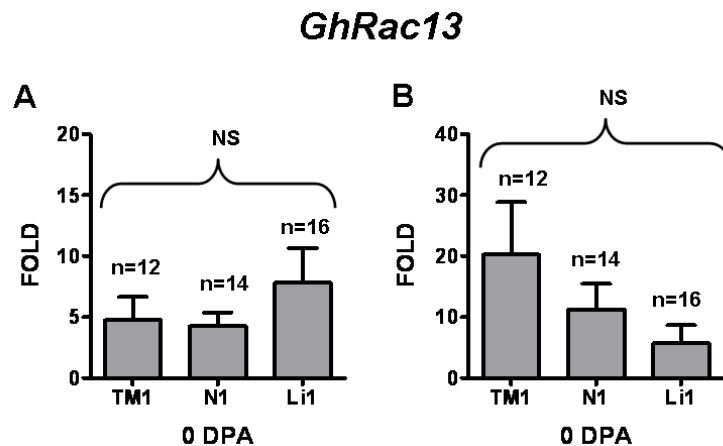


Figure 2-17. *GhRac13* transcript level comparison among *Gossypium hirsutum* TM1, N1, and Li1 ovules on the day of anthesis. The relative transcript abundance of *GhRac13* was measured by Q-RT-PCR with gene specific primers for *GhRac13*. Conditions for Q-RT-PCR are identical to those shown in Figure 2-9. A) *GhRac13* transcript levels normalized with respect to the transcript level of *18S rRNA*. B) *GhRac13* transcript levels normalized with respect to the transcript level of *UCP*. NS indicates no significant difference, and n indicates the sample size.

The one-way ANOVA analysis determined the mean *GhRac13* transcript level in TM1, N1, and Li1 ovules indicated was not significantly different ($p=0.4502$, $n=3$). The Tukey-Kramer multiple comparison post-test results confirmed the ANOVA analysis results ($p>0.05$). *GhRac13* transcripts were also normalized with respect to *UCP* transcript levels (Figure 2-17B).

When normalized with *UCP*, *GhRac13* transcripts accumulated to highest levels in TM1 ovules and to lowest levels in Li1 ovules. Transcripts accumulated 3.5 times more in TM1 ovules than in Li1 ovules. Transcripts accumulated two times more in TM1 ovules than N1 ovules and in N1 ovules than Li1. *GhRac13* transcript levels were analyzed statistically with a one-way ANOVA. Although the mean *GhRac13* transcription level appeared significant between TM1 and Li1 ovules (Figure 2-17B), the mean *GhRac13* transcript accumulation in TM1, N1, and Li1 ovules on the day of anthesis was not significantly different ($p=0.1840$, $n=3$). The results of the Tukey-Kramer post-test confirmed the ANOVA results ($p>0.05$).

Transcript levels of *GhRac1* (Figure 2-13) and *GhRac13* (Figure 2-17) in TM1, N1, and Li1 ovules harvested on the day of anthesis were not significantly different regardless of which gene was used as a normalizer. The C_T values of *GhRac1* and *GhRac13* were much higher than the C_T values of *GhRac2*, *GhRac3*, and *GhRac9*, indicating that *GhRac1* and *GhRac13* were less abundant mRNAs in the transcriptome compared to *GhRac2*, *GhRac3*, and *GhRac9*.

Temporal gene expression pattern of cotton *Rop/Rac* GTPases in TM1 and N1 ovules during fiber initiation and elongation. We compared the relative transcript expression pattern in *GhRac1*, *GhRac2*, *GhRac3*, *GhRac9*, and *GhRac13* during fiber initiation and elongation in ovules harvested from a wild type line (TM1) and a near isogenic fiberless mutant (N1) impaired in fiber initiation using Q-RT-PCR. Li1 was not included in the analysis, because insufficient tissue was harvested for total RNA extraction from plants grown during the summer of 2004. For these experiments, fiber tissue was not separated from developing TM1 and N1 ovules. From the results presented in Figures 2-13 to 2-17, *UCP* was used as the transcript normalizer. Based on C_T value alone, *UCP* and *18S rRNA* were more abundant in the

transcriptome than the cotton *Rop/Rac* G-proteins, but the C_T values quantified for *UCP* were more constant among the TM1, N1, and Lil ovule samples than the C_T values for *18S*, suggesting that *UCP* may be a more dependable normalizer than *18S rRNA*. Our conclusion that *18S rRNA* transcripts may not be suitable a normalizer for Q-RT-PCR of cotton ovule transcripts is consistent with the findings of Burton et al. (2004) in their Q-RT-PCR analysis of the cellulose synthase gene family in barley.

The expression pattern of *GhRac2* in TM1 0-10 DPA ovules during fiber initiation and elongation is shown in Figure 2-18A.

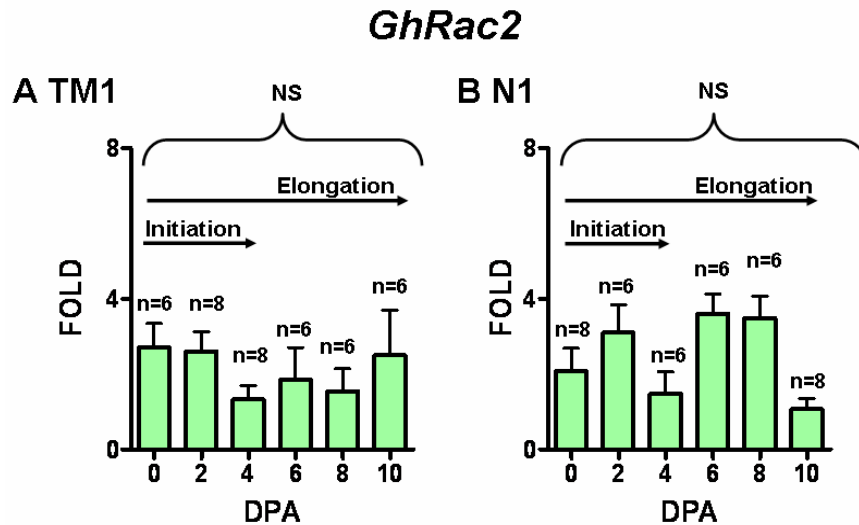


Figure 2-18. *GhRac2* transcript level comparison among *Gossypium hirsutum* TM1 and N1 ovules from 0 to 10 DPA. The relative transcript abundance of *GhRac2* measured by Q-RT-PCR with gene specific primers for *GhRac2*. Transcripts are normalized with respect to the transcript level of *UCP*. Conditions for Q-RT-PCR are identical to those shown in Figure 2-9. A) *GhRac2* transcript levels in TM1 ovules. B) *GhRac2* transcript levels in N1 ovules. NS indicates no significant difference, n indicates the sample size.

There appeared to be a slight dip in transcript levels at the middle range of fiber DPA; the results obtained from a one-way ANOVA analysis determined that the mean *GhRac2* transcript levels were not significantly different from 0-10 DPA in TM1 ovules ($p=0.6121$, $n=6$). The results of the Tukey-Kramer post-test affirmed the ANOVA analysis ($p>0.05$). The gene expression pattern of *GhRac2* in N1 0-10 DPA ovules during initiation and elongation was shown in Figure

2-18B. The results obtained from the ANOVA analysis determined that the mean *GhRac2* transcript levels were not significantly different from 0-10 DPA in the N1 ovules ($p=0.4769$, $n=6$). The Tukey-Kramer multiple comparison post-test confirmed the ANOVA results with two exceptions. Mean *GhRac2* transcript levels in N1 0-10 DPA ovules were only significantly different when comparing transcript levels at 6 versus 10 DPA ($p<0.05$) and 8 versus 10 DPA ($p<0.05$). Overall, these results determined that *GhRac2* transcripts remained at a constant level in ovules throughout fiber initiation and elongation even in a mutant that did not produce fiber.

GhRac3 transcripts in TM1 0 to 10 DPA ovules during initiation and elongation are shown in Figure 2-19A.

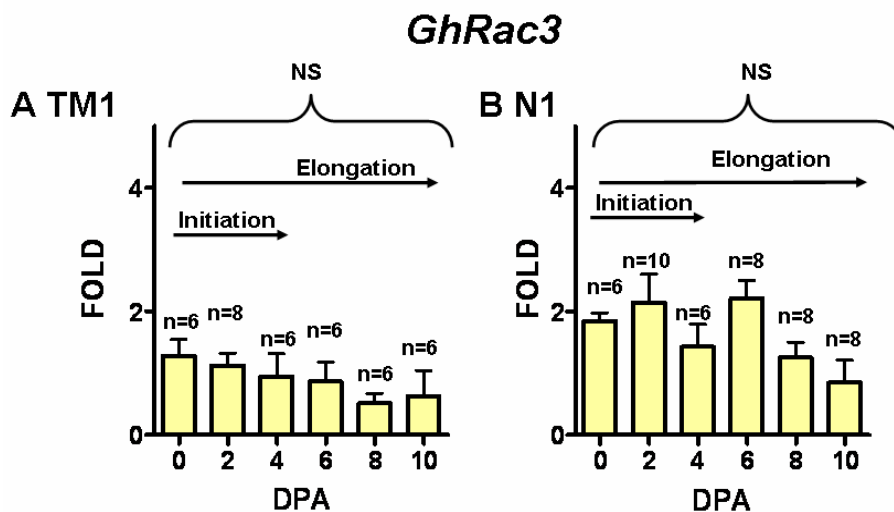


Figure 2-19. *GhRac3* transcript level comparison among *Gossypium hirsutum* TM1 and N1 ovules from 0 to 10 DPA. The relative transcript abundance of *GhRac3* measured by Q-RT-PCR with gene specific primers for *GhRac3*. Transcripts are normalized with respect to the transcript level of *UCP*. Conditions for Q-RT-PCR are identical to those shown in Figure 2-9. A) *GhRac3* transcript levels in TM1 ovules. B) *GhRac3* transcript levels in N1 ovules. NS indicates no significant difference, n indicates the sample size.

Although the figure suggests that *GhRac3* transcript levels were highest at 0 DPA (1X) and decrease as the ovules age, the ANOVA analysis determined that the mean *GhRac3* transcript levels were not significantly different from 0-10 DPA in TM1 ovules ($p=0.4088$, $n=6$). The Tukey-Kramer post-test results confirmed the ANOVA analysis results ($p>0.05$). The temporal

gene expression pattern of *GhRac3* in N1 0-10 DPA ovules during initiation and elongation is shown in Figure 2-19B. Results obtained from the ANOVA reported that the mean *GhRac3* transcript levels were not significantly different in N1 0-10 DPA ($p=0.0616$, $n=6$). The Tukey-Kramer post-test results affirmed the ANOVA results ($p>0.05$). These results determined that *GhRac3* transcripts remained at a constant level throughout fiber development, and *GhRac3* expression was not significantly different in a wild type versus the initiation-impaired N1 mutant.

Delmer et al. (1995) determined the transcription *GhRac9* expression pattern using northern blot analysis. Delmer and colleagues (1995) reported that *GhRac9* transcript expression was very low during fiber elongation and postulated that *GhRac9* may not be a very abundant mRNA in the transcriptome [Delmer et al., 1995]. The Q-RT-PCR analysis of the temporal gene expression pattern of *GhRac9* in TM1 and N1 0-10 DPA ovules during fiber initiation and elongation is illustrated in Figure 2-20A.

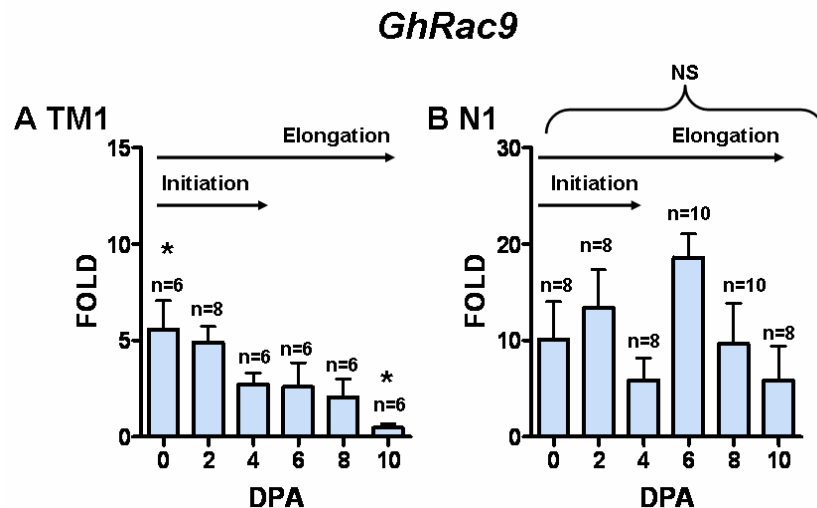


Figure 2-20. *GhRac9* transcript level comparison among *Gossypium hirsutum* TM1 and N1 ovules from 0 to 10 DPA. The relative transcript abundance of *GhRac9* measured by Q-RT-PCR with gene specific primers for *GhRac9*. Transcripts are normalized with respect to the transcript level of *UCP*. Conditions for Q-RT-PCR are identical to those shown in Figure 2-9. A) *GhRac9* transcript levels in TM1 ovules. B) *GhRac9* transcript levels in N1 ovules. The asterisks (*) indicate significant differences, NS indicates no significant difference, and n indicates the sample size.

GhRac9 transcript levels were highest at 0 DPA and declined as the ovules increased with age. The results obtained from the ANOVA analysis determined that the mean *GhRac9* transcript levels were significantly different from 0 to 10 DPA in TM1 ovules ($p=0.0251$, $n=6$), but the Tukey-Kramer post-test results obtained determined that the only significant difference in mean *GhRac9* transcript levels was the comparison between 0 DPA versus 10 DPA ($p<0.05$). The temporal gene expression of *GhRac9* in N1 0 to 10 DPA ovules is shown in Figure 2-20B. *GhRac9* transcript levels were highest at 6 DPA and lowest at 10 DPA. The results obtained from a one-way ANOVA analysis determined that the mean *GhRac9* transcript accumulation was not significantly different from 0 to 10 DPA in N1 ovules ($p=0.0999$, $n=6$). The Tukey-Kramer multiple comparison analysis confirmed the ANOVA results ($p>0.05$).

Our analysis of the temporal gene expression pattern of *GhRac9* using Q-RT-PCR contrasted with the previous results indicating that *GhRac9* may not be a very abundant mRNA in the fiber transcriptome. Our Q-RT-PCR analysis suggested that *GhRac9* was an abundant mRNA in elongating *Gossypium hirsutum* fibers. The difference may be explained by the increased sensitivity of real-time reverse transcription PCR as an analytical method for measuring RNA abundance versus northern blot analysis [Gachon et al., 2004].

Attempts to determine the temporal expression patterns of *GhRac1* and *GhRac13* in TM1 and N1 0 to 10 DPA ovules were unsuccessful. The C_T value for these reactions was ≥ 40 . A C_T value of 40 means very little amplification has occurred [ABI User Bulletin No. 2]. It is quite possible that *GhRac1* and *GhRac13* are not abundant mRNAs in *Gossypium hirsutum* ovules. It may be possible to obtain temporal expression profiles of less abundant genes with a more sensitive SYBR® green assay. Recently, Bio-Rad announced a new SYBR® green Q-RT-PCR mix purportedly more sensitive than the SYBR® Green mix from Applied Biosystems.

Tests were conducted to determine if the Bio-Rad SYBR® green mix could detect low abundance mRNAs, such as *GhRac1* and *GhRac13*. Again, the temporal patterns of *GhRac1* and *GhRac13* in TM1 and N1 ovule tissue from 0 to 10 DPA could not be determined. The SYBR® Green mix from both commercial sources resulted in C_T values ≥ 40 for both *GhRac1* and *GhRac13*.

Conclusions. Two full-length *Rop/Rac* G-protein cDNAs, *GhRac2* and *GhRac3*, were cloned and sequenced from *Gossypium hirsutum*. *GhRac2* and *GhRac3* were PCR amplified from cDNA prepared from 4 DPA TM1 ovules, representing the early phases of cotton fiber development. *GhRac2* shows the greatest sequence similarity to subfamily II and *GhRac3* shares the greatest sequence similarity to subfamily I of the *Rop/Rac* G-protein family from *Arabidopsis thaliana*. At present, the functions of *GhRac2* and *GhRac3* remain an enigma. The role of *Rop/Rac* genes in regulating growth in *Arabidopsis thaliana* pollen tubes [Lin and Yang, 1997; Li et al., 1998; Zheng and Yang, 2000a; Fu and Yang, 2001; Fu et al., 2001; Fu et al., 2002; Chen et al., 2003] and root hairs [Fu and Yang, 2001; Molendijk et al., 2001; Jones et al., 2002], two cells with exaggerated polar growth, suggested that elucidating the function of cotton *Rop/Rac* G-proteins might provide important clues about the regulation of cotton fiber development. By monitoring changes in *GhRac2* and *GhRac3* transcript levels in wild type ovules, a mutant impaired in fiber elongation, and a mutant impaired in fiber initiation, we aimed to provide supporting evidence for the roles of these genes in fiber development. Based on our analysis of gene expression using real-time reverse transcription PCR, *GhRac2* and *GhRac3* may be involved in fiber elongation. Cotton fibers elongate by a combination of tip growth and diffuse growth [Seagull, 1990]. During diffuse growth, actin filaments are required for the reorganization of microtubules and may control their orientation [Li et al., 2005]. Actin is

preferentially expressed in cotton fiber, is developmentally regulated, and is critical for fiber cell elongation [Li et al., 2005]. Regulation of the actin cytoskeleton organization is unclear in cotton and other higher plants. The Q-RT-PCR results suggests that *GhRac2* and *GhRac3* may not be important for fiber initiation, because *GhRac2* and *GhRac3* transcripts are not significantly different between a wild type and a mutant impaired in fiber initiation. The Q-RT-PCR results suggest that *GhRac2* and *GhRac3* may be transcriptionally regulated during fiber elongation. *GhRac2* and *GhRac3* transcript levels are significantly lower in ovules from a mutant impaired in fiber elongation when compared to wild type. Maximal *GhRac2* expression occurs during stages of fiber development when the rate of elongation is highest with transcript levels significantly decreasing as fibers enter into the secondary cell wall biosynthesis stage. *GhRac3* transcript levels double from 10 to 12 DPA and remain fairly constant as fibers enter the cellulose biosynthesis stage of fiber development. This result suggests that *GhRac3* may participate in signaling events responsible for the transition from elongation to secondary wall thickening. Since the timing of the transition period is a critical determinant for fiber quality parameters, additional inquiry into the function of *GhRac3* may have significance for improving cotton fiber quality, a long term objective of the cotton fiber bioscience team.

References

- Agrawal GK, Iwahashi H, Rakwal R (2003) Small GTPase *Rop*: molecular switch for plant defense responses, *FEBS Lett* 546(2-3):173-80.
- Altschul SF, Gish W, Miller W, Myers EW, Lipman DJ (1990) Basic local alignment search tool, *J Mol Biol*, 215: 403–410.
- Altschul SF, Madden TL, Schaffer AA, Zhang J, Zhang Z, Miller W, Lipman DJ (1997) Gapped BLAST and PSI-BLAST: a new generation of protein database search programs, *Nucleic Acids Res* 17:3389-402.
- Ambion, TURBO DNA-free™ DNase Treatment and Removal Protocol, Version 0405, 3-5.
- Arabidopsis* Genome Initiative (2000) Analysis of the genome sequence of the flowering plant *Arabidopsis thaliana*, *Nature* 408: 796-815.
- Applied Biosystems, User Bulletin No. 2, ABI PRISM 7700 Sequence Detection System, Revision A, 11–14.
- Basra AS, Malik CP (1984) Development of the cotton fiber, *Int Rev Cytol* 89: 65-113.
- Basra AS, Saha S (1999) Growth Regulation of Cotton Fibers, *In* AS Basra [ed.] *Cotton Fibers: Developmental Biology, Quality Improvement, and Textile Processing*, 47-58. Food Products Press, Binghamton, NY.
- Baxter-Burrell A, Yang Z, Springer PS, Bailey-Serres J (2002) *RopGAP4*-dependent *Rop* GTPase rheostat control of *Arabidopsis* oxygen deprivation tolerance. *Science* 296(5575): 2026-8.
- Bernard P, Gabant P, Bahassi EM, Couturier M (1994) Positive-selection vectors using the F plasmid *ccdB* killer gene, *Gene* 148: 71-74.
- Bio-Rad, Quantum Prep™ Freeze ‘N Squeeze DNA Gel Extraction Spin Columns, Revision B.
- Bischoff F, Molendijk A, Rajendrakumar CS, Palme K (1999) GTP binding proteins in plants, *Cell Mol Life Sci* 55(2): 233-256.
- Bischoff F, Vahlkamp L, Molendijk A, Palme K (2000) Localization of *AtRop4* and *AtRop6* and interaction with the guanine nucleotide dissociation inhibitor *AtRhoGDII* from *Arabidopsis*, *Plant Molec Biol* 42: 515-530.
- Blewitt M, Matz EC, Davy DF, Burr B (1999) ESTs from developing cotton fiber, GenBank unpublished data.

- Boguski M, McCormick F (1993) Proteins regulating *Ras* and its relatives, *Nature* 366: 643-654.
- Brookes AJ (1999) The essence of SNPs, *Gene* 234:177-186.
- Brubaker CL, Patterson AH, Wendel JF (1999) Comparative genetic mapping of allotetraploid cotton and its diploid progenitors, *Genome* 42: 184-203.
- Burrige K, Wennerberg K (2004) *Rho* and *Rac* take center stage, *Cell* 116(2): 167-179.
- Burton RA, Shirley NJ, King BJ, Harvey AJ, Fincher GB (2004) The *CesA* gene family of barley. Quantitative analysis of transcripts reveals two groups of co-expressed genes, *Plant Physiol* 134: 224-236.
- Bustin SA (2000) Absolute quantification of mRNA using real-time reverse transcription polymerase chain reaction assays, *J Molec Endo*, 25: 169-193.
- Campbell PM, Der CJ (2004) Oncogenic *Ras* and its role in tumor cell invasion and metastasis, *Seminars Cancer Biol* 14(2): 105-114.
- Chen CY, Cheung AY, Wu H (2003) Actin polymerizing factor mediates *Rac/Rop* GTPase-regulated pollen tube growth, *Plant Cell* 15: 237-249.
- Chou Q, Russel M, Birch D, Raymond J, Bloch W (1992) Prevention of pre-PCR mis-priming and primer dimerization improves low-copy-number amplifications, *Nucl Acids Res* 20: 1717-1723.
- Clontech, Marathon™ cDNA Amplification Kit User Manual Protocol Number PT1115-1, Version PR15735, 28-32.
- DeLanghe E (1986) Lint Development, *In* JR Mauney and J Stewart [eds.] *Cotton Physiology* Number One The Cotton Foundation Reference Book Series, 325-349. The Cotton Foundation, Memphis, TN.
- Delmer DP (1999) Cellulose Biosynthesis in Developing Cotton Fibers, *In* AS Basra [ed.] *Cotton Fibers: Developmental Biology, Quality Improvement, and Textile Processing*, 85-112. Food Products Press, Binghamton, NY.
- Delmer DP, Pear JR, Andrawis A, Stalker DM (1995) Genes encoding small GTP-binding proteins analogous to mammalian *Rac* are preferentially expressed in developing cotton fibers, *Mol Gen Genet* 248(1): 43-451.
- Drivas G, Shih A, Coutavas E, Rush MG, D'Eustachio P (1990) Characterization of four novel *Ras*-related genes expressed in a human teratocarcinoma cell line, *Mol Cell Biol* 10: 1793-1798.

- Endrizzi JE, Turcotte EL, Kohel RJ (1984) Qualitative Genetics, Cytology, and Cytogenetics, *In* RJ Kohel and CF Lewis [eds.], Cotton, Agronomy Monograph No. 24, 81-129. Crop Science Society of America, Madison, WI.
- Etienne-Manneville, S (2004) *Cdc42*-the centre of polarity, *J Cell Science* 117: 1291-1300.
- Fu Y, Li H, Yang Z (2002) The *Rop2* GTPase controls the formation of cortical fine F-actin and the early phase of directional cell expansion during *Arabidopsis* organogenesis, *Plant Cell* 14: 777-794.
- Fu Y, Wu G, Yang Z (2001) *Rop* GTPase-dependent dynamics of tip-localized F-actin controls tip growth in pollen tubes, *J Cell Biol* 152: 1019-1032.
- Fu Y, Yang Z (2001) *Rop* GTPase: a master switch of cell polarity development in plants, *Trends Plant Sci* 6: 545-547.
- Fujisawa Y, Kato H, Iwasaki Y (2001) Structure and function of heterotrimeric G-proteins in plants, *Plant Cell Physiol* 42(8): 789-794.
- Gachon C, Mingam A, Charrier B (2004) Real-time PCR: What relevance to plant studies? *J Exp Bot* 55(402): 1445-1454.
- Gasteiger E, Gattiker A, Hoogland C, Ivanyi I, Appel RD, Bairoch A (2003). ExPASy: the proteomics server for in-depth protein knowledge and analysis, *Nucleic Acid Res* 31: 3784-3788.
- Gilbert DG (1997) PhyloDendron, Java software for phylogenetic tree drawing. Bionet Software, <http://iubio.bio.indiana.edu/treeapp/> (Accessed March 2005).
- Gu Y, Vernoud V, Fu Y, Yang Z (2003) *Rop* GTPase regulation of pollen tube growth through the dynamics of tip-localized F-actin, *J Exp Botany* 54(380): 93-101.
- Gu Y, Wang Z, Yang Z (2004) *Rop/Rac* GTPase: an old new master regulator for plant signaling, *Curr Opin Plant Biol* 7: 527-536.
- Hassanain HH, Sharma YK, Moldovan L, Khramtsov V, Berliner LJ, Duvick JP, Goldschmidt-Clermont PJ (2000) Plant Rac proteins induce superoxide production in mammalian cells, *Biochem Biophys Res Commun* 272(3): 783-788.
- Heyworth PG, Knaus UG, Settleman J, Curnutte JT, Bokoch GM (1993) Regulation of NADPH oxidase activity by Rac GTPase activating protein(s), *Mol Biol Cell* 11:1217-1223.
- Invitrogen, TOPO® XL PCR Cloning Kit Manual, Version M, 9-13.

- Iskandar HM, Simpson RS, Casu RE, Bonnett GD, Maclean DJ, Manners JM (2004) Comparison of reference genes for quantitative real-time polymerase chain reaction analysis of gene expression in sugarcane, *Plant Molec Bio Rep* 22: 325-337.
- Jones A, Assmann S (2004) Plants: the latest model system for G-protein research, *EMBO Rep* 5(6): 572-578.
- Jones M, Shen J, Fu Y, Li H, Yang Z, Grierson C (2002) The *Arabidopsis Rop2* GTPase is a positive regulator of both root hair inhibition and tip growth, *Plant Cell* 14: 763-776.
- Josefsson LG, Rask L (1997) Cloning of a putative G-protein-coupled receptor from *Arabidopsis thaliana*, *Eur J Biochem* 249(2): 415-20.
- Kahn RA, Gilman AG (1986) The protein cofactor necessary for ADP-ribosylation of Gs by cholera toxin is itself a GTP Binding Protein, *J Biol Chem* 261(17): 7906-7911.
- Kawasaki T, Henmi K, Ono E, Hatakeyama S, Iwano M, Satoh H, Shimamoto K (1999) The small GTP-binding protein *Rac* is a regulator of cell death in plants, *Proc Nat Acad Sci, USA* 96(19): 10922-10926.
- Kim BR, Nam HY, Kim SU, Kim SI, Chang YJ (2003) Normalization of reverse transcription quantitative-PCR with housekeeping genes in rice *Biotechnol Lett* 21: 1869-1872.
- Kim H, Yu, Y, Kudrna D, Hatfield J, Stum D, Mueller C, Udall JA, Rapp RA, Wendel JF, Rao K, Soderlund C, Wing RA (2004) Global assembly of cotton ESTs, GenBank unpublished data.
- Kim HJ, Charalambopoulos J, Triplett BA (2000) Isolation of a cDNA encoding a *Rac* like G-Protein from immature cotton locules (Accession No. AF165925) from cotton (*Gossypium hirsutum* L.), PGR00-012, *Plant Physiol* 122: 291.
- Kim HJ, Pesacreta TC, Triplett BA (2004) Cotton-fiber germin-like protein II: immunolocalization, purification, and functional analysis, *Planta* 218(4): 525-35
- Kim HJ, Triplett BA (2001) Cotton fiber growth in planta and in vitro. Models for plant cell elongation and cell wall biogenesis, *Plant Physiol* 127: 1361-1366.
- Kim HJ, Triplett BA (2004a) Characterization of *GhRac1* GTPase expressed in developing cotton (*Gossypium hirsutum* L.) fibers, *Biochim Biophys Acta* 1679(3): 214-221.
- Kim HJ, Triplett BA (2004b) Cotton fiber germin-like protein I. Molecular cloning and gene expression, *Planta* 218: 516-524.

- Kohel RJ (1999) Cotton Germplasm Resources and the Potential for Improved Fiber Productivity and Quality, *In* AS Basra [ed.] Cotton Fibers: Developmental Biology, Quality Improvement, and Textile Processing, 167-182. Food Products Press, Binghamton, NY.
- Kohel RJ, Lewis CF, Richmond TR (1970) Texas Marker-1: description of a genetic standard for *Gossypium hirsutum*, *Crop Sci* 10: 670–671.
- Kohel RJ, Quisenberry JE, Benedict CR (1974) Fiber elongation and dry weight changes in mutant lines of cotton, *Crop Sci* 14: 471-474.
- Kost B, Lemichez E, Spielhofer P, Hong Y, Tolia K, Carpenter C, Chua NH (1999) *Rac* homologues and compartmentalized phosphatidylinositol 4, 5-bisphosphate act in a common pathway to regulate polar pollen tube growth, *J Cell Biol* 145(2): 317-330.
- Lavy M, Bracha-Drori K, Sternberg H, Yalovsky S (2002) A cell-specific, prenylation-independent mechanism regulates targeting of type II *Racs*, *Plant Cell* 14: 2431-2450.
- Lee JA (1984) Cotton as a World Crop. *In* RJ Kohel and CL Lewis [eds.], Cotton, Agronomy Monograph No. 24, 1-25. Crop Science Society of America, Madison, WI.
- Lemichez E, Wu Y, Sanchez JP, Mettouchi A, Mathur J, Chua NH (2001) Inactivation of *AtRac1* by abscisic acid is essential for stomatal closure, *Genes & Dev* 15: 1808-1816.
- Li H, Jun-Jiang S, Zhi-Liang Z, Yakang L, Yang Z (2001) The *Rop* GTPase switch controls multiple developmental processes in *Arabidopsis*, *Plant Physiol* 126: 670-684.
- Li H, Lin Y, Heath RM, Zhu MX, Yang Z (1999) Control of pollen tube tip growth by a *Rop* GTPase-dependent pathway that leads to tip-localized calcium influx, *Plant Cell* 11: 1731-1742.
- Li H, Wu G, Ware D, Davis KR, Yang Z (1998) *Arabidopsis* *Rho*-related GTPases: differential gene expression in pollen and polar localization in fission yeast, *Plant Physiol* 118: 407–417.
- Li XB, Fan XP, Wang XL, Cai L, Yang WC (2005) The cotton *ACTIN1* gene is functionally expressed in fibers and participates in fiber elongation, *Plant Cell* 17: 859-875.
- Lin Y, Yang Z (1997) Inhibition of pollen tube elongation by microinjected anti-Rop1Ps antibodies suggests a crucial role for *Rho*-type GTPases in the control of tip growth, *Plant Cell* 9: 1647-1659.
- Livak KJ, Schmittgen TD (2001) Analysis of relative gene expression data using real-time quantitative PCR and the $2^{(-\Delta\Delta C_T)}$ method, *Methods* 4: 402-8.

- Ma H, Yanofsky MF, Meyerowitz EM (1990) Molecular cloning and characterization of *GPA1*, a G-protein α subunit gene from *Arabidopsis thaliana*, Proc Nat Acad Sci, USA 87: 3821–3825.
- Mackay DJ, Hall A (1998) *Rho* GTPases, J Biol Chem 273: 20685–20688.
- Mason MG, Botella JR (2000) Completing the heterotrimer: isolation and characterization of an *Arabidopsis thaliana* G-protein γ -subunit cDNA, Proc Nat Acad Sci, USA 97: 14784–14788.
- Mason MG, Botella JR (2001) Isolation of a novel G-protein γ -subunit from *Arabidopsis thaliana* and its interaction with G β , Biochim Biophys Acta 1520: 147–153.
- Memon AR (2004) The role of ADP ribosylation factor and *SARI* in vesicular trafficking in plants, Biochim Biophys Acta 1664(1): 9-30.
- Molendijk AJ, Bischoff F, Chadalavada S, Rajendrakumar V, Friml J, Braun M, Gilroy S, Palme K (2001) *Arabidopsis thaliana Rop* GTPases are localized to tips of root hairs and control polar growth, EMBO 20: 2779-2788.
- Molendijk AJ, Ruperti B, Palme K (2004) Small GTPases in vesicle trafficking, Curr Opin Plant Biol 7(6): 694-700.
- Morel J, Fromentin J, Blein JP, Simon-Plas F, Elmayan T (2004) *Rac* regulation of NtrbohD, the oxidase responsible for the oxidative burst in elicited tobacco cell, Plant J 37(2): 282-93.
- Morrison TB, Weis JJ, Wittwer CT (1998) Quantification of low-copy transcripts by continuous SYBR Green I monitoring during amplification, Biotechniques 6: 954-8, 960, 962.
- National Cotton Council. <http://www.cotton.org> (accessed March 2005).
- Pandey S, Assmann SM (2004) The *Arabidopsis* putative G-protein-coupled receptor, *GCR1*, interacts with the G-protein α -subunit, *GPA1* and regulates abscisic acid signaling, Plant Cell 16(6):1616-32.
- Park J, Gu Y, Lee Y, Yang Z, Lee Y (2004) Phosphatidic acid induces leaf cell death in *Arabidopsis* by activating the *Rho*-related small G-protein GTPase-mediated pathway of reactive oxygen species generation, Plant Physiol 134:129-136.
- Plakidou-Dymock S, Dymock D, Hooley R (1998) A higher plant seven-transmembrane receptor that influences sensitivity to cytokinins, Curr Biol 8(6): 315-24.
- Potikha TS, Collins CC, Johnson DI, Delmer DP, Levine A. (1999) The involvement of hydrogen peroxide in the differentiation of secondary walls in cotton fibers, Plant Physiol 119: 849–858.

Promega, Technical Bulletin Number 117, Wizard Plus Minipreps DNA Purification System, 3-6.

Qiagen, RNeasy Mini Handbook, Third Edition, 76-81.

Qiu JL, Jilk R, Marks MD, Szymanski DB (2002) The *Arabidopsis SPIKE1* gene is required for normal cell shape control and tissue development, *Plant Cell* 14: 101–118.

Ridley AJ, Hall A (1992) The small GTP-binding protein *Rho* regulated the assembly of focal adhesions and actin stress fibers in response to growth factors, *Cell* 70: 389-399.

Ridley AJ, Patterson HF, Johnston CL., Diekmann D., Hall A (1992) The small GTP-binding protein *Rac* regulates growth factor-induced membrane ruffling, *Cell* 70: 401-410.

Sambrook J, Fritsch EF, Maniatis T (1989) *Molecular Cloning: A Laboratory Manual*, 2nd ed. Cold Spring Harbor Laboratory Press, Cold Spring Harbor, New York.

Schultz DJ, Craig R, Cox-Foster D, Mumma R, Medford J (1994) RNA isolation from recalcitrant plant tissue, *Plant Mol Bio Rep* 12(4): 310-316.

Seagull RW (1990) Tip Growth and Transition to Secondary Wall Synthesis in Developing Cotton Hairs, *In* IB Heath [eds.], *Tip Growth in Plant and Fungal Cells*, 261-284 Academic Press, San Diego, CA.

Sharkey DJ, Scalice ER, Christy KG Jr, Atwood SM, Daiss JL (1994) Antibodies as thermolabile switches: high temperature triggering for the polymerase chain reaction, *Biotechnology* 5: 506-9.

Shuman S (1994) Novel approach to molecular cloning and polynucleotide synthesis using *Vaccinia* DNA topoisomerase, *J Biol Chem* 269: 32678-32684.

Suharsono U, Fujisawa Y, Kawasaki T, Iwasaki Y, Satoh H, Shimamoto K (2002) The heterotrimeric G-protein α -subunit acts upstream of the small GTPase *Rac* in disease resistance of rice, *Proceedings National Academy of Sciences, USA* 99: 13307–13312.

Takai Y, Sasaki T, Matozaki T (2001) Small GTP-binding proteins, *Physiol Rev* 81(1): 154-208.

Tao LZ, Cheung AY, Wu HM (2002) Plant *Rac*-like GTPases are activated by auxin and mediate auxin-responsive gene expression, *Plant Cell* 14(11): 2745-60.

The Institute of Genomic Research.

http://www.tigr.org/tigrscripts/tgi/T_index.cgi?species=cotton (accessed March 2005)

- Thompson JD, Higgins DG, Gibson TJ (1994) CLUSTAL W: improving the sensitivity of progressive multiple sequence alignment through sequence weighting, position-specific gap penalties, and weight matrix choice, *Nucleic Acids Res* 22: 4673-4680.
- Thuring RWJ, Sanders JPM, Borst P (1975). A freeze-squeeze method for recovering long DNA from agarose gels, *Anal Biochem* 66: 213-220.
- Tranin T, Shmuel M, Delmer DP (1996) In vitro prenylation of the small GTPase *Rac13* of cotton *Plant Physiol* 112: 1491-1497.
- Ullah H, Chen JG, Temple B, Boyes DC, Alonso JM, Davis KR, Ecker JR, Jones AM (2003) The β -subunit of the *Arabidopsis* G-protein negatively regulates auxin-induced cell division and affects multiple developmental processes, *Plant Cell* 15: 393–409.
- Ullah H, Chen JG, Wang S, Jones AM (2002) Role of G-protein in regulation of *Arabidopsis* seed germination, *Plant Physiol* 129: 897–907.
- Ullah H, Chen JG, Young J, Im KH, Sussman MR, Jones AM (2001) Modulation of cell proliferation by heterotrimeric G-protein in *Arabidopsis*, *Science* 292: 2066–2069.
- United States Department of Agriculture Economic Research Service. <http://www.ers.usda.gov> (accessed March 2005).
- Vernoud V, Horton AC, Yang Z, Nielson E (2003) Analysis of the small GTPase superfamily of *Arabidopsis*, *Plant Physiol* 131(3): 1191-1208.
- Wang X-Q, Ullah H, Jones AM, Assmann SM (2001) G-protein regulation of ion channels and abscisic acid signalling in *Arabidopsis* guard cells, *Science* 292: 2070–2072.
- Wendel JF, Cronn RC (2003) Polyploidy and the evolutionary history of cotton, *Adv Agronomy* 78: 139-186.
- Weiss CA, Garnaat CW, Mukai K, Hu Y, Ma H (1994) Isolation of cDNAs encoding guanine nucleotide-binding protein β -subunit homologues from maize (*ZG β 1*) and *Arabidopsis* (*AG β 1*), *Proceedings National Academy of Sciences, USA* 91: 9554–9558.
- Whittaker DJ, Triplett BA (1999) Gene specific changes in alpha tubulin transcript accumulation in developing cotton fibers, *Plant Physiol* 121: 181-188.
- Wing RA, Frisch D, Yu Y, Main D, Rambo T, Simmons J, Henry D, Wood TC, Leslie A, Wilkins TA (2000) An integrated analysis of the genetics, development, and evolution of the cotton fiber, GenBank unpublished data.
- Winge P, Brembu T, Bones AM (1997) Cloning and characterization of *Rac*-like cDNAs from *Arabidopsis thaliana*, *Plant Mol Biol* 35(4): 483-495.

- Winge P, Brembu T, Kristensen R, Bones AM (2000) Genetic structure and evolution of *Rac* GTPases in *Arabidopsis thaliana*, *Genetics* 156: 1959-1971.
- Wu G, Li H, Yang Z (2000) *Arabidopsis RopGAPs* are a novel family of *Rho* GTPase-activating proteins that require the *Cdc42/Rac*-interactive binding motif for *Rop*-specific GTPase stimulation, *Plant Physiol* 124: 1625-1636.
- Yalovsky S, Rodriguez-Concepcion M, Gruissem W (1999) Lipid modifications of proteins-slipping in and out of membranes, *Trends Plant Sci* 4: 439-445.
- Yang Z (2002) Small GTPases: versatile signaling switches in plants, *Plant Cell Supplement*, S375-S388.
- Yang Z, Watson JC (1993) Molecular cloning and characterization of *Rho*, a *Ras*-related small GTP-binding protein from the garden pea, *Proc Nat Acad Sci, USA* 90: 8732-8736.
- Zheng ZL, Nafisi M, Tam A, Li H, Crowell DN, Chary SN, Schroeder JI, Shen J, Yang Z (2002) Plasma membrane-associated *Rop10* small GTPase is a specific negative regulator of abscisic acid responses in *Arabidopsis*, *Plant Cell* 14(11): 2787-2797.
- Zheng ZL, Yang Z (2000a) The *Rop* GTPase switch turns on polar growth in pollen, *Trends Plant Sci* 5:298-303.
- Zheng ZL, Yang Z (2000b) The *Rop* GTPase: an emerging signaling switch in plants, *Plant Mol Biol* 44: 1-9.

Appendix 1

Buffers, media, and reagents

Agarose (0.8%)²

In a baked 500 mL glass container, add 1.6 g Ultra Pure™ Agarose (Invitrogen) to 200 mL H₂O. Swirl gently. Microwave on high power ~ 2 minutes to dissolve agarose. Cool to 65°C before use. Store at room temperature.

Boric Acid Stock Solution (0.5 M)

Dissolve 7.73 g boric acid (MW= 61.83) into 225 mL H₂O. Adjust the final volume to 250 mL with H₂O. Add 0.1% (v/v) of DEPC. Shake well. Let stand under a chemical fume hood, overnight. Autoclave for 20 minutes, 121°C, 20 psi. Store at room temperature.

Diethylpyrocarbonate (DEPC)-treated Water

Add 0.1% (v/v) of DEPC to 1 L of H₂O. Shake well. Let stand under a chemical fume hood, overnight. Autoclave for 20 minutes, 121°C, 20 psi. Store at room temperature.

DNA Gel Loading Buffer (6X)

0.25% bromophenol blue (w/v)

0.25% xylene cyanol (w/v)

15% Ficoll type 400 (w/v)

Adjust volume to 10 mL with H₂O. Store at room temperature.

Ethanol Solution (70%)

In a baked 500 mL glass container, add 175 mL of absolute ethyl alcohol (200 proof) to 325 mL DEPC-treated H₂O. Label for RNA use only. Store at -20°C.

Ethidium Bromide Solution (10 mg/mL)

Prepare under chemical fume hood. Dissolve 100 mg ethidium bromide in 10 mL H₂O. Vortex. Wrap in foil. Store at 4°C.

Ethylenediaminetetraacetic Acid (EDTA) Solution, pH 8.0 (0.2 M)³

Dissolve 3.7 g EDTA disodium salt dihydrate (MW= 372.26) in 30 mL DEPC-treated H₂O. Add 10 M NaOH until pH reaches 8.0. Adjust final volume to 50 mL with the addition of DEPC-treated H₂O. Filter sterilize with a 0.22 µM Nalgene filter unit (Nalge Nunc International, Rochester, NY). Store at room temperature in a baked glass container labeled for RNA use only.

² Prepare agarose (0.8%) for RNA gel electrophoresis with DEPC-treated H₂O.

³ EDTA does not go into solution until the pH of the solution is adjusted to ~ 8.0 with the addition of NaOH [Sambrook et al., 1989].

Appendix 1 (continued)

Ethylene Glycol Bis-N,N,N',N'-Tetraacetic Acid (EGTA) Solution, pH 8.0 (0.2 M)⁴

Dissolve 19.02 g EGTA (MW= 380.4) in 200 mL DEPC-treated H₂O. Adjust pH to 8.0 with the addition of 10 M NaOH. Adjust final volume to 250 mL with the addition of DEPC-treated H₂O. Filter sterilize with a 0.22 μM Nalgene filter unit. Store at room temperature in a baked glass container labeled for RNA use only.

Glycerol Solution (80%)

Pour 80 mL glycerol into 20 mL H₂O. Vortex. Autoclave for 20 minutes, 121°C, 20 psi. Store at room temperature.

Kanamycin Stock Solution (50 ug/mL)

Dissolve 0.25g kanamycin in 5 mL autoclaved H₂O (final volume). Vortex. Filter sterilize with a 0.22 μM Nalgene filter unit. Store as 1 mL aliquots at -20°C.

Luria-Bertani (LB) Liquid Media

Dissolve 10 g bacto-tryptone, 5 g bacto-yeast extract, and 10 g NaCl into 900 mL distilled H₂O. Adjust pH to 7.0 with the addition of 5 M NaOH. Adjust final volume to 1 L with the addition of H₂O. Divide into 4 glass containers (250 mL each). Autoclave for 20 minutes, 121°C, 20 psi. Store at room temperature.

LB plates

Dissolve 2.5 g bacto-tryptone, 1.25 g bacto-yeast extract, 2.5 g NaCl, and into 200 mL distilled H₂O. Adjust pH to 7.0 with the addition of 5 M NaOH. Adjust final volume to 250 L with the addition of H₂O. Add 3.3 g bacto-agar and dissolve. Autoclave for 20 minutes, 121°C, 20 psi. Place in a 65°C water bath for 30 minutes before adding 150 μL of kanamycin stock solution (50 μg/mL). Pour ~30 mL per plate. Allow to harden at room temperature. Store plates at 4°C.

Lithium Chloride Solution (8 M)

Dissolve 17.0 g LiCl (MW= 42.4) into 30 mL H₂O. Adjust final volume to 50 mL with the addition of H₂O. Add 0.1% (v/v) DEPC. Shake well. Let stand under a chemical fume hood, overnight. Autoclave for 20 minutes, 121°C, 20 psi. Store at room temperature.

3% Polyvinylpyrrolidone (PVPP): Chloroform Solution

Prepare under a chemical fume hood. In a 500 mL baked glass container, dissolve 9 g of PVPP (high molecular weight) in 300 mL chloroform. Do not autoclave. Store at room temperature under a chemical fume hood. Shake well before use.

⁴ EGTA does not go into solution until the pH of the solution is adjusted to ~ 8.0 with the addition of NaOH [Sambrook et al., 1989].

Appendix 1 (continued)

React 3 Buffer (10X)

500 mM Tris-HCl, pH 8.0 (final concentration)

100 mM MgCl₂ (final concentration)

1 M NaCl (final concentration)

This buffer is purchased from Invitrogen.

RNA Dye (2X)

Prepare under a chemical fume hood.

0.25% bromophenol blue (w/v)

0.25% xylene cyanol (w/v)

1 mM EDTA, pH 8.0 (final concentration)

50% glycerol

1 mg/ml ethidium bromide solution (final concentration)

Adjust final volume to 10 mL with DEPC-treated H₂O. Divide into 2.0 mL aliquots. Store at -80°C.

Sodium Acetate Solution (3 M)

Dissolve 12.3 g sodium acetate (MW= 82.03) into 30 mL H₂O. Add glacial acetic acid until the pH is 5.2. Adjust the final volume to 50 mL with the addition of H₂O. Add 0.1% (v/v) of DEPC. Shake well. Let stand under a chemical fume hood, overnight. Autoclave for 20 minutes, 121°C, 20 psi. Store at room temperature.

Sodium Chloride (NaCl) Solution (5 M)

Dissolve 143 g NaCl (MW= 58.44) in 450 mL H₂O. Adjust final volume to 500 mL with H₂O. Add 0.1% (v/v) of DEPC. Shake well. Let stand under a chemical fume hood, overnight. Autoclave for 20 minutes, 121°C, 20 psi. Store at room temperature.

Sodium Dodecyl Sulfate (SDS) Solution (10%)

Dissolve 10 g SDS (MW= 288.38) into 90 mL DEPC-treated H₂O. Heat solution to 65°C to assist in dissolution. Adjust final volume to 100 mL with DEPC-treated H₂O. Filter sterilize with a 0.22 µm Nalgene filter unit. Store at room temperature.

Sodium Hydroxide (NaOH) Solution (5 M)

Prepare under a chemical fume hood. In a baked glass container, dissolve 20 g of NaOH (MW= 40.0) into 80 mL H₂O. Adjust final volume to 100 mL with the addition of H₂O.

Appendix 1 (continued)

SOC Liquid Media

Dissolve 20 g bacto-tryptone and 5 g bacto-yeast extract in 900 mL H₂O. Add 2 mL of 5 M NaCl (10 mM final concentration), 2.5 mL of 1 M KCl (2.5 mM final concentration), 10 mL of 1 M MgCl₂ (10 mM final concentration), and 10 mL of 1 M MgSO₄ (10 mM final concentration). Adjust pH to 7.0 with 5 M NaOH. Adjust volume to 980 mL with the addition of H₂O. Autoclave for 20 minutes, 121°C, 20 psi. Cool to 60°C and add 20 mL of sterile 1 M glucose (20 mM final concentration). This media is supplied in the TOPO[®] XL PCR Cloning Kit (Invitrogen).

Total RNA Extraction Buffer

In a baked 500 mL glass container, dissolve 30 g of *p*-aminosalicylic acid (6% final concentration) and 5 g polyvinylpyrrolidone (MW= 40,000, 1% final concentration) into 50 mL of 1 M Tris-HCl (pH 8.0) solution (100 mM final concentration), 125 mL of 0.2M EGTA (pH 8.0) solution (50 mM final concentration), 10 mL of 5 M NaCl solution (100 mM final concentration 100), and 50 mL 10% SDS solution (1% final concentration). Adjust final volume to 500 mL with the addition of DEPC-treated H₂O. Do not autoclave. Wrap container in foil. Store at room temperature under a chemical fume hood. Just before use, aliquot 15 mL total RNA extraction buffer/total RNA tissue sample in a baked glass container. Add 1% β -mercaptoethanol and an equal volume of 3% PVPP: chloroform solution.

Total RNA Re-suspension Buffer

In a baked 500 mL glass container, add 25 mL of 0.5 M boric acid solution (final concentration 25 mM), 25 mL of 1 M Tris-HCL (pH 8.0) solution (final concentration 50 mM), 3.13 mL of 0.2 M EDTA (pH 8.0) solution (final concentration 1.25 mM), and 10 mL of 5 M NaCl solution (final concentration 0.1 M). Adjust volume to 500 mL with DEPC-treated H₂O. Do not autoclave. Store under chemical fume hood at room temperature.

Tris-Borate-EDTA (TBE) Buffer (1X)⁵

In a baked 1 L glass container, dissolve 1 packet of Ultra Pure TBE Gel Running Mate (89 mM Tris, 89 mM boric acid, and 2 mM EDTA, pH 8.3 (Invitrogen) into 900 mL H₂O. Adjust final volume to 1 L with the addition of H₂O. Store at room temperature.

Tris-HCl Stock Solution, pH 8.0 (1.0 M)

Dissolve 60.6 g Trizma base (MW= 121.14) into 400 mL DEPC-treated H₂O. Add concentrated HCl (~12 M) until pH is 8.0. Adjust final volume to 500 mL. Autoclave for 20 minutes, 121°C, 20 psi. Store at room temperature.

⁵ TBE buffer (1X) for RNA gel electrophoresis was prepared with DEPC-treated H₂O.

Appendix 1 (continued)

Preparation of plasticware, glassware, electrophoresis equipment, and pH meter for RNA work

Soak all plasticware in distilled H₂O and treat all with 0.1% (v/v) of DEPC. Let stand under a chemical fume hood, overnight. Autoclave for 20 minutes, 121°, 20 psi. Cool to room temperature before use. Treat all glassware with a small volume of RNaseZap (Ambion), rinse twice with DEPC-treated water, and bake (12 hours at 212°C) to remove contaminating RNases. Cool to room temperature before use. Treat all electrophoresis equipment with a small amount of RNaseZap, rinse twice with DEPC-treated water, and dry before use. Treat pH meter electrode with a small volume of Electro Zap (Ambion) and rinse electrode with DEPC-treated water.

Appendix 2

3'-Rapid Amplification of cDNA Ends PCR Primers

| <u>Name</u> | <u>Sequence</u> | <u>Purpose</u> |
|-------------|--|---|
| G1 | 5'-ATGAGYRCYKCVARRTTYATMAARTGY-3' Translation codes: Y= C+T, R= A+G, K= G+T, V= A+C+G, M= A+C | Degenerate forward primer designed to amplify the protein-coding region and 3' UTR from a <i>Gossypium hirsutum</i> Rop/Rac G-protein from any subfamily. |
| G2 | 5'-ATGGCTTCAAGCGCTTCAAGATTTATC-3' | Forward primer designed to amplify the protein-coding region and 3' UTR from a <i>Gossypium hirsutum</i> subfamily II Rop/Rac G-protein. |
| Nic1 | 5'-ATGAGCGCCTCGAGATTCATAAAGTGC-3' | Forward primer designed to amplify the protein-coding region and 3' UTR from a <i>Gossypium hirsutum</i> subfamily I Rop/Rac G-protein. |

Appendix 3

Real-time Reverse Transcription PCR Primers

| <u>Name</u> | <u>Sequence</u> | <u>Purpose</u> |
|------------------|----------------------------------|--|
| <i>GhRac2-F</i> | 5'-GAGGAACTTCGTGCCTGCTAA-3' | Forward primer used with <i>GhRac2-R</i> to amplify a 71 base pair fragment of the <i>GhRac2</i> gene. |
| <i>GhRac2-R</i> | 5'-GCAAGAGGAACACAAGCATTG-3' | Reverse primer used with <i>GhRac2-F</i> . |
| <i>GhRac3-F</i> | 5'-AGATTGCGGCTCCTGCATAC-3' | Forward primer used with <i>GhRac3-R</i> to amplify a 71 base pair fragment of the <i>GhRac3</i> gene. |
| <i>GhRac3-R</i> | 5'-TGCATCAAACACTGCCTTCAC-3' | Reverse primer used with <i>GhRac3-F</i> . |
| <i>NicRac9-F</i> | 5'-ACGTCGAGGTTTATCAAGTGTGTC-3' | Forward primer used with <i>NicRac9-R</i> to amplify a 73 base pair fragment of the <i>GhRac9</i> gene. |
| <i>NicRac9-R</i> | 5'-TTGCTAGTATACGAAATAAGCATGCA-3' | Reverse primer used with <i>NicRac9-F</i> . |
| <i>GhRac1-F</i> | 5'-GAAATGGATTCCAGAATTGAGACA-3' | Forward primer used with <i>GhRac1-R</i> to amplify a 73 base pair fragment of the <i>GhRac1</i> gene. |
| <i>GhRac1-R</i> | 5'-TGTTGGGACTAAGCTTGATCTT-3' | Reverse primer used with <i>GhRac1-F</i> . |
| <i>GhRac13-F</i> | 5'-GTGAAGGCTGTTTTTCGATGCT-3' | Forward primer used with <i>GhRac13-R</i> to amplify a 73 base pair fragment of the <i>GhRac13</i> gene. |

Appendix 3 (continued)

| | | |
|----------------------|-------------------------------|--|
| <i>GhRac13-R</i> | 5'-CCAAAGAGAAAGCCTTGCAAAA-3' | Reverse primer used with <i>GhRac13-F</i> . |
| <i>GhGLP1-F</i> | 5'-CCGTACCGCAGGCAACAC-3' | Forward primer used with <i>GhGLP1-R</i> to amplify a 70 base pair fragment of the <i>Gossypium hirsutum</i> germin-like protein gene. |
| <i>GhGLP1-R</i> | 5'-CGGGAATTGAGTCGAAAAGG-3' | Reverse primer used with <i>GhGLP1-F</i> . |
| <i>UCP-F</i> | 5'-CGGAAAGAGGTGAAGATGTCAAC-3' | Forward primer used with <i>UCP-R</i> to amplify a 74 base pair fragment of the ubiquitin-conjugating enzyme protein gene. |
| <i>UCP-R</i> | 5'-GGATCTTGCTGCAACCTCTTAAA-3' | Reverse primer used with <i>UCP-F</i> . |
| <i>18S rRNA-F</i> | 5'-CGTCCCTGCCCTTTGTACA-3' | Forward primer used with <i>18S rRNA-R</i> to amplify a 61 base pair fragment of the 18S ribosomal subunit gene. |
| <i>18S rRNA-R</i> | 5'-AACACTTCACCGGACCATTC-3' | Reverse primer used with <i>18S rRNA-F</i> . |
| <i>α-tubulin 4-F</i> | 5'-GATCTCGCTGCCCTGGAA-3' | Forward primer used with <i>α-tubulin 4-R</i> to amplify a 51 base pair fragment of the cotton <i>α-tubulin 4</i> gene. |
| <i>α-tubulin 4-R</i> | 5'-ACCAGACTCAGCGCCAACTT-3' | Reverse primer used with <i>α-tubulin 4-F</i> . |

Vita

Nicole Marie Asprodites was born in New Orleans, Louisiana in 1973. She earned her Bachelor of Science Degree in Zoology from Louisiana State University in May of 1996. Nicole entered the Master of Science program at the University of New Orleans in August of 2001 and performed her research at the United States Department of Agriculture, Southern Regional Research Center in New Orleans, Louisiana. Throughout her thesis research, Nicole worked in the laboratory of Dr. Barbara A. Triplett. In the spring of 2005, Nicole won third place in the oral competition in the cotton physiology division at the Beltwide Cotton Conference. In May of 2005, she received her Master of Science degree in Biological Sciences from the University of New Orleans.